Giant porphyry copper deposits require large magma reservoirs at the verge of eruption

Working Paper

Author(s):
Large, Simon J.E.; Buret, Yannick; Wotzlaw, Jörn-Frederik; Karakas, Özge; Guillong, Marcel; von Quadt, Albrecht; Heinrich, Christoph A.

Publication date:
2019-02-02

Permanent link:
https://doi.org/10.3929/ethz-b-000473491

Giant porphyry copper deposits require large magma reservoirs at the verge of eruption

S.J.E. Large[1*,†], Y. Buret[1,†], J.F. Wotzlaw[1], O. Karakas[1], M. Guillong[1], A. von Quadt[1], C.A. Heinrich[1,2]

[1]Department of Earth Sciences, Eidgenössische Technische Hochschule (ETH) Zurich, 8092 Zürich, Switzerland.

[2]Faculty of Mathematics and Natural Sciences, University of Zurich, 8006 Zürich, Switzerland.

† Current address: Department of Earth Sciences, Natural History Museum, Cromwell Road, London, SW7 5BD, UK

*Corresponding author. Email: s.large@nhm.ac.uk

Volatile-rich silicic magma reservoirs can feed devastating volcanic eruptions but also generate valuable magmatic-hydrothermal ore deposits that supply most of the world's copper. The rate of hydrous magma injection into the upper crust and the subsequent thermal evolution are decisive for the two contrasting modes of volatile release. Here, we integrate zircon petrochronology with geophysical data and thermal modelling to reconstruct the magmatic evolution of the ~3000 km^3 magma reservoir that sourced the giant Cu-Mo-Au deposits at Bingham Canyon (USA). The magmatic body was assembled rapidly in a pre-heated upper crust by a high magma flux, similar to reservoirs that feed volcanic super-eruptions. The subsequent ~800 kyr of recorded upper-crustal magma evolution are dominated by monotonous cooling and crystallisation that resulted in rapid fluid extraction forming the subvolcanic Cu-Au deposit in <150 kyr. Based on these findings we argue that giant porphyry deposits are formed by magma supply rates approaching those preceding volcanic super-eruptions, whereby thermal weakening of the upper crust by preceding lower-crustal magmatism contributes to focussed ejection of fluids only while avoiding destructive eruption.

Porphyry Cu (-Au-Mo) deposits currently provide ~75 %, 20 % and 50 % of the global demand for Cu, Au and Mo, respectively[1] and are an essential source of society's future metal demand. These magmatic-hydrothermal deposits form at the interface between the plutonic and volcanic domains of upper-crustal magmatic systems. Focused fluid extraction from large upper-crustal magma bodies results in the chemical concentration of economic mineralisation around sub-volcanic porphyritic intrusions[1,2]. The chemical evolution of ore fluids and fluid-saturating plutons have been investigated in detail[3-5] and questions now centre on the physical evolution of the upper-crustal magma reservoirs and the extraction of fluids to generate the deposits. The existence of large melt-rich bodies invoked for ore

formation[6-8] has been questioned because of lacking geophysical evidence for low-crystallinity melt zones underlying active volcanoes[9,10] and thermal arguments implying the necessity of sustained magma input to prevent rapid ($<10^4$ yr) solidification[11,12]. In combination with geochronological evidence from plutons, this has led to the inference that long-lived reservoirs ($>10^5$ kyr) are incrementally assembled by a sustained magma flux, whereby the magma is predominantly stored in a crystal-rich mush at near-solidus temperatures[12,13] and melt can percolate through this mush on a crustal scale[14,15]. However, thermal models incorporating lower-crustal magma storage predict significant pre-heating of the upper crust, which can extend the life-time of upper-crustal magma chambers to several 100 kyr[16,17]. The thermal lifetime of upper-crustal magma reservoirs has broader significance, because it implies that the rate of magma input may determine whether the magma reservoir cools to form a pluton, generates a porphyry-mineralising magma chamber, or leads to a large volcanic eruption[11,18,19]. High-precision single-zircon U-Pb geochronology has so far not documented systematic differences in the lifetimes of upper-crustal magma reservoirs resulting in barren plutons[12,20-22], ore deposits[23-27] or volcanic eruptions[13,28,29]. These partial and seemingly contradictory observations call for an integrated study in which independent information about the size of the magma reservoir is combined with observational data for its time–temperature evolution, which can then be compared with geologically constrained thermal modelling. Igneous complexes generating giant ore deposits provide a particularly stringent test of thermal models, because the accumulation of a large tonnage of copper contributes additional constraints on magma and fluid volumes[7,30,31], and small rapidly-quenched porphyry intrusions provide successive samples of the crystallising magma reservoir[7,32,33]. Here, we present high-precision zircon U-Pb geochronology and in-situ geochemistry including Ti-in-zircon temperatures and combine these data with thermal

modelling to constrain the evolution of the magma reservoir that provided the source of thermal energy, metals and volatiles to a giant Cu-Au-Mo deposit.

Rapid Cu-Au ore fluid extraction from a long-lived magmatic system at Bingham Canyon

Bingham Canyon (USA, Fig.1), is one of the world's largest (>26 Mt Cu, ~1500 t Au, ~1.5 Mt Mo)[34] and best studied porphyry deposits. Economic mineralisation is centred around an equigranular monzonite (EM) stock and a sequence of porphyries intruding into Carboniferous quartzites and limestones[32]. An aeromagnetic anomaly under Bingham Canyon has been inverted, assuming the EM to represent the apical part of a larger intrusion, resulting in an estimated magma volume of 1500 to 3500 km^3 that is consistent with the quantity of fluids and metals required to form the deposit[30]. Field relationships show that the EM was intruded by the quartz monzonite porphyry (QMP), then the latite porphyry (LP) and finally the quartz latite porphyry (QLP; Supplementary Fig.1). Each porphyry intrusion is associated with veining and alteration that decreases in intensity with each intrusion[32,34]. Most Cu-Au-mineralised veins are truncated by the latite porphyry, indicating that ~90% of Cu and Au was deposited between the emplacement of the QMP and LP[32]. Molybdenum-bearing veins postdate all intrusions and account for 60–90 % of the Mo-ore[32,35].

We obtained geochemical information by in-situ LA-ICP-MS analysis of individual zircon grains and subsequently dated the same grains at high-precision, employing chemical abrasion isotope dilution thermal ionisation mass spectrometry (CA-ID-TIMS, see methods). This petrochronology approach provides reliable temporal resolution for the spatially resolved chemical information and allows a detailed reconstruction of the magma reservoir evolution.

$^{206}Pb/^{238}U$ dates from Bingham Canyon span a total of 817±62 kyr (38.553±0.025 to 37.736±0.057 Ma; Fig. 1). Zircons from each porphyry intrusion record a range of crystallisation ages, which is short in the oldest intrusion (EM: 34±50 kyr) and extends to

progressively longer timespans in the younger intrusions (QLP: 410±61 kyr). We interpret these ranges in zircon dates to reflect continuous zircon crystallisation within a magma batch up to the point of its emplacement into the sub-volcanic environment and rapid cooling to a porphyry. The youngest individual zircon dates of each porphyry intrusion therefore define the emplacement ages (Fig. 1c; QMP: 38.284 ± 0.024 Ma; LP: 38.157 ± 0.021 Ma; QLP: 37.736 ± 0.057 Ma), in line with cross-cutting field relationships[32,34]. Emplacement ages of the QMP and LP[32] constrain the maximum duration of the main ore-forming event to 127±23 kyr, whereas Mo-ore formation occurred >400 kyr after the main period of Cu-Au ore mineralisation after emplacement of the QLP.

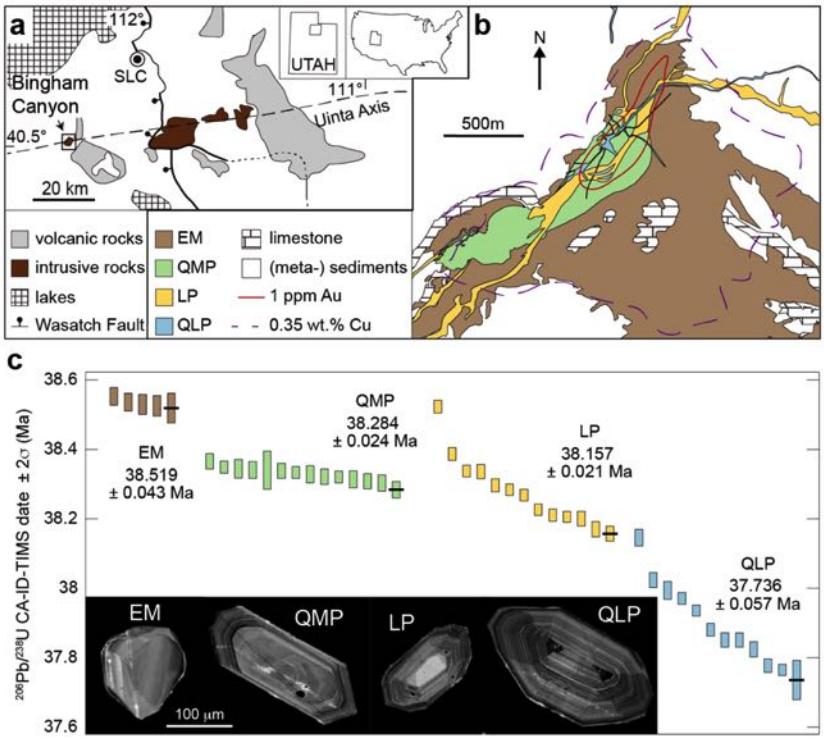

Figure 1: High-precision geochronology of intrusive rock units at Bingham Canyon. a, Overview map modified from ref. 35. **b**, Geological map of the mine area, both modified from ref. 32. **c**, Individual $^{206}Pb/^{238}U$ zircon dates with 2σ uncertainty of the four main intrusions, with colours matching intrusive units shown in map **b**; youngest zircon dates determine maximum emplacement ages. Inset shows representative cathodoluminescence images of zircons.

A crystallising and continuously cooling upper-crustal magma reservoir

The punctuated intrusion of porphyries contrasts with a surprisingly continuous trend in the trace element evolution from the oldest zircon in the earliest intrusion to the youngest zircon in the latest porphyry (Fig. 2), recording the evolution of a single underlying magma reservoir. Systematic changes in trace element ratios (Fig. 2a) document the co-crystallisation of zircon, titanite, apatite and hornblende and correlate with decreasing Ti-in-zircon temperatures[36] (Fig. 2).

The data obtained from Bingham Canyon are the first-ever documentation of a time-resolved trace element evolution that quantifies cooling and progressive fractional crystallisation of a single magma reservoir over a well-defined period of ~800 kyr (Fig. 2). Zircon crystals from the oldest EM are irregular and anhedral, indicating interstitial crystallisation after emplacement of the EM as an initially zircon-undersaturated magma. The subsequent hiatus in zircon crystallisation over 132±46 kyr indicates renewed zircon-undersaturation in the magma reservoir, interpreted to reflect further influx of high-temperature melt into the reservoir. These observations (and the absence of systematic variation of zircon geochemistry within the small range of ages; Fig. 2b, c) demonstrate that zircon crystallisation and subsequent fractional crystallisation did not start in the lower crust. Rather, the influx of hot monzonitic magma established a large upper-crustal melt-rich magma reservoir which then partly crystallised over ~100 kyr until extraction of the QMP, immediately followed by the most intense quartz–chalcopyrite veining. Titanium-in-zircon temperatures systematically decrease from ~900°C in the EM to ~650°C in the QLP (Fig. 2c) and correlate with zircon saturation temperatures ($T_{zrc\text{-}sat}$) based on published melt inclusion compositions[37]. The short interval of Cu-Au ore formation coincides with the sharpest drop in Ti-in-zircon temperatures (Fig. 2c). We interpret this drop to reflect a period of rapid

crystallisation driving massive fluid release from the large volume of magma. After the resulting main Cu-Au ore mineralisation, zircons from the QLP record consistently low crystallisation temperatures (Fig. 2c), reflecting a more crystalline state of the reservoir (Fig. 2a, b).

The pyroxene bearing EM corresponds to the early crystallised, zircon undersaturated apical part of the large magma reservoir and reflects relatively primitive and only moderately water-rich source magma. Upper-crustal fractionation resulted in successively more evolved magmas being ejected into the porphyry environment culminating in the emplacement of the quartz and amphibole rich QLP. Bingham is therefore the first porphyry deposit providing clear evidence that phenocryst and zircon crystallisation was associated with extensive fractionation and progressive volatile enrichment in an upper-crustal magma reservoir and does not record antecrystic growth in a longer-lived lower-crustal hot zone.

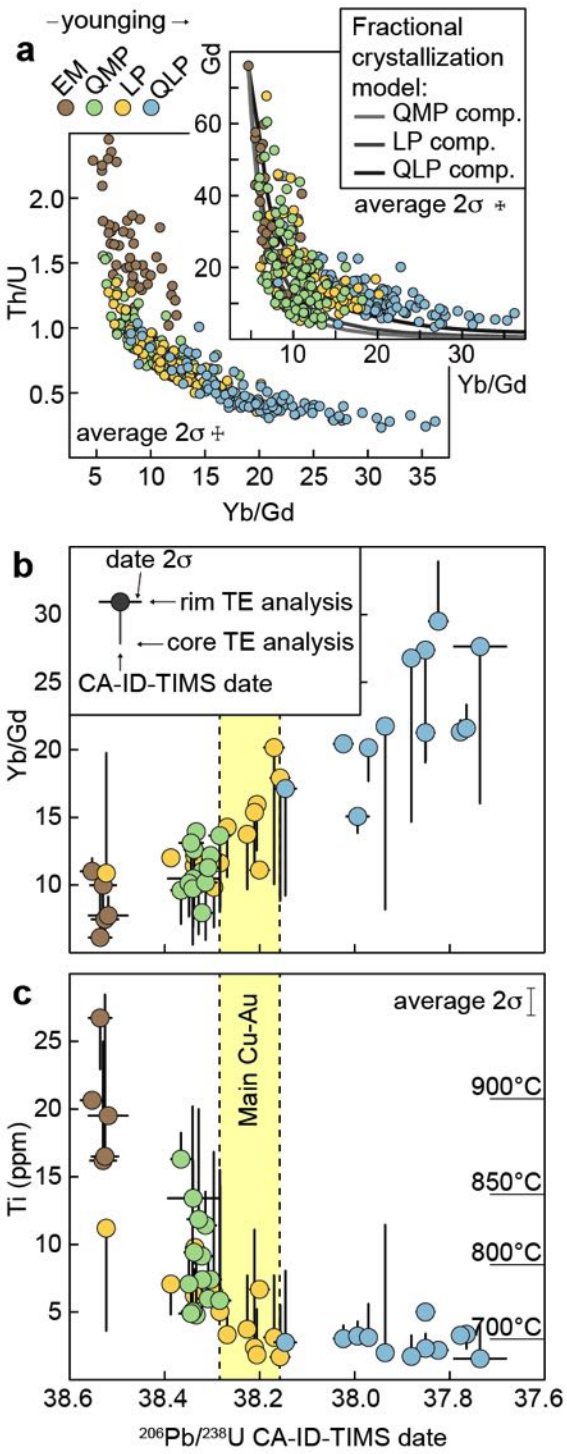

Figure 2: Time-calibrated geochemical evolution of the Bingham Canyon magma reservoir resolved by zircon petrochronology. a, Trace element co-variation diagrams illustrating progressive fractional crystallisation with lines marking results of crystallisation modelling (see methods for further information). **b**, and **c**, Trace element composition of ID-TIMS-dated zircons recording fractional crystallisation (increasing Yb/Dy) and cooling (decreasing Ti) of a single magma reservoir through time. Interval of main Cu-Au ore formation after ref. 32.

Thermal modelling constraints on the assembly and evolution of a long-lived, homogeneous magma reservoir

The time – temperature evolution observed in zircons can be confronted with a thermal evolution model[17] using geometric constraints of a 3000 km^3 subvolcanic body defined from geophysical data[30]. In a first stage of the model, we computed the thermal evolution of the crust by simulating injections of basaltic andesite dikes and sills into the lower crust over 2 Ma. This stage significantly pre-heats the middle to upper crust and is consistent with widespread Eocene magmatic activity around Bingham Canyon[37] (Fig. 1a). In the second stage, we simulated monzonitic dike and sill injections into this pre-heated upper crust between 5 and 8 km depth[30]. The total duration of magma injection into the upper crust was varied from 1.5 to 0.1 Ma, corresponding to fluxes from moderately low (~0.0025 km^3/yr) to very high (~0.035 km^3/yr), but always resulting in a similar volume of total injected magma. We modelled a total of 8 emplacement scenarios (see Supplementary Material for additional models), three of which are compared with the petrochronological results in Figure 3.

An extended period of slow magma injection (Fig. 3a) cannot explain the time-temperature evolution of the Bingham Canyon reservoir, nor can any rate of magma injection into cold crust[17]. In contrast, models with moderately high (0.0065 km^3/yr) to very high (0.035 km^3/yr) magma flux during 0.5 to 0.1 Myr into pre-heated upper crust reproduce the petrochronological data almost perfectly (Fig. 3b, c). The calculated thermal evolutions start with an interval of increasing temperatures during reservoir assembly followed by continuous cooling once magmatic recharge is stopped, leading to full solidification >600 kyr after zircon saturation. In these scenarios a partially molten domain persists at depths between 5-8 km (Fig. 3d-f), providing a source of metal-rich fluids and porphyry magmas that were successively injected to the sub-volcanic environment. Total melt volumes at the time of QMP emplacement in excess of 250 km^3 are sufficient to source all metals and sulphur at

Bingham Canyon based on melt inclusion data and mass balance calculations[30,37]. The calculated crystallinity of the melt-rich domain at the time of QMP emplacement (Supplementary Material) is consistent with the phenocryst contents (50-60 %) of the QMP[32], and the corresponding melt fraction allows efficient flow of exsolving volatiles through the crystal mush and its focussing to the apex of the magma chamber[38]. Calculated temperatures of the melt-rich domain agree with Ti-in-zircon temperatures (Fig. 3) and the sharp temperature increase above $T_{zrc\text{-}sat}$ during assembly of the large reservoir is agreement with the lack of recorded zircon crystallisation ages.

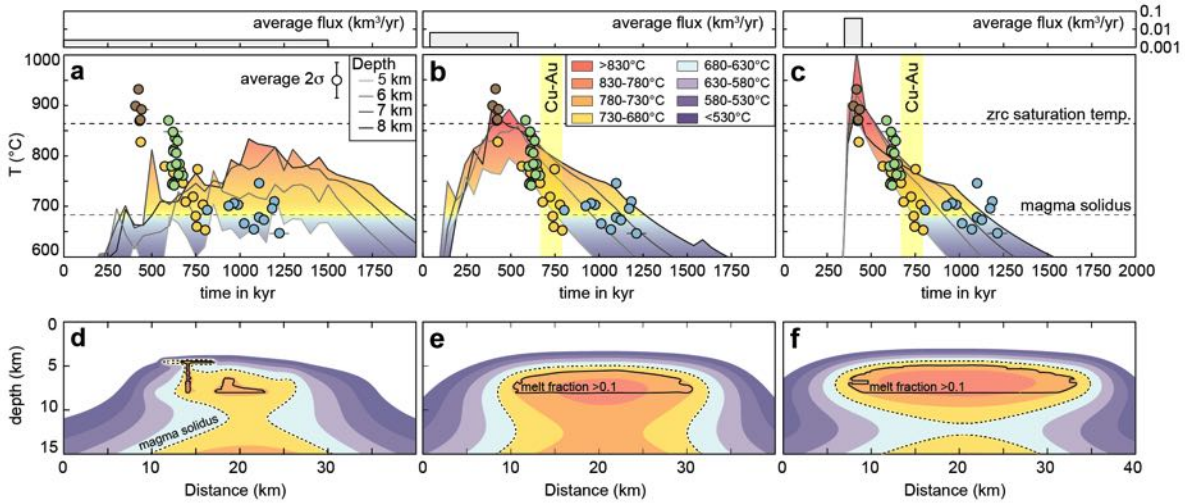

Figure 3: Comparison of zircon petrochronology data with thermal modelling results. **a,-c,** Filled symbols show time-temperature evolution recorded by zircons (rim data as in Figure 2); grey lines illustrate temperature evolution at different depth along a vertical profile through the centre of the magma reservoir, as predicted by the thermal model, with colour shading according to model temperatures. The high-temperature EM zircons were adjusted to the temperature peak of the thermal model for consistent comparison. Dashed lines mark the temperatures of zircon saturation of monzonite and the solidus of granite. **d,-f,** 2-D temperature profiles with coherent melt regions, shown for the time of QMP emplacement, i.e. the onset of Cu-Au ore formation.

Giant-porphyry forming magma reservoirs are confined super-eruptions

The remarkable agreement between the zircon analytical data and geologically-constrained thermal simulations shows that a minimum flux of 0.0065 km^3/yr is needed for the formation of a fertile magma reservoir that can source a Bingham Canyon sized porphyry deposit. Reservoir assembly at higher fluxes will also provide permissive conditions but is more likely to overpressure the magma reservoir to the point of eruption[39,40], destroying any chance of ore formation[23]. The magma volume and input rate identified at Bingham Canyon resemble values that have been typically associated with volcanic super-eruptions[11,16-18] (Fig. 4). Magma fluxes suggested for barren plutons and small porphyry deposits are much lower and are reflected by more convoluted zircon age-composition trends indicating an open system evolution[21,23,25,27,28].

The short metal mineralisation event concurs with timescales from studies on smaller porphyry deposits (<1-7 Mt Cu)[23,25,27]. Lacking systematics between zircon crystallisation age and trace-element patterns seen in these studies can be explained by insufficient duration of high fluxes to establish a closed-system petrochronology signal or by less rapidly assembled reservoirs (<0.001 km^3/yr) generating small isolated melt lenses[17]. These low fluxes might be sufficient to source smaller eruptions and deposits but not a giant deposit like Bingham Canyon.

The timescales and fluxes obtained in this study challenge earlier investigations based on numerical models alone[18,19,41,42]. These models suggested that multi-million-year upper-crustal magmatism and extended periods of hydrothermal ore formation are essential for the formation of giant porphyry ore deposits. Their idea was motivated by the pulsed nature of porphyry emplacement[1,32,33] and extended ranges of magmatic and hydrothermal age dates in many major mineral camps[1,43-46]. We reinterpret the latter observations to reflect the required thermal preparation of the upper crust. The multi-million-year timescales of upper-crustal

magmatism are not consistent with large upper-crustal magma chambers with sufficiently sized melt-rich domain to release and focus large volumes of metal-bearing fluids over a short time interval (127±23 kyr for Bingham Canyon), but more likely represent the time scale of mid to lower-crustal hot zones[47,48]. Extended crustal pre-heating followed by high-flux magma injection into the upper crust are two essential conditions for establishing the capability to exsolve and focus large volumes of metal-rich fluid within a short period of time, by rapid cooling, fractional crystallisation and "second boiling"[6,30]. Similarities with eruption-feeding magma reservoirs in terms of lifetime and magma flux are in agreement with rare observations that porphyry deposits and major ignimbrites can be sourced from the same magma reservoir[23]. We argue that the generation of super-eruptions and giant porphyry Cu deposits both require rapid magma emplacement into pre-heated upper crust. Pre-heating by extended lower-crustal magmatism not only explains multi-Ma upper-crustal magmatism preceding ore formation[46], but also lowers the viscoelastic strength of the upper crust resulting in favourable conditions for the accumulation of large volumes of magma to feed giant porphyry deposits or voluminous eruptions[40]. The degree of thermal weakening is probably decisive between catastrophic eruption of fluids together with magma, or the controlled release of low-viscosity fluid only through a multitude of narrow fractures characterising porphyry ore deposits[1,31,49]. Some of the richest deposits are hosted by carbonate sequences[1,26,32] which, being particularly susceptible to thermal weakening, might contribute to preventing magmas and fluids from uncontrolled eruption. In summary, the formation of a giant porphyry deposits more closely resembles a barely-prevented volcanic super-eruption, rather than a plutonic system in which multiple magma pulses feed a gradual buildup of porphyries and hydrothermal veins.

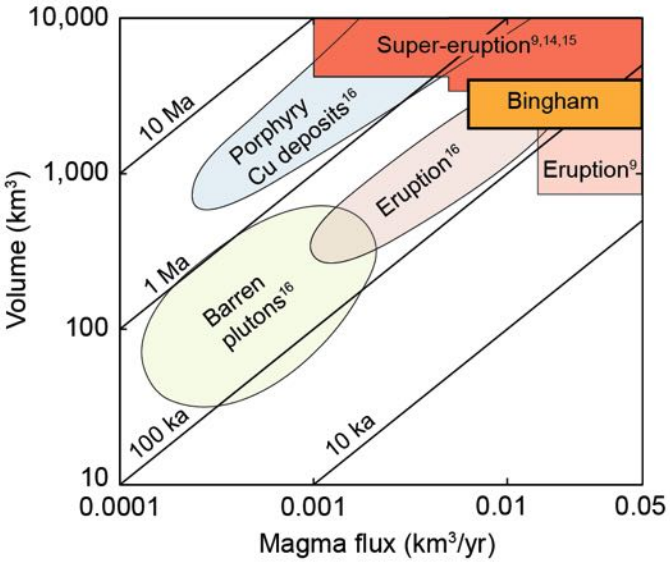

Figure 4: Magma flux and volume at Bingham Canyon compared to other systems. Possible conditions for reservoir assembly and ore formation at Bingham Canyon (red square) are compared to compiled literature data of fluxes and injected volumes suggested for different magmatic systems.

Acknowledgments: S.J.E.L., Y.B. and C.A.H. acknowledge funding from Swiss National Science Foundation (SNF) project 200026-166151.

Author contributions: S.J.E.L. and Y.B. performed data acquisition and interpretation (DI) and science interpretation (SI). J.F.W. and. C.A.H. provided DI and SI. O.K. wrote the modelling code and produced numerical results. A.v.Q. and M.G. provided essential laboratory resources for the study. S.J.E.L., Y.B., J.F.W., O.K., C.A.H. jointly designed the numerical experiments and drafted the manuscript. S.J.E.L. prepared the figures. Authors declare no competing interests.

References

1. Sillitoe RH. Porphyry copper systems. *Economic geology* 2010, **105**(1)**:** 3-41.

2. Hedenquist JW, Lowenstern JB. The role of magmas in the formation of hydrothermal ore deposits. *Nature* 1994, **370**(6490)**:** 519-527.

3. Landtwing MR, Furrer C, Redmond PB, Pettke T, Guillong M, Heinrich CA. The Bingham Canyon porphyry Cu-Mo-Au deposit. III. Zoned copper-gold ore deposition by magmatic vapor expansion. *Economic Geology* 2010, **105**(1)**:** 91-118.

4. Kouzmanov K, Pokrovski GS. Hydrothermal controls on metal distribution in porphyry Cu (-Mo-Au) systems. 2012.

5. Roedder E. Fluid inclusion studies on the porphyry-type ore deposits at Bingham, Utah, Butte, Montana, and Climax, Colorado. *Economic Geology* 1971, **66**(1)**:** 98-118.

6. Cloos M. Bubbling Magma Chambers, Cupolas, and Porphyry Copper Deposits. *International Geology Review* 2001, **43**(4)**:** 285-311.

7. Dilles JH. Petrology of the Yerington Batholith, Nevada; evidence for evolution of porphyry copper ore fluids. *Economic Geology* 1987, **82**(7)**:** 1750-1789.

8. Shinohara H, Hedenquist J. Constraints on magma degassing beneath the Far Southeast porphyry Cu–Au deposit, Philippines. *Journal of Petrology* 1997, **38**(12)**:** 1741-1752.

9. Huang H-H, Lin F-C, Schmandt B, Farrell J, Smith RB, Tsai VC. The Yellowstone magmatic system from the mantle plume to the upper crust. *Science* 2015, **348**(6236)**:** 773-776.

10. Delph JR, Ward KM, Zandt G, Ducea MN, Beck SL. Imaging a magma plumbing system from MASH zone to magma reservoir. *Earth and Planetary Science Letters* 2017, **457:** 313-324.

11. Annen C. From plutons to magma chambers: Thermal constraints on the accumulation of eruptible silicic magma in the upper crust. *Earth and Planetary Science Letters* 2009, **284**(3-4)**:** 409-416.

12. Barboni M, Annen C, Schoene B. Evaluating the construction and evolution of upper crustal magma reservoirs with coupled U/Pb zircon geochronology and thermal modeling: A case study from the Mt. Capanne pluton (Elba, Italy). *Earth and Planetary Science Letters* 2015, **432:** 436-448.

13. Szymanowski D, Wotzlaw J-F, Ellis BS, Bachmann O, Guillong M, von Quadt A. Protracted near-solidus storage and pre-eruptive rejuvenation of large magma reservoirs. *Nature Geoscience* 2017, **10**(10)**:** 777-782.

14. Cashman KV, Sparks RS, Blundy JD. Vertically extensive and unstable magmatic systems: A unified view of igneous processes. *Science* 2017, **355**(6331).

15. Jackson MD, Blundy J, Sparks RSJ. Chemical differentiation, cold storage and remobilization of magma in the Earth's crust. *Nature* 2018, **564**(7736)**:** 405-409.

16. Gelman SE, Gutiérrez FJ, Bachmann O. On the longevity of large upper crustal silicic magma reservoirs. *Geology* 2013, **41**(7)**:** 759-762.

17. Karakas O, Degruyter W, Bachmann O, Dufek J. Lifetime and size of shallow magma bodies controlled by crustal-scale magmatism. *Nature Geoscience* 2017, **10**(6)**:** 446-450.

18. Caricchi L, Simpson G, Schaltegger U. Zircons reveal magma fluxes in the Earth's crust. *Nature* 2014, **511**(7510)**:** 457-461.

19. Schöpa A, Annen C, Dilles JH, Sparks RSJ, Blundy JD. Magma Emplacement Rates and Porphyry Copper Deposits: Thermal Modelling of the Yerington Batholith, Nevada, USA. EGU General Assembly Conference Abstracts; 2017; 2017. p. 13127.

20. Glazner AF, Bartley JM, Coleman DS, Gray W, Taylor RZ. Are plutons assembled over millions of years by amalgamation from small magma chambers? *GSA Today* 2004, **14**(4).

21. Schoene B, Schaltegger U, Brack P, Latkoczy C, Stracke A, Günther D. Rates of magma differentiation and emplacement in a ballooning pluton recorded by U–Pb TIMS-TEA, Adamello batholith, Italy. *Earth and Planetary Science Letters* 2012, **355-356:** 162-173.

22. Ratschbacher BC, Keller CB, Schoene B, Paterson SR, Anderson JL, Okaya D*, et al.* A New Workflow to Assess Emplacement Duration and Melt Residence Time of Compositionally Diverse Magmas Emplaced in a Sub-volcanic Reservoir. *Journal of Petrology* 2018.

23. Buret Y, Wotzlaw J-F, Roozen S, Guillong M, von Quadt A, Heinrich CA. Zircon petrochronological evidence for a plutonic-volcanic connection in porphyry copper deposits. *Geology* 2017, **45**(7)**:** 623-626.

24. Gilmer AK, Sparks RSJ, Rust AC, Tapster S, Webb AD, Barfod DN. Geology of the Don Manuel igneous complex, central Chile: Implications for igneous processes in porphyry copper systems. *Geological Society of America Bulletin* 2017, **129**(7-8)**:** 920-946.

25. Chelle-Michou C, Chiaradia M, Ovtcharova M, Ulianov A, Wotzlaw J-F. Zircon petrochronology reveals the temporal link between porphyry systems and the magmatic evolution of their hidden plutonic roots (the Eocene Coroccohuayco deposit, Peru). *Lithos* 2014, **198-199:** 129-140.

26. Large SJE, Quadt Av, Wotzlaw J-F, Guillong M, Heinrich CA. Magma Evolution Leading to Porphyry Au-Cu Mineralization at the Ok Tedi Deposit, Papua New

Guinea: Trace Element Geochemistry and High-Precision Geochronology of Igneous Zircon. *Economic Geology* 2018, **113**(1)**:** 39-61.

27. Tapster S, Condon DJ, Naden J, Noble SR, Petterson MG, Roberts NMW*, et al.* Rapid thermal rejuvenation of high-crystallinity magma linked to porphyry copper deposit formation; evidence from the Koloula Porphyry Prospect, Solomon Islands. *Earth and Planetary Science Letters* 2016, **442:** 206-217.

28. Deering CD, Keller B, Schoene B, Bachmann O, Beane R, Ovtcharova M. Zircon record of the plutonic-volcanic connection and protracted rhyolite melt evolution. *Geology* 2016, **44**(4)**:** 267-270.

29. Wotzlaw J-F, Schaltegger U, Frick DA, Dungan MA, Gerdes A, Günther D. Tracking the evolution of large-volume silicic magma reservoirs from assembly to supereruption. *Geology* 2013, **41**(8)**:** 867-870.

30. Steinberger I, Hinks D, Driesner T, Heinrich CA. Source plutons driving porphyry copper ore formation: combining geomagnetic data, thermal constraints, and chemical mass balance to quantify the magma chamber beneath the Bingham Canyon deposit. *Economic Geology* 2013, **108**(4)**:** 605-624.

31. Weis P, Driesner T, Heinrich CA. Porphyry-copper ore shells form at stable pressure-temperature fronts within dynamic fluid plumes. *Science* 2012, **338**(6114)**:** 1613-1616.

32. Redmond PB, Einaudi MT. The Bingham Canyon porphyry Cu-Mo-Au deposit. I. Sequence of intrusions, vein formation, and sulfide deposition. *Economic Geology* 2010, **105**(1)**:** 43-68.

33. Seedorff E, Einaudi MT. Henderson porphyry molybdenum system, Colorado: I. Sequence and abundance of hydrothermal mineral assemblages, flow paths of evolving fluids, and evolutionary style. *Economic Geology* 2004, **99**(1)**:** 3-37.

34. Porter J, Schroeder K, Austin G. Geology of the Bingham Canyon porphyry Cu-Mo-Au deposit, Utah. *Econ Geol Spec Publ* 2012, **16:** 127-146.

35. Gruen G, Heinrich CA, Schroeder K. The Bingham Canyon porphyry Cu-Mo-Au deposit. II. Vein geometry and ore shell formation by pressure-driven rock extension. *Economic Geology* 2010, **105**(1)**:** 69-90.

36. Ferry JM, Watson EB. New thermodynamic models and revised calibrations for the Ti-in-zircon and Zr-in-rutile thermometers. *Contributions to Mineralogy and Petrology* 2007, **154**(4)**:** 429-437.

37. Grondahl C, Zajacz Z. Magmatic controls on the genesis of porphyry Cu–Mo–Au deposits: The Bingham Canyon example. *Earth and Planetary Science Letters* 2017, **480:** 53-65.

38. Parmigiani A, Faroughi S, Huber C, Bachmann O, Su Y. Bubble accumulation and its role in the evolution of magma reservoirs in the upper crust. *Nature* 2016, **532**(7600)**:** 492-495.

39. Degruyter W, Huber C. A model for eruption frequency of upper crustal silicic magma chambers. *Earth and Planetary Science Letters* 2014, **403:** 117-130.

40. Jellinek AM, DePaolo DJ. A model for the origin of large silicic magma chambers: precursors of caldera-forming eruptions. *Bulletin of Volcanology* 2003, **65**(5)**:** 363-381.

41. Chelle-Michou C, Rottier B, Caricchi L, Simpson G. Tempo of magma degassing and the genesis of porphyry copper deposits. *Sci Rep* 2017, **7:** 40566.

42. Chiaradia M, Caricchi L. Stochastic modelling of deep magmatic controls on porphyry copper deposit endowment. *Sci Rep* 2017, **7:** 44523.

43. Lee RG, Dilles JH, Tosdal RM, Wooden JL, Mazdab FK. Magmatic Evolution of Granodiorite Intrusions at the El Salvador Porphyry Copper Deposit, Chile, Based on Trace Element Composition and U/Pb Age of Zircons. *Economic Geology* 2017, **112**(2)**:** 245-273.

44. Piquer J, Skarmeta J, Cooke DR. Structural Evolution of the Rio Blanco-Los Bronces District, Andes of Central Chile: Controls on Stratigraphy, Magmatism, and Mineralization. *Economic Geology* 2015, **110**(8)**:** 1995-2023.

45. Correa KJ, Rabbia OM, Hernández LB, Selby D, Astengo M. The timing of magmatism and ore formation in the El Abra porphyry copper deposit, northern Chile: Implications for long-lived multiple-event magmatic-hydrothermal porphyry systems. *Economic Geology* 2016, **111**(1)**:** 1-28.

46. Rezeau H, Moritz R, Wotzlaw J-F, Tayan R, Melkonyan R, Ulianov A*, et al.* Temporal and genetic link between incremental pluton assembly and pulsed porphyry Cu-Mo formation in accretionary orogens. *Geology* 2016, **44**(8)**:** 627-630.

47. Annen C, Blundy J, Sparks R. The genesis of intermediate and silicic magmas in deep crustal hot zones. *Journal of Petrology* 2005, **47**(3)**:** 505-539.

48. Rohrlach BD, Loucks RR, Porter T. Multi-million-year cyclic ramp-up of volatiles in a lower crustal magma reservoir trapped below the Tampakan copper-gold deposit by Mio-Pliocene crustal compression in the southern Philippines. *Super porphyry copper and gold deposits: A global perspective* 2005, **2:** 369-407.

49. Fournier RO. Hydrothermal processes related to movement of fluid from plastic into brittle rock in the magmatic-epithermal environment. *Economic Geology* 1999, **94**(8)**:** 1193-1211.

Materials and Methods

Sample preparation

Heavy mineral separates of the of the equigranular monzonite, quartz monzonite porphyry, latite porphyry and quartz latite porphyry (samples are described in Supplementary Material, Supplementary Fig. 2) were obtained by disintegration with a high-voltage pulses in a Selfrag LabTM at ETH Zurich followed by conventional panning, heavy liquid (methylene iodide: 3.3 g/cm^3) and magnetic separation techniques. Hand-picked zircons were annealed at 900°C in quartz crucibles for 48 hours in a muffle furnace. Zircons and titanites were mounted in epoxy resin, ground and polished to expose crystal interiors. Polished grain mounts were imaged with backscattered electrons (titanite) or cathodoluminescence (zircon) using a JEOL JSM-6390 LA scanning electron microscope at ETH Zürich.

Zircon morphology and textures

Extracted zircons from all investigated intrusions range from 100 – 300 μm in length with aspect ratios of 1:2 to 1:5. Zircons from the equigranular monzonite exhibit broken and subhedral crystal shapes and CL-imaging reveals sector zoning or no zoning making the identification of core and rim domains difficult (Supplementary Fig. 2a). Zircons from the quartz monzonite porphyry, latite porphyry and quartz latite porphyry all display euhedral bi-pyramidal crystal shapes (Supplementary Fig. 2b, c, d). Zircons from the quartz monzonite porphyry contain distinct growth bands and minor oscillatory zoning, whereas oscillatory zoning is the prominent zoning pattern in the latite porphyry and especially the quartz latite porphyry.

LA-ICP-MS analyses

In-situ trace element analyses and U-Pb geochronology (Supplementary tables 2 – 5) were conducted by laser ablation-inductively coupled plasma-mass spectrometry (LA-ICP-MS) on a Thermo Element XR ICP-MS coupled to an ASI Resolution 193 nm Resonetics ArF excimer laser, with a spot diameter of 30 μm. Spots within the grains were selected based on prior images and generally one spot was chosen in the interior (core) and one for the exterior (rim) part. The total ablation time was set to 40 seconds with a gas blank/background measurement of 10s and a baseline of 30 seconds. Dwell times ranged from 5 - 30 ms and peak-hopping was employed. Oxide generation was optimised at $ThO^+/Th^+ = <0.2\%$.

For trace element analyses NIST 610 glass was used as reference material and stochiometric concentrations of Si (zircon) and Ca (titanite) as internal standards. Elemental concentrations were calculated using the IGOR based Iolite software[50]. The accuracy of the measurements was monitored by repeated analyses of secondary zircon standards (GJ-1, 91500 and synthetic zircon). Most trace elements have uncertainties better than ±5% (2 RSD) based on glass standard reproducibility. Concentrations of Al, P, Ca, Mn or Fe were monitored as proxies for possible mineral or melt inclusion contamination. Concentrations for Ti were corrected against reference material 91500 after ref. 51.

For reconnaissance, in-situ zircon U-Pb geochronology analyses the masses 202, 204, 206, 207, 208, 232, 235 and 238 were measured. The primary reference material was GJ-1[52] and secondary reference materials were 91500[53], Temora[54], AusZ7.1[55] and AusZ7.5[56]. Data reduction was performed with the IGOR based Iolite v2.5[50] and Vizual Age[57] software packages. Obtained isotope ratios and dates are corrected for mass bias, instrumental drift and downhole fractionation using primary reference material.

CA-ID-TIMS geochronology

After in-situ geochemistry, zircons were selected from the grain mounts based on the absence of mineral- or melt inclusions or inherited zircon domains for high-precision U-Pb chemical abrasion-isotope dilution-thermal ionisation mass spectrometry (CA-ID-TIMS) at the Institute of Geochemistry and Petrology of ETH Zurich (Supplementary table 1 and Supplementary Fig. 3). All zircons were pre-treated using chemical abrasion (CA) techniques modified from ref. 58 where selected annealed zircons were hand-picked from the grain mounts, placed into 3 ml Savillex beakers, rinsed with 4 N HNO_3 and subsequently transferred into 200 µl Savillex micro-capsules with 80 µl concentrated HF + trace HNO_3. The capsules were placed in a high-pressure Parr bomb and chemically abraded for 12 – 15 hours at 180°C. Chemically abraded zircons were transferred back into their 3 ml Savillex beakers, fluxed for 12 hours in 6 N HCl at ~85°C and ultrasonically cleaned in ultrapure H_2O and 4N HNO_3. Zircons were then loaded back into their pre-cleaned micro-capsules with a microdrop of 7.5N HNO_3 and 70 µl concentrated HF. Samples were spiked with 6 – 9 mg of the EARTHTIME ^{202}Pb-^{205}Pb-^{233}U-^{235}U tracer solution (ET2535[59,60]) and dissolved in high-pressure Parr bombs at 210°C for >60 hours. Dissolved samples were dried down and redissolved in 6N HCl at 180°C for 12 hours to convert the samples to chlorides. The solutions were dried again and redissolved in 3N HCl in preparation of ion exchange chromatography. U and Pb were separated using an HCl-based ion exchange chemistry following procedures modified from ref. 61. The U-Pb fractions were dried down with a microdrop of 0.02 M H_3PO_4 and loaded onto zone-refined single Re filaments with one microdrop of a silica gel emitter[62]. All measurements were performed at the Institute of Petrology and Geochemistry at ETH Zurich employing a Thermo Scientific TRITON Plus thermal ionisation mass spectrometer (TIMS). Pb was measured sequentially on a dynamic MassCom secondary electron multiplier and U was measured in static mode as U-oxide using Faraday cups fitted with 10^{13} Ω resistor amplifiers[56,63]. If intensities of U during static measurements were sufficient an online UO_2 interference correction was applied[63]. The

linearity of the MasCom secondary electron multiplier was calibrated through repeated measurements of SRM982 over a range of intensities up to 1.4 Mcps. Instrumental mass fractionation was corrected by calculating the deviation of the measured $^{202}Pb/^{205}Pb$ and $^{233}U/^{235}U$, respectively, from the known tracer composition of the ET2535 tracer solution (ET2535 v 3.0[59,60]), and assuming a sample and blank $^{238}U/^{235}U$ of 137.818 ± 0.045 (2σ)[64]. Comparison with total procedural blank measurements indicated that analysed zircons did not contain common Pb and that all common Pb in the zircon analyses was derived from the laboratory blank. All common Pb in zircon analyses was therefore corrected using the long-term average laboratory blank composition of $^{206}Pb/^{204}Pb$ = 18.40 ± 0.20, $^{207}Pb/^{204}Pb$ = 15.19 ± 0.19 and $^{208}Pb/^{204}Pb$ = 36.93 ± 0.45 (1σ abs; n=16). Data reduction and error propagation of the U-Pb data was carried out using the Tripoli and U-Pb Redux software packages[65] applying the algorithms of ref. 66. U-Pb ages were calculated relative to the EARTHTIME tracer calibration v.3[59] and the U decay constants of ref. 67. All uncertainties of U-Pb ages are reported at the 95% confidence interval (2σ) and do not include decay constant uncertainties. Results of analyses of ET2535 spiked aliquots of the EARTHTIME 100 synthetic solution[59] as well as analyses of zircon reference materials were performed over the course of this study and are compiled in ref. 56 and 63.

All $^{206}Pb/^{238}U$ dates were corrected for initial ^{230}Th-^{238}U disequilibrium in the ^{238}U-^{206}Pb decay chain[68] using a constant Th/U partition coefficient ratio assuming that variations in Th/U of the zircons result from different Th/U of the melt in equilibrium during zircon crystallisation and not from variations in relative zircon-melt partitioning of Th and U. For this study, a constant $D_{Th/U}$ of 0.25 ± 0.10[69] is used for all zircons with Th/U < 1.5. Zircons from the EM displayed very high Th/U ratios and were corrected with an assumed Th/U of the melt of 4 ± 1 (c.f. ref. 70 and 71).

Mineral thermometry

Mineral thermometry was applied to zircon and titanite to constrain crystallisation temperatures of individual mineral domains. The variables for the application of mineral thermometry on zircon, after ref. 36, and titanite, after ref. 72, are the activities of SiO_2 ($aSiO_2$) and TiO_2 ($aTiO_2$) in the melt and in the case of titanite thermometry the pressure. Based on the occurrence of quartz an $aSiO_2$ of 1 was assumed and the pressure was fixed at 2 kbar based on an assumed depth of 5-8 km of the magma reservoir[30]. The melt activity of $aTiO_2$ is difficult to quantify, especially in altered rocks related to porphyry deposits. We therefore use a new approach where we correlate the Ti-in-zircon and Zr-in-titanite thermometers (Supplementary Fig. 5). Based on the co-occurrence of titanite and zircon in the QLP and the co-crystallisation evidenced by the geochemical evolution of zircon (Figure 2a, Supplementary Fig. 4) we assume that the majority of the titanite and zircon populations from the QLP must have crystallised at the same temperature. Applying values for $aSiO_2$ and pressure as outlined above, and varying the $aTiO_2$ we identify an $aTiO_2$ value of 0.5 as the best fit for our data-set (Supplementary Fig. 5). As no magmatic titanite could be recovered from the other samples due to strong alteration intensities, we also applied this value to the other samples. We consider this to be the most robust way of estimating the $aTiO_2$. We further included an uncertainty of ±0.1 on the activity of $aTiO_2$ for the calculation of the zircon crystallisation temperature. In general, variation of $aTiO_2$ and $aSiO_2$ would not significantly alter any of our described relative time-temperature relationships but would slightly shift absolute values (see Supplementary Fig. 5a, b, c).

Trace element modelling and zircon saturation temperature calculation

Trace element fractional crystallisation modelling is based on the crystallisation of phenocryst assemblages of the Bingham Canyon intrusions[32] (See Supplementary Table 6 for details on

the input parameters for the modelling) using the least fractionated zircon of the EM as the starting composition and calculating crystallisation steps of 5%.

The zircon saturation temperature is calculated applying the experimental calibration by ref. 73 using the average melt inclusion composition of unaltered contemporaneous latitic volcanic rocks outcropping to the southeast of the Bingham Canyon deposit[37].

Linking spatially-resolved trace element data with high-precision geochronology

Linking the crystallisation age of a zircon grain or zircon fragment, obtained by high-precision CA-ID-TIMS geochronology, to geochemical data derived from the same zircon volume (TIMS-TEA)[74] is a powerful tool in exploring the magmatic evolution of the crystallising reservoir[e.g.21,29,75]. Here, we link high-precision geochronological data with previously obtained geochemical in-situ LA-ICP-MS data on the same zircon grains that provide further spatially information of the geochemical data.

To test the validity of plotting in-situ data against bulk zircon crystallisation ages we compared Th/U ratios obtained by LA-ICP-MS and ID-TIMS. The latter are calculated from the measured radiogenic ^{208}Pb component for the same volume of zircon that was used to obtain a high-precision CA-ID-TIMS U-Pb date based on the assumption of concordance between the U-Pb and Th-Pb systems. The obtained ratios display an excellent fit with in-situ data obtained for rim analyses, whereas in-situ core analyses result in systematically slightly higher Th/U ratios (Supplementary Fig. 6). This is in agreement with ref. 75 who demonstrated that rim-analyses represent a much larger volume of the zircon than core analyses.

In Figure 2 all available trace element information of a zircon grain are plotted against its zircon crystallisation age by displaying core and rim analyses. As for the good correlation of in-situ rim and whole fragment analyses rims are visually emphasised. For clarity, only rim analyses are plotted in Figure 3.

Modelling the thermal evolution of the magma reservoirs in the lower and upper crust

We used a two-dimensional thermal model to quantify the evolution of magmas incrementally emplaced first in the lower, and then in the upper crust. The model is modified from ref. 17 to simulate the magma evolution at Bingham Canyon and constrain the conditions under which the magma reservoir that sourced the giant porphyry Cu-Au-Mo deposit based on the timescales suggested by geochronology in this study. The numerical model follows the finite volume scheme described by ref. 76. The entire domain consists of a 60 km by 60 km section of the crust and upper mantle with 40 m resolution on both horizontal and vertical directions. The heat conduction equation is solved for each grid with a timestep of 100 years. Careful treatment of latent heat evolution during melting and crystallisation is key while solving the heat equation. The evolution of the system as a result of cooling and crystallisation of intruded magmas and the surrounded crustal material is calculated following the experimental conditions and rhyolite-MELTS modelling results[77] for the compositions determined for the Bingham Canyon system. For the lower and upper crustal material, we used the experimental results of ref. 78 using metapelitic rocks. For the lower crustal magmas, we used the melt fraction versus temperature relationship based on the results of fractional crystallisation experiments of primitive, hydrous arc magmas[79]. The upper crustal melt fraction versus temperature relationship is determined from rhyolite-MELTS calculations based on ref. 37 using the average whole-rock composition of latites from the nearly co-eval volcanic sequence southeast of the Bingham Canyon deposit at 2 kbar and with 4.8 wt.% H_2O (Supplementary Fig. 11).

The initial thermal profile of the domain is determined by a steady-state geotherm with exponential distribution of the radiogenic element concentration in the uppermost crust. The surface temperature (x=0 km) is fixed at 0°C. The side temperatures and temperature at the

bottom of the domain is determined based on the initial geothermal gradient. We assume constant boundary conditions, where the temperatures are fixed at the lateral boundaries. In the second step of simulations, we use constant heat flux boundary condition at the bottom boundary, assuming that the rate of change of average temperature in upper crust is minimal after 2 Ma of lower crustal magmatism[17], which is assumed based on abundant Eocene magmatic activity within the region[80].

The equations and solutions for the conservation of mass and enthalpy, and mixture properties of density, thermal conductivity, and heat capacity terms are discussed in ref. 17. The intrusion frequency, volume, and timing are randomised following the L'Ecuyer random number generator algorithm. Latent heat evolution during phase changes is calculated using the predictor-corrector algorithm and iterative approach following[81]. The details of the assumptions and calculations are described in ref. 82. The results of all 8 modelling runs conducted in this study are displayed in Supplementary Fig. 7-11.

Code Availability:

The code applied in this study is described in full detail in ref. 17 and is available from OK on request.

Data Availability statement:

Authors can confirm that all relevant data are included in the paper and its supplementary information files.

Continued references:

50. Paton C, Hellstrom J, Paul B, Woodhead J, Hergt J. Iolite: Freeware for the visualisation and processing of mass spectrometric data. *Journal of Analytical Atomic Spectrometry* 2011, **26**(12)**:** 2508-2518.

51. Szymanowski D, Fehr MA, Guillong M, Coble MA, Wotzlaw J-F, Nasdala L*, et al.* Isotope-dilution anchoring of zircon reference materials for accurate Ti-in-zircon thermometry. *Chemical Geology* 2018, **481:** 146-154.

52. Jackson SE, Pearson NJ, Griffin WL, Belousova EA. The application of laser ablation-inductively coupled plasma-mass spectrometry to in situ U–Pb zircon geochronology. *Chemical Geology* 2004, **211**(1-2)**:** 47-69.

53. Wiedenbeck M, Alle P, Corfu F, Griffin W, Meier M, Oberli Fv*, et al.* Three natural zircon standards for U-Th-Pb, Lu-Hf, trace element and REE analyses. *Geostandards newsletter* 1995, **19**(1)**:** 1-23.

54. Black LP, Kamo SL, Allen CM, Aleinikoff JN, Davis DW, Korsch RJ*, et al.* TEMORA 1: a new zircon standard for Phanerozoic U–Pb geochronology. *Chemical geology* 2003, **200**(1-2)**:** 155-170.

55. Kennedy AK, Wotzlaw J-F, Schaltegger U, Crowley JL, Schmitz M. Eocene zircon reference material for microanalysis of U-Th-Pb isotopes and trace elements. *The Canadian Mineralogist* 2014, **52**(3)**:** 409-421.

56. von Quadt A, Wotzlaw J-F, Buret Y, Large SJ, Peytcheva I, Trinquier A. High-precision zircon U/Pb geochronology by ID-TIMS using new 10 13 ohm resistors. *Journal of Analytical Atomic Spectrometry* 2016, **31**(3)**:** 658-665.

57. Petrus JA, Kamber BS. VizualAge: A novel approach to laser ablation ICP-MS U-Pb geochronology data reduction. *Geostandards and Geoanalytical Research* 2012, **36**(3)**:** 247-270.

58. Mattinson JM. Zircon U–Pb chemical abrasion ("CA-TIMS") method: combined annealing and multi-step partial dissolution analysis for improved precision and accuracy of zircon ages. *Chemical Geology* 2005, **220**(1)**:** 47-66.

59. Condon D, Schoene B, McLean N, Bowring S, Parrish R. Metrology and traceability of U–Pb isotope dilution geochronology (EARTHTIME Tracer Calibration Part I). *Geochimica et Cosmochimica Acta* 2015, **164:** 464-480.

60. McLean NM, Condon DJ, Schoene B, Bowring SA. Evaluating uncertainties in the calibration of isotopic reference materials and multi-element isotopic tracers (EARTHTIME Tracer Calibration Part II). *Geochimica et Cosmochimica Acta* 2015, **164:** 481-501.

61. Krogh T. A low-contamination method for hydrothermal decomposition of zircon and extraction of U and Pb for isotopic age determinations. *Geochimica et Cosmochimica Acta* 1973, **37**(3)**:** 485-494.

62. Gerstenberger H, Haase G. A highly effective emitter substance for mass spectrometric Pb isotope ratio determinations. *Chemical geology* 1997, **136**(3-4)**:** 309-312.

63. Wotzlaw J-F, Buret Y, Large SJ, Szymanowski D, von Quadt A. ID-TIMS U–Pb geochronology at the 0.1‰ level using 10 13 Ω resistors and simultaneous U and 18 O/16 O isotope ratio determination for accurate UO 2 interference correction. *Journal of Analytical Atomic Spectrometry* 2017, **32**(3)**:** 579-586.

64. Hiess J, Condon DJ, McLean N, Noble SR. 238U/235U systematics in terrestrial uranium-bearing minerals. *Science* 2012, **335**(6076)**:** 1610-1614.

65. Bowring JF, McLean NM, Bowring S. Engineering cyber infrastructure for U-Pb geochronology: Tripoli and U-Pb_Redux. *Geochemistry, Geophysics, Geosystems* 2011, **12**(6).

66. McLean NM, Bowring JF, Bowring S. An algorithm for U-Pb isotope dilution data reduction and uncertainty propagation. *Geochemistry, Geophysics, Geosystems* 2011, **12**(6).

67. Jaffey A, Flynn K, Glendenin L, Bentley Wt, Essling A. Precision measurement of half-lives and specific activities of U 235 and U 238. *Physical Review C* 1971, **4**(5)**:** 1889.

68. Schärer U. The effect of initial 230 Th disequilibrium on young U Pb ages: The Makalu case, Himalaya. *Earth and Planetary Science Letters* 1984, **67**(2)**:** 191-204.

69. Rubatto D, Hermann J. Experimental zircon/melt and zircon/garnet trace element partitioning and implications for the geochronology of crustal rocks. *Chemical Geology* 2007, **241**(1)**:** 38-61.

70. Blackburn TJ, Olsen PE, Bowring SA, McLean NM, Kent DV, Puffer J*, et al.* Zircon U-Pb geochronology links the end-Triassic extinction with the Central Atlantic Magmatic Province. *Science* 2013, **340**(6135)**:** 941-945.

71. Rioux M, Bowring S, Kelemen P, Gordon S, Dudás F, Miller R. Rapid crustal accretion and magma assimilation in the Oman-UAE ophiolite: High precision U-Pb zircon geochronology of the gabbroic crust. *Journal of Geophysical Research: Solid Earth* 2012, **117**(B7).

72. Hayden LA, Watson EB, Wark DA. A thermobarometer for sphene (titanite). *Contributions to Mineralogy and Petrology* 2007, **155**(4)**:** 529-540.

73. Watson EB, Harrison TM. Zircon saturation revisited: temperature and composition effects in a variety of crustal magma types. *Earth and Planetary Science Letters* 1983, **64**(2)**:** 295-304.

74. Schoene B, Latkoczy C, Schaltegger U, Günther D. A new method integrating high-precision U–Pb geochronology with zircon trace element analysis (U–Pb TIMS-TEA). *Geochimica et Cosmochimica Acta* 2010, **74**(24)**:** 7144-7159.

75. Samperton KM, Schoene B, Cottle JM, Brenhin Keller C, Crowley JL, Schmitz MD. Magma emplacement, differentiation and cooling in the middle crust: Integrated zircon geochronological–geochemical constraints from the Bergell Intrusion, Central Alps. *Chemical Geology* 2015, **417:** 322-340.

76. Patankar S. *Numerical heat transfer and fluid flow*. CRC press, 1980.

77. Gualda GA, Ghiorso MS, Lemons RV, Carley TL. Rhyolite-MELTS: a modified calibration of MELTS optimized for silica-rich, fluid-bearing magmatic systems. *Journal of Petrology* 2012, **53**(5)**:** 875-890.

78. Vielzeuf D, Holloway JR. Experimental determination of the fluid-absent melting relations in the pelitic system. *Contributions to Mineralogy and Petrology* 1988, **98**(3)**:** 257-276.

79. Nandedkar RH, Ulmer P, Müntener O. Fractional crystallization of primitive, hydrous arc magmas: an experimental study at 0.7 GPa. *Contributions to Mineralogy and Petrology* 2014, **167**(6).

80. Krahulec K. Tertiary intrusion-related copper, molybdenum, and tungsten mining districts of the eastern Great Basin. New Concepts and Discoveries: Geological Society of Nevada 2015 Symposium CD; 2015; 2015. p. 219-250.

81. Voller V, Swaminathan C. ERAL Source-based method for solidification phase change. *Numerical Heat Transfer, Part B Fundamentals* 1991, **19**(2)**:** 175-189.

82. Karakas O, Dufek J. Melt evolution and residence in extending crust: Thermal modeling of the crust and crustal magmas. *Earth and Planetary Science Letters* 2015, **425:** 131-144.

Supplementary Materials for

Giant porphyry copper deposits require large magma reservoirs at the verge of eruption

S.J.E. Large, Y. Buret, J.-F. Wotzlaw, Ö. Karakas, M. Guillong, A. von Quadt, C.A. Heinrich

Correspondence to: s.large@nhm.ac.uk

Supplementary geological background

The Bingham Canyon Cu-Au-Mo deposit is one of the world's largest magmatic-hydrothermal porphyry-skarn deposits with an estimated >25 Mt of Cu, ~1000 t of Au and ~0.8 Mt Mo[1]. The deposit is located within the Oquirrh Mountains on the eastern edge of the Basin and Range province, ~30 km southwest of Salt Lake City, Utah. It is part of the Eocene Wasatch igneous belt striking east from the Basin and Range province, across the Wasatch fault into the Rocky Mountains block (Fig. 1). The deposit is centred on the sub-volcanic intrusive rocks of the Bingham stock that intruded into the (meta-) sedimentary sequence of the Pennsylvanian Oquirrh Group[2]. The Bingham stock as well as the nearby Last Chance, Settlement and Stockton stocks are dominated by equigranular monzonite. At Bingham the equigranular monzonite is succeeded by at least 5 porphyritic intrusions[3]. In this study we focused on the four most prominent igneous rock types (Fig. 1, Supplementary Fig. 1, 2: e.g. ref. 1-4: the initial, premineralisation (i) equigranular monzonite (EM); the strongly mineralised (ii) quartz monzonite porphyry (QMP); and the smaller and less mineralised (iii) latite porphyry (LP) and (iv) quartz latite porphyry (QLP).

The laterally extensive equigranular monzonite (Supplementary Fig. 2a) comprises most of the ~3 x 3 km Bingham stock and pre-dates all economic hydrothermal activity[4]. It consists of plagioclase, orthoclase, minor quartz and ~30 vol.% clinopyroxene and amphibole (all <3 mm[5]). The strongly Cu-Au mineralised, veined and potassically altered quartz monzonite porphyry (Supplementary Fig. 2b) is the largest porphyritic intrusion at Bingham Canyon. The dike-like body has an average width of ~350 m, strikes roughly northeast, dips 60° to the northwest and intruded along the contact of the equigranular monzonite and the host quartzites (Supplementary Fig. 1). The quartz monzonite porphyry contains 40 – 60 vol.% medium- to coarse-grained phenocrysts of plagioclase, orthoclase, hornblende, biotite and rare quartz eyes that are hosted in an aplitic groundmass. It has long been identified as the igneous body spatially and temporally related to the Cu-Au ore formation event[2,3]. Several thin (10 - 80 m) dikes of latite porphyry (Supplementary Fig. 2c) strike northeast extending over ~3km, mainly along the northern margin of the quartz monzonite porphyry (Supplementary Fig. 1). Compositionally the latite porphyry is very similar to the quartz monzonite porphyry. Dikes of the quartz latite porphyry (Supplementary Fig. 2d) range from <10 – 50 m in width and dominantly strike north-east with some north-westerly striking apophyses. The quartz latite porphyry contains 30 – 40 vol. % phenocrysts and is characterised by abundant quartz eyes (3 – 7 vol. %: 21) with otherwise similar phenocryst proportions as the quartz monzonite porphyry and the latite porphyry but with.

Geophysical anomalies and abundant volcanic sequences indicate that the rocks of the Bingham stock are part of a vertically extensive Eocene magmatic system. A WSW-ENE striking positive aeromagnetic anomaly suggests a large batholith underlying the Wasatch igneous belt[6]. By combining geophysical observations with thermal constraints and mass balance calculations[7] depicted the igneous body underlying the Oquirrh Mountains to be 2 – 3.5 km thick, to lie 2 – 3.5 km below today's surface and to range between 1400 and 4000 km3 in volume. Volcanic rocks exposed on the eastern flank of the Oquirrh Mountains were deposited roughly contemporaneously with the injection of the intrusive stocks[8] and are considered to have a co-magmatic origin[6,8].

A clear correlation between Cu-Au grades and intensity of potassic alteration and veining intensity was identified early[1-3]. Ref. 1 reports no systematic difference in Cu- and Au grades between the different lithologies, whereas ref. 3 conclude that ore grades can be truncated abruptly at later intrusive contacts. They argue that older grade-maps were

smoothed along intrusive contacts (e.g. Supplementary Fig. 1a, b) and detailed mapping demonstrated a lithological control on ore grades (Supplementary Fig. 1d) as well as on vein and alteration intensities. It is estimated that >90% of quartz stockwork veins within the quartz monzonite porphyry are truncated by the later latite porphyry suggesting that the majority of Cu-Au mineralisation occurred between emplacement of the quartz monzonite porphyry and the latite porphyry. Sporadically, Cu-Fe-sulphide bearing veins (<10 %) crosscut the contact of the two porphyries indicating that only minor (<10%) Cu-Au mineralisation was associated with the emplacement of the latite porphyry. In turn the younger quartz latite porphyry that only contains a fractional amount of stockwork veinlets and Cu-Au mineralisation truncates stockwork veins within the latite porphyry. The overall quartz vein content within the porphyries decreases systematically from 5 -15 % in the quartz monzonite porphyry to <1 % in the quartz latite porphyry. There is also a systematic shift from relatively high bornite and digenite to chalcopyrite ratios in the quartz monzonite porphyry to a strongly chalcopyrite dominated Cu-sulphide suite in the latite porphyry and quartz latite porphyry[3]. In summary, crosscutting relationships and abrupt changes in alteration and Cu-Au grades indicate that the amount of introduced Cu and Au decreased with each intrusive-hydrothermal cycle[3].

References:

1. Porter J, Schroeder K, Austin G. Geology of the Bingham Canyon porphyry Cu-Mo-Au deposit, Utah. *Econ Geol Spec Publ* 2012, **16:** 127-146.
2. Lanier G, John E, Swensen A, Reid J, Bard C, Caddey S*, et al.* General geology of the Bingham mine, Bingham canyon, Utah. *Economic Geology* 1978, **73**(7)**:** 1228-1241.
3. Redmond PB, Einaudi MT. The Bingham Canyon porphyry Cu-Mo-Au deposit. I. Sequence of intrusions, vein formation, and sulfide deposition. *Economic Geology* 2010, **105**(1)**:** 43-68.
4. Babcock Jr R, Ballantyne G, Phillips C. Summary of the geology of the Bingham district, Utah. *Porphyry copper deposits of the American Cordillera: Arizona Geological Society Digest* 1995, **20:** 316-335.
5. Moore WJ. Igneous rocks in Bingham mining district, Utah: US Govt. Print. Off.; 1973. Report No.: 2330-7102.
6. Waite KA, Keith JD, Christiansen EH, Whitney JA, Hattori K, Tingey DG*, et al.* Petrogenesis of the volcanic and intrusive rocks associated with the Bingham Canyon porphyry Cu-Au-Mo deposit, Utah. *Soc Econ Geol Guidebook Ser* 1997, **29:** 91-128.
7. Steinberger I, Hinks D, Driesner T, Heinrich CA. Source plutons driving porphyry copper ore formation: combining geomagnetic data, thermal constraints, and chemical mass balance to quantify the magma chamber beneath the Bingham Canyon deposit. *Economic Geology* 2013, **108**(4)**:** 605-624.
8. Maughan D, Keith J, Christiansen E, Pulsipher T, Hattori K, Evans N. Contributions from mafic alkaline magmas to the Bingham porphyry Cu-Au-Mo deposit, Utah, USA. *Mineralium Deposita* 2002, **37**(1)**:** 14-37.
9. Bachmann O, Dungan MA, Bussy F. Insights into shallow magmatic processes in large silicic magma bodies: the trace element record in the Fish Canyon magma body, Colorado. *Contributions to Mineralogy and Petrology* 2005, **149**(3)**:** 338-349.
10. Colombini LL, Miller CF, Gualda GAR, Wooden JL, Miller JS. Sphene and zircon in the Highland Range volcanic sequence (Miocene, southern Nevada, USA): elemental partitioning, phase relations, and influence on evolution of silicic magma. *Mineralogy and*

Petrology 2011, **102**(1-4)**:** 29-50.
11. Ferry JM, Watson EB. New thermodynamic models and revised calibrations for the Ti-in-zircon and Zr-in-rutile thermometers. *Contributions to Mineralogy and Petrology* 2007, **154**(4)**:** 429-437.
12. Hayden LA, Watson EB, Wark DA. A thermobarometer for sphene (titanite). *Contributions to Mineralogy and Petrology* 2007, **155**(4)**:** 529-540.
13. Grondahl C, Zajacz Z. Magmatic controls on the genesis of porphyry Cu–Mo–Au deposits: The Bingham Canyon example. *Earth and Planetary Science Letters* 2017, **480:** 53-65.

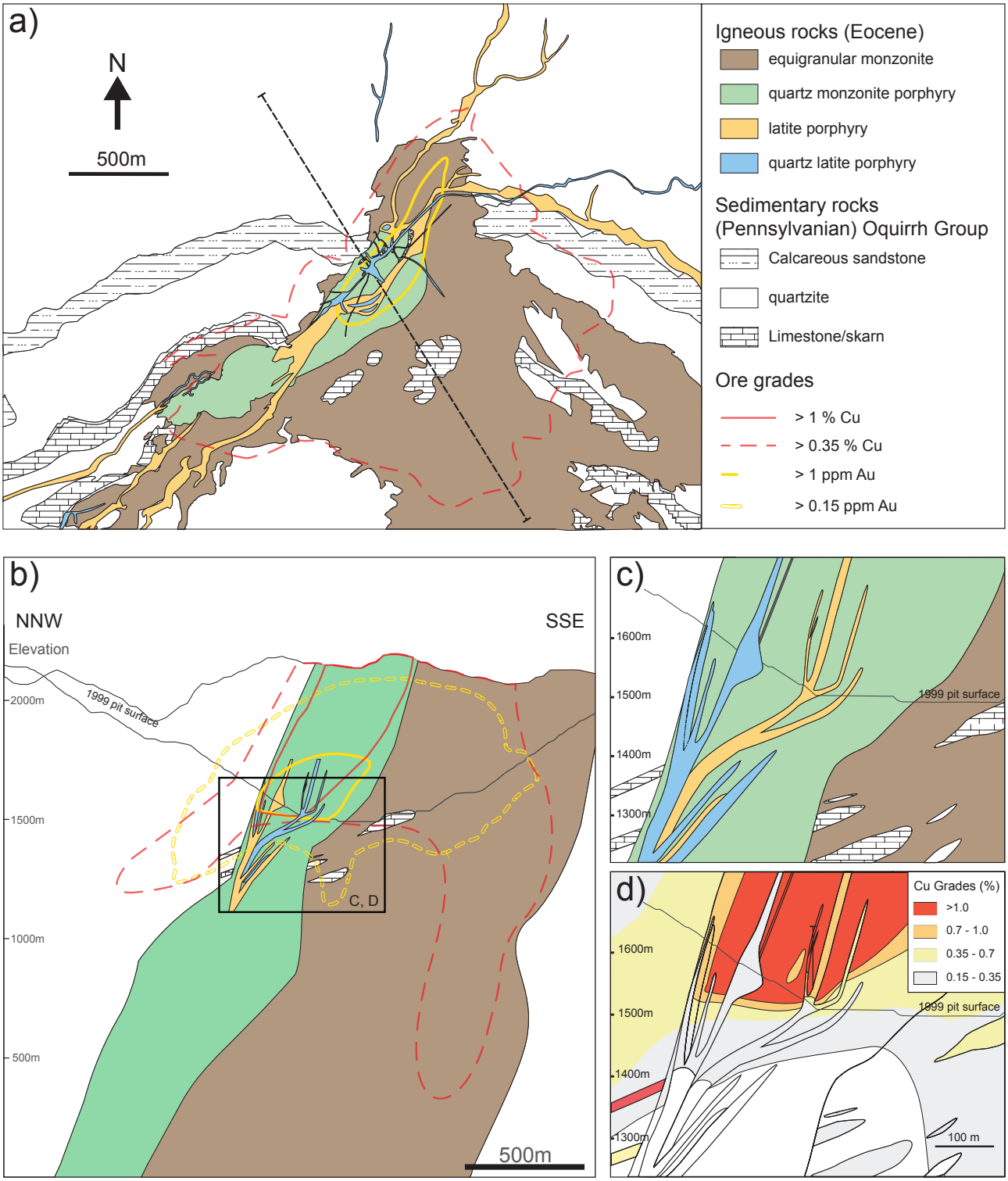

Fig. S1: Geological maps and cross-sections of the Bingham Canyon porphyry deposit. **a,** Geological map of the mine area. Northeast elongated porphyry stocks and dikes intruded into the equigranular monzonite and the sedimentary rock sequence. 0.35% Cu and 1 ppm Au contours are centred on the quartz monzonite porphyry. **b,** Cross-section through the deposit. Note the characteristic ore shell with a barren core at depth centred on the quartz monzonite porphyry. **c,** Detailed cross-section (square in B indicates the depicted area). **d,** Grade distribution of the cross-section in **c**. Note the grade cuts at the contacts of the quartz monzonite porphyry to the latite porphyry and quartz latite porphyry. **a,** – **c,** have the same legend. Legend for **c** in the small inset. Maps and cross-sections modified from ref. 3.

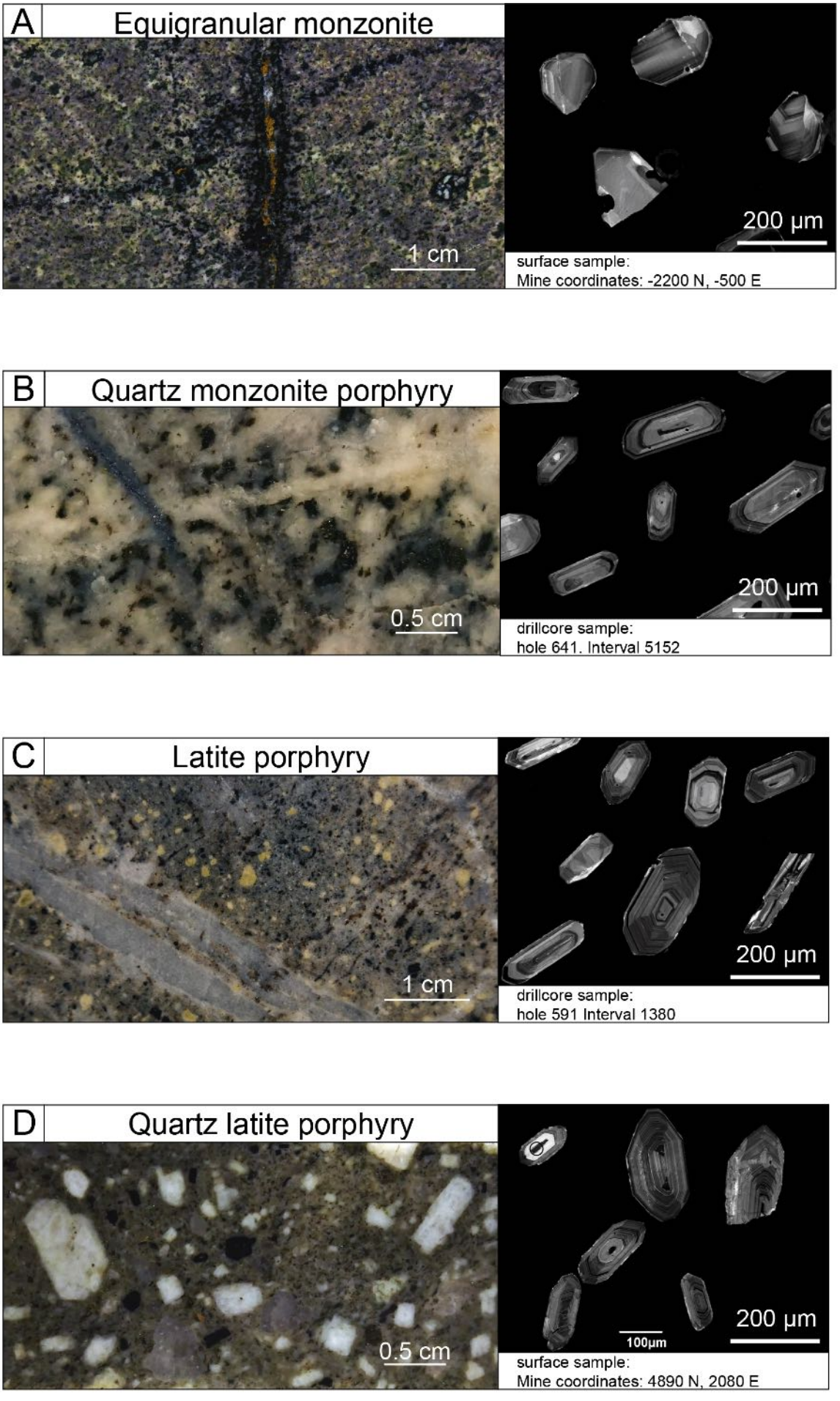

Fig. S2: Analysed samples with selected Cathodoluminescence images and sample locations.

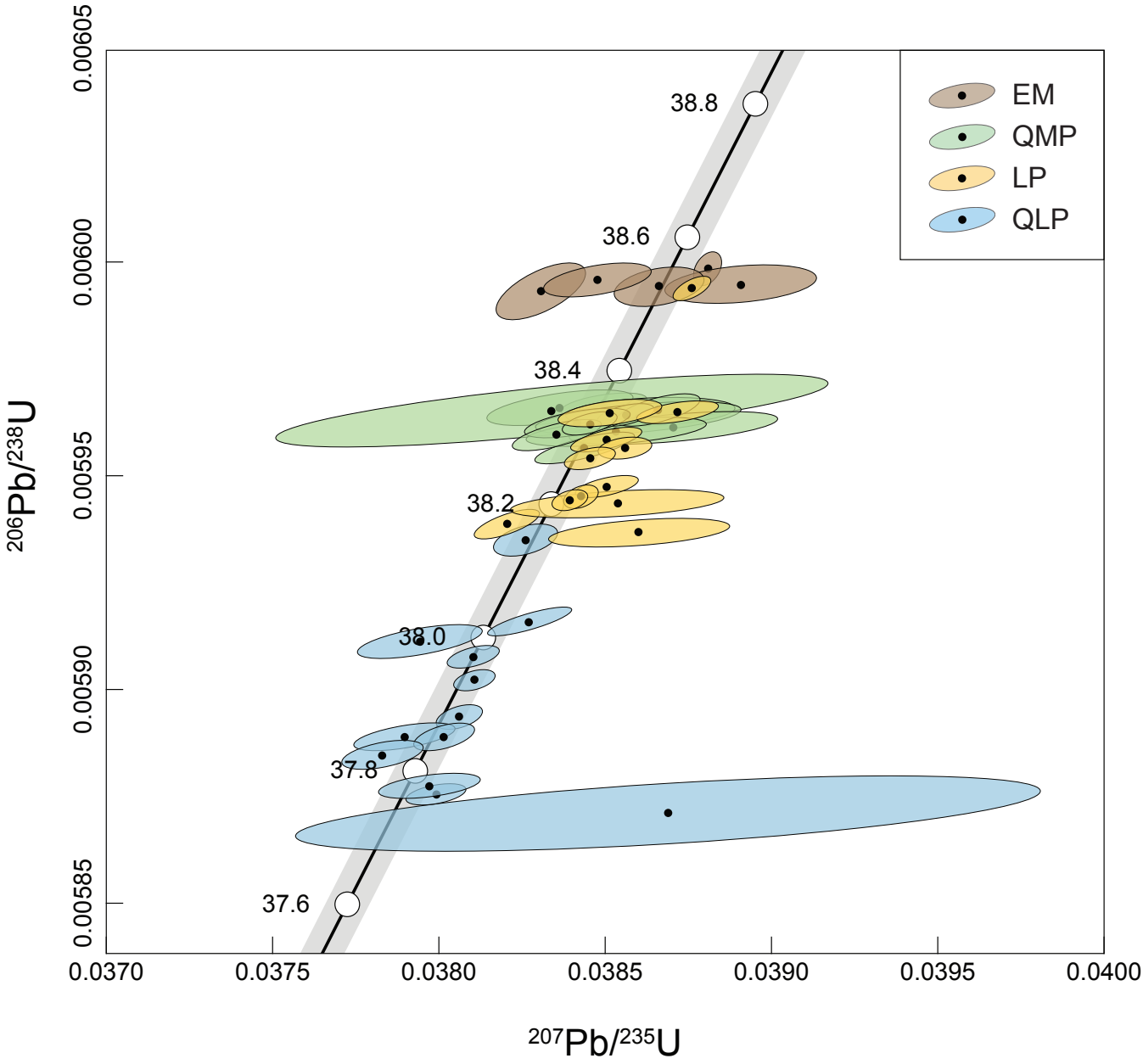

Fig. S3: Concordia diagram for Bingham Canyon zircons dated by ID–TIMS (full data presented in Supplementary Table 1).

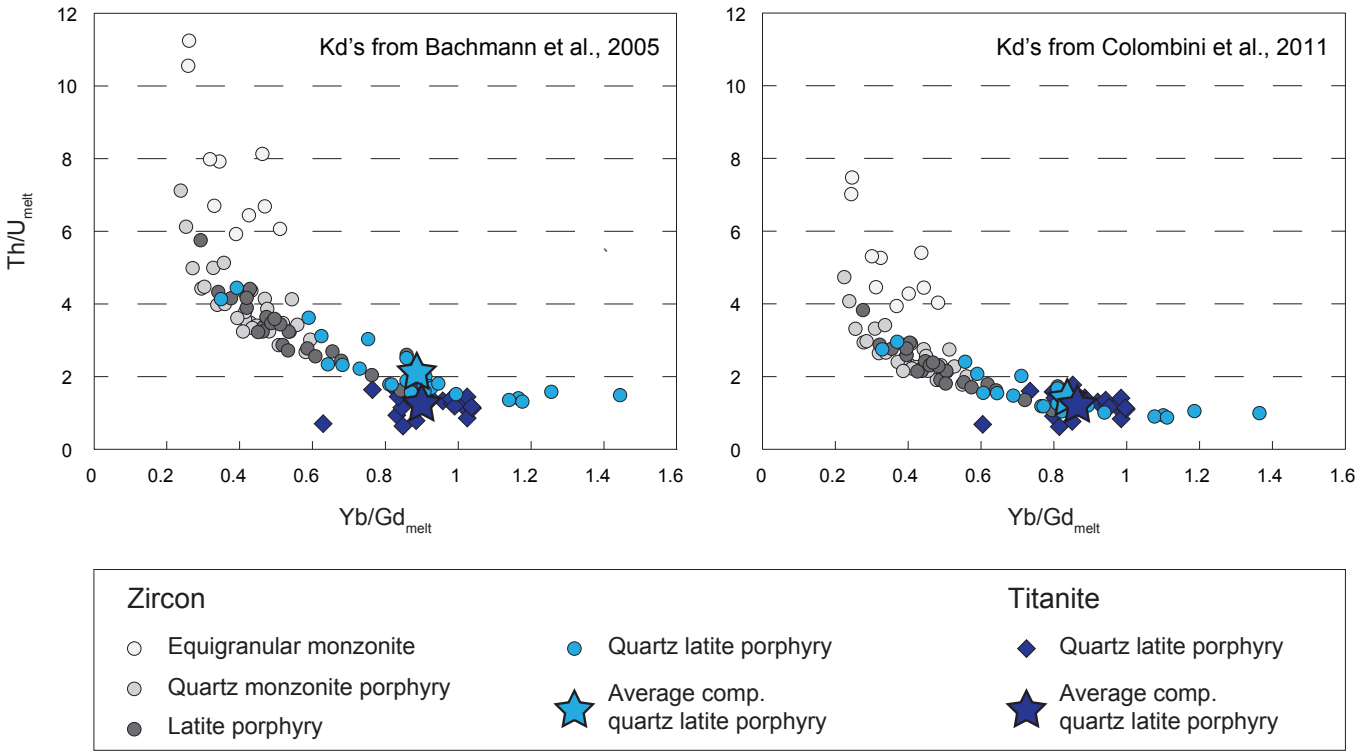

Fig. S4: Comparison of backcalulated melt compositions based on zircon and titanite geochemistry using partition coefficients by ref. 9 and ref. 10. Stars indicate averaged compositions of zircons and titanites. Partition coefficients of ref. 10 result in excellent overlap of the melt composition calculated from titanites and zircons from the QLP. This is in agreement with co-crystallisation of zircon and titanite in the same melt.

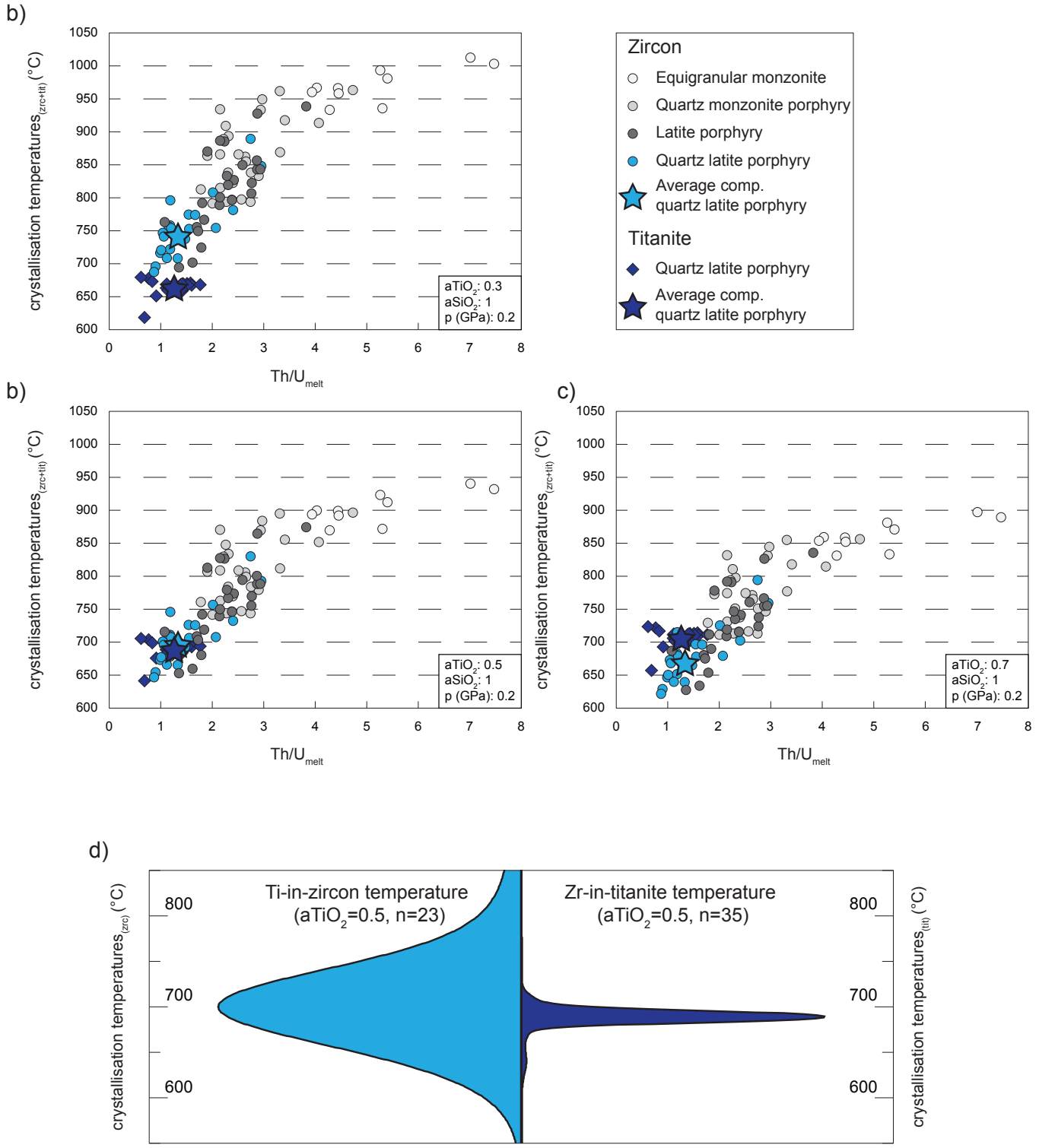

Fig. S5: Diagrams illustrating the sensitivity of Ti in zircon and Zr in titanite thermometry (calculated using calibrations from ref. 11 and ref. 12) on changing TiO_2 activities ($aTiO_2$). Absolute values vary but general crystallisation trend is not disturbed by differing $aTiO_2$. Based on co-crystallisation of zircon and titanite an $aTiO_2$ of 0.5 is the preferred value (**b, c**) and applied in this study.

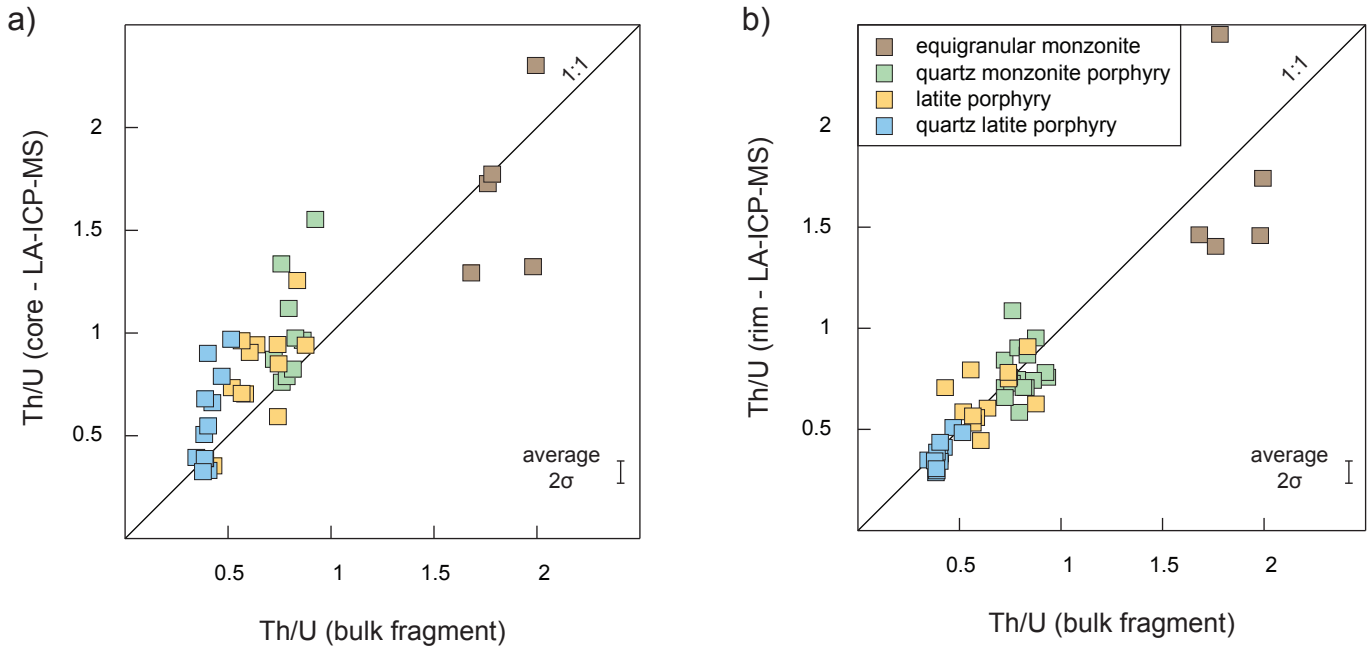

Fig. S6: Comparison of Th/U ratios obtained by CA-ID-TIMS analysis, from the same volume of zircon as high-precision crystallisation ages with Th/U ratios obtained by in-situ analysis on the same grain. A: Core analysis by LA-ICP-MS plotted against bulk fragment analysis. B: Rim analysis by LA-ICP-MS plotted against bulk fragment analysis. Bulk fragment and spatially resolved analyses of the rims display an excellent correlation.

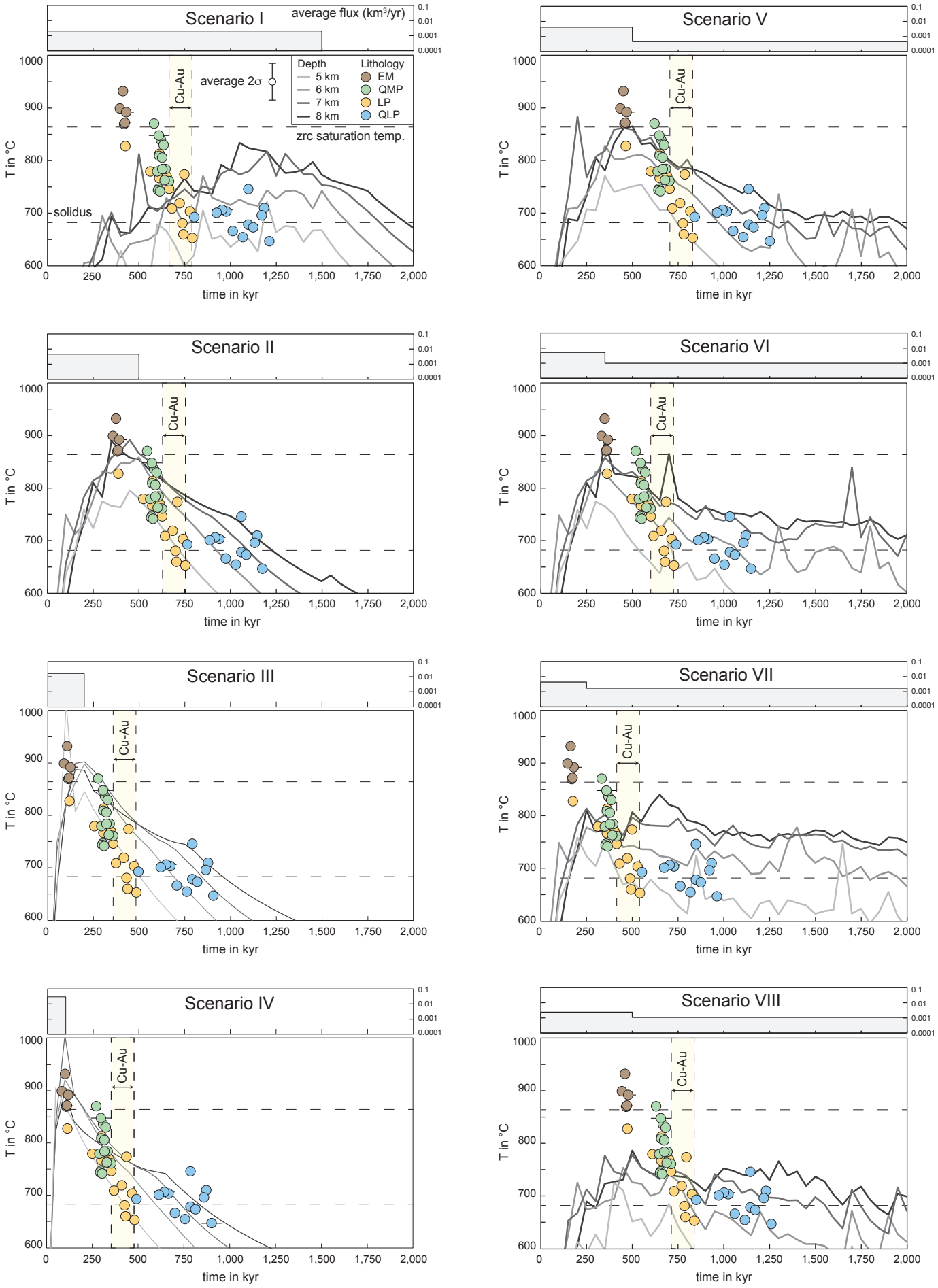

Fig. S7: Results of all thermal models run in this study in comparison with analytical zircon data. Averaged fluxes are illustrated at the top of each diagram.

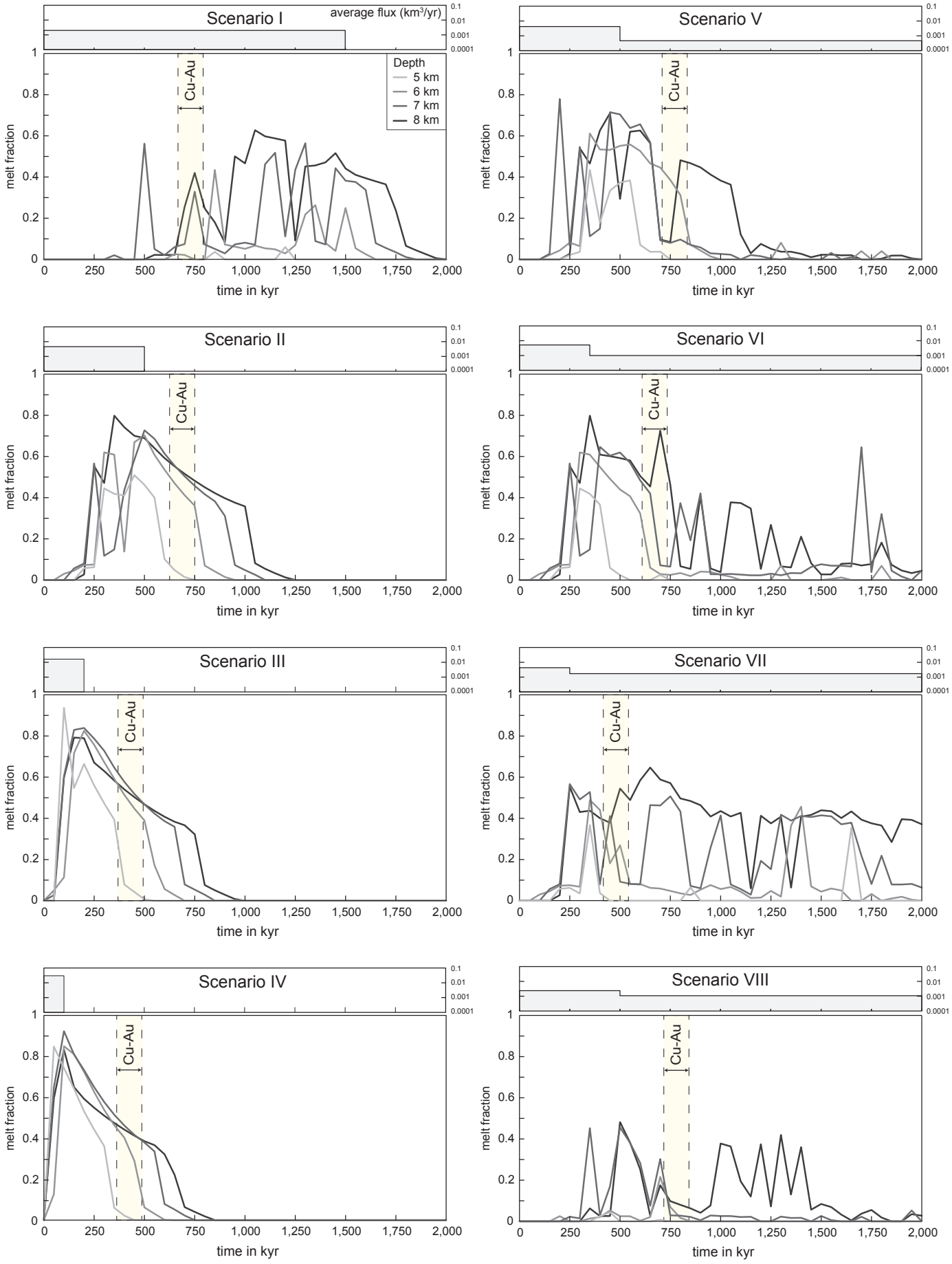

Fig. S8: Evolution of melt fractions at different depths within the modelled magma reservoir as provided by the thermal models. Illustrated events correspond to timing in Fig. S7.

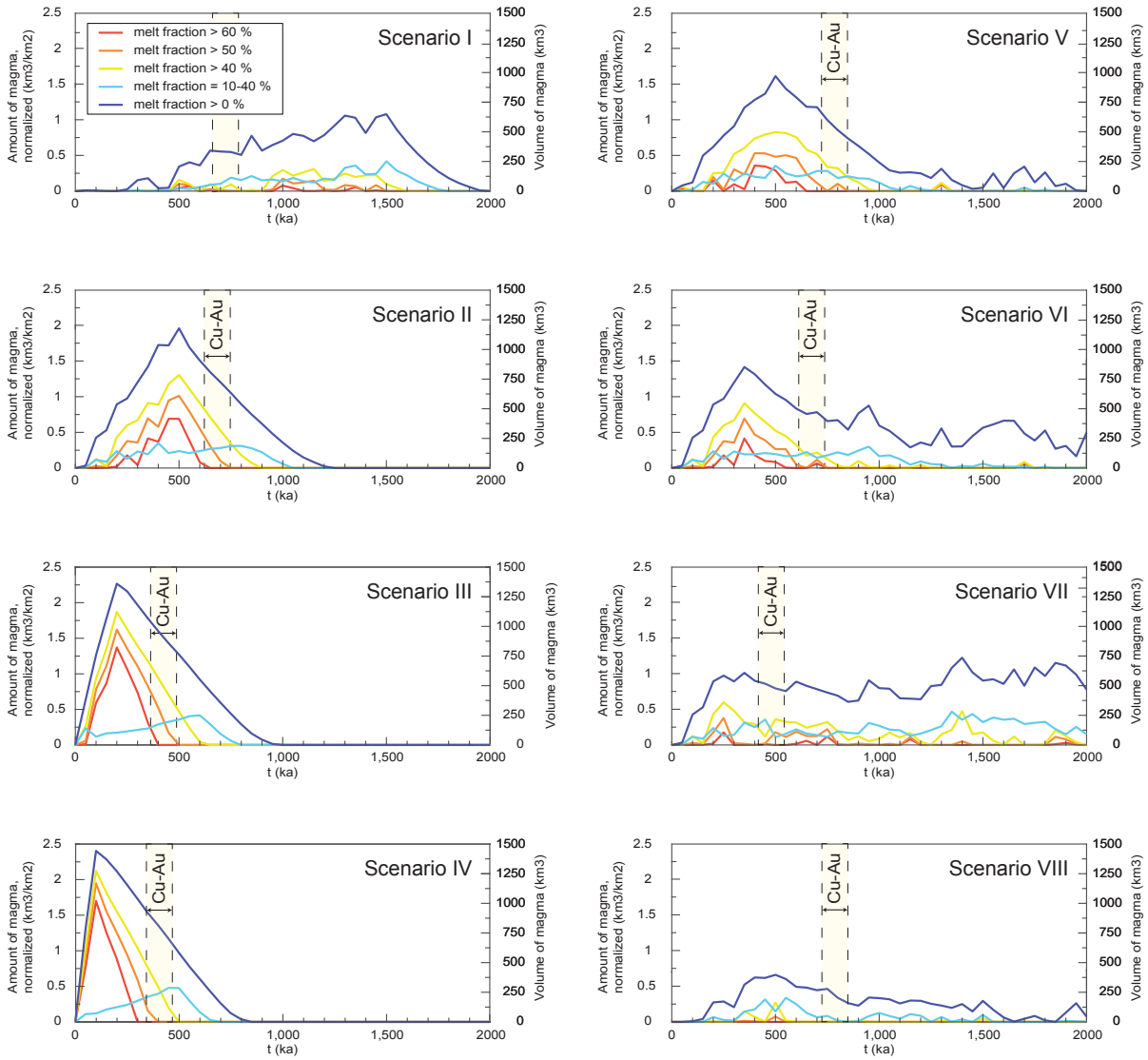

Fig. S9: Evolution of melt fractions within the whole modelled magma reservoir as provided by the thermal models. Illustrated events correspond to timing in Fig. S7.

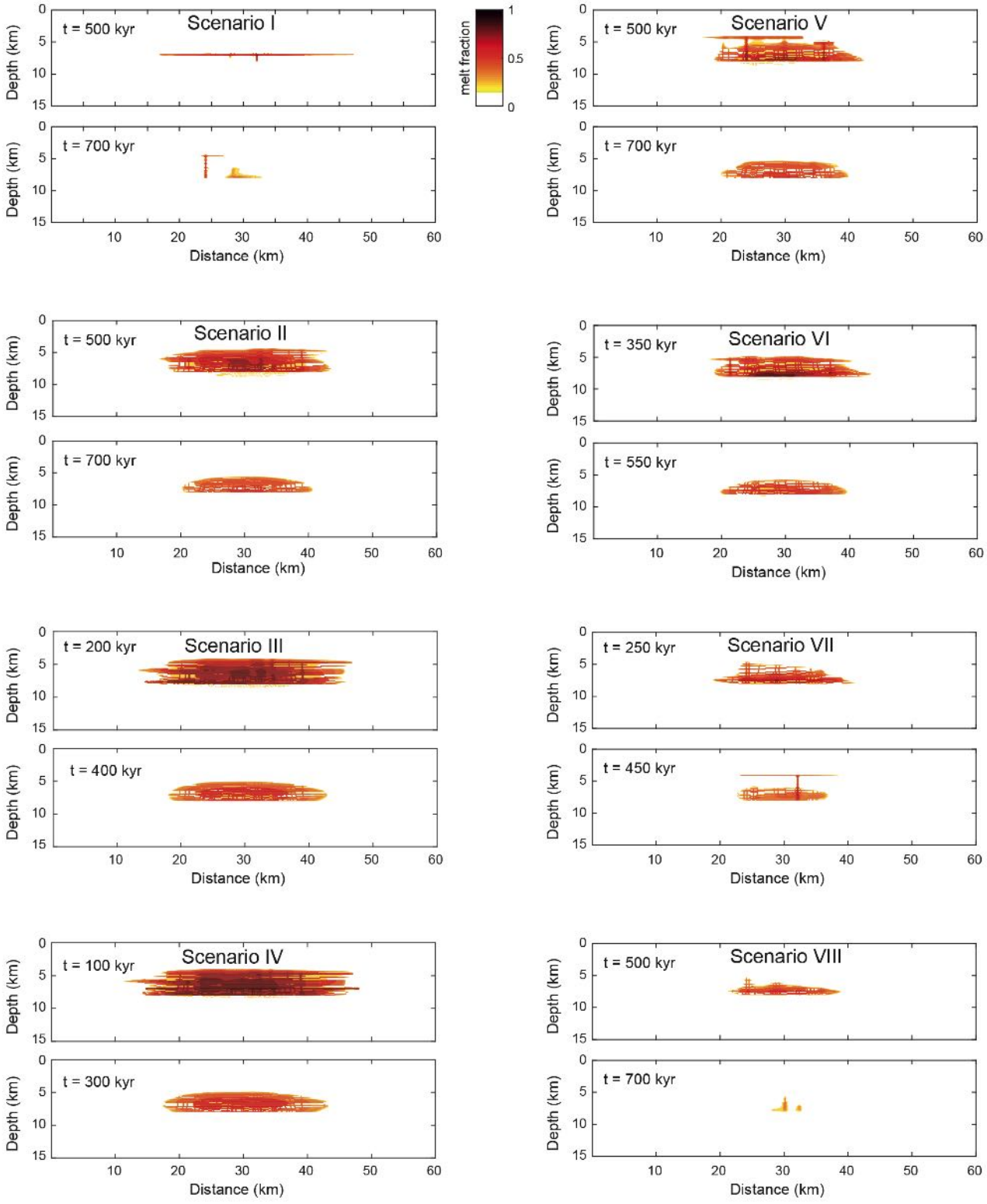

Fig. S10: Melt distribution within the crust at the time of stop/reduction of recharge and inferred time of ore formation for all modelled scenarios. Timing of ore formation is based on correlation of zircon data and thermal model (Fig. S7). Illustrated domains contain melt fractions >0.1. Melt-rich domains at the time of ore formation in Scenarios II-IV are sufficiently sized to provide all Cu, S and Cl at Bingham Canyon based on mass-balance calculations of ref. 7 and ref. 13. The different Scenarios illustrate that high-flux models result in the accumulation of larger melt-rich domains.

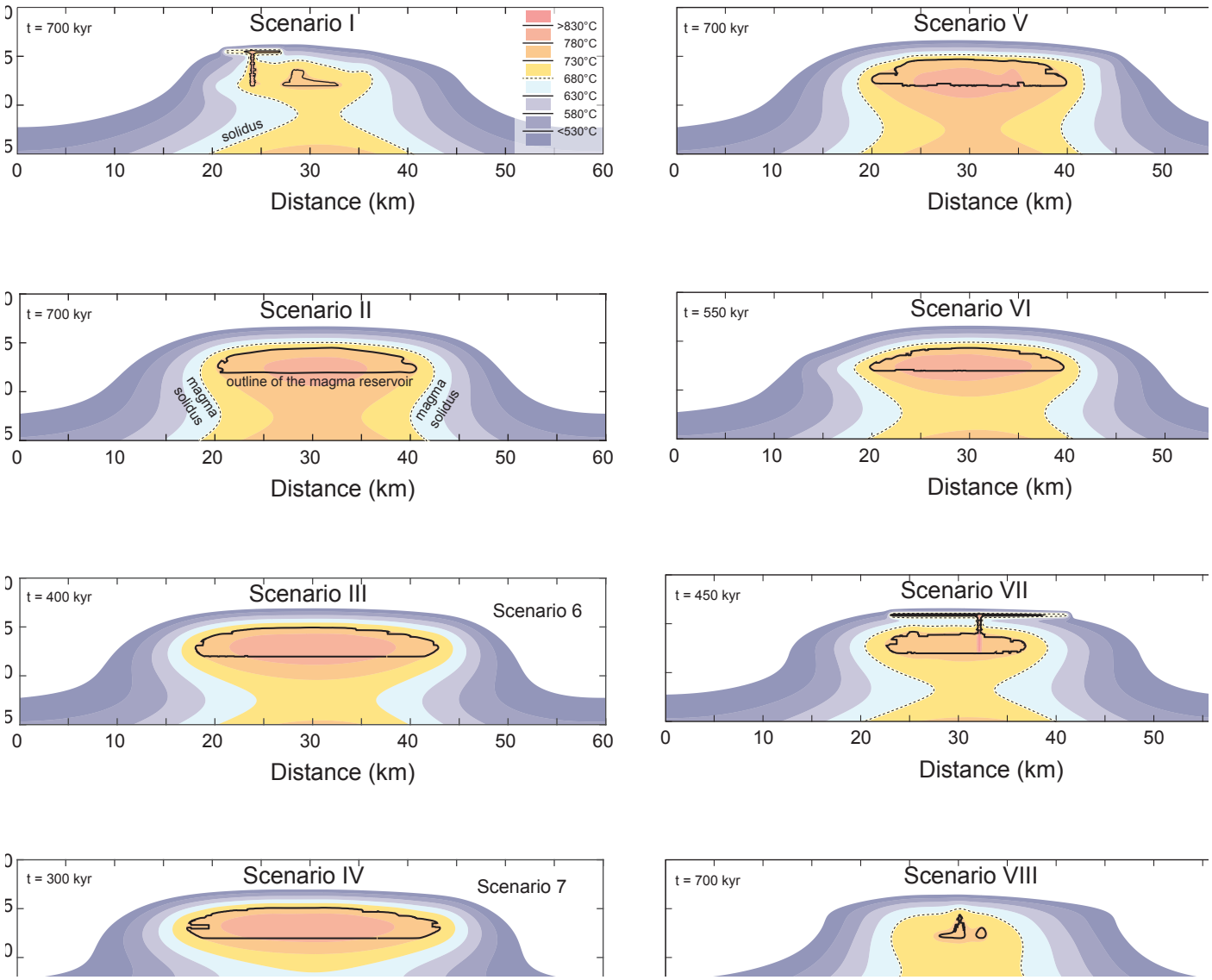

Fig. S11: Thermal state of the upper crust of all Scenarios at the time of inferred ore formation. Outline of domain with melt-fractions of dominantly >0.1. Thin sills and dikes in Scenario IV and VI are the result of a recently intruded dike.

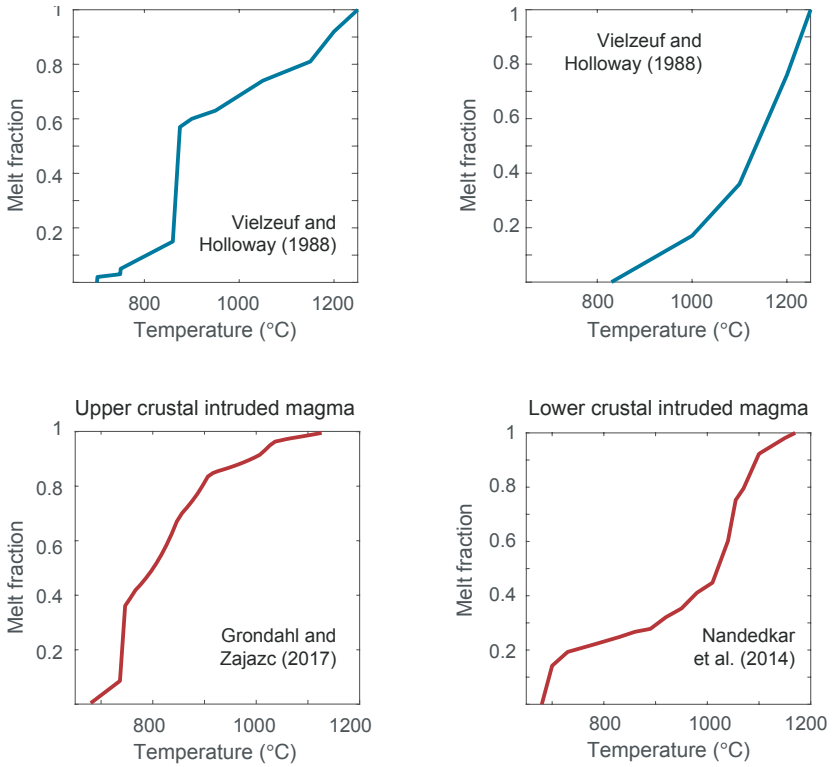

Fig. S12: Temperature-melt fraction relationships of the host-lithologies and injected magma in the upper- and lower-crustal domains used in the thermal model.

Table S1.

CA-ID-TIMS zircon geochronology

Bingham Canyon

Sample	Composition				Isotopic Ratios								Dates (Ma)					
	Th/U[1]	Pb* (pg)[2]	Pbc (pg)[3]	Pb*/ Pb_c[4]	$^{206}Pb/^{204}Pb$[5]	$^{206}Pb/^{238}U$[6]	±2σ (%)	$^{207}Pb/^{235}U$[6]	±2σ (%)	$^{207}Pb/^{206}Pb$[6]	±2σ (%)	Corr. coef.	$^{206}Pb/^{238}U<Th>$[7]	±2σ (abs)	$^{20}7Pb/^{235}U$[8]	±2σ (abs)	$^{207}Pb/^{206}Pb$[8]	±2σ (abs)
Equigranular Monzonite																		
EM_z02	1.69	31.03	0.19	166.76	7564	0.0059834	0.100	0.03831	0.35	0.04646	0.29	0.705	38.519	0.043	38.17	0.13	20.5	6.9
EM_z11	1.99	70.89	0.12	569.10	24281	0.0059899	0.035	0.03881	0.11	0.04702	0.08	0.726	38.553	0.025	38.66	0.04	49.0	2.0
EM_z28	1.77	48.97	1.48	33.07	1490	0.0059854	0.056	0.03891	0.59	0.04717	0.56	0.427	38.530	0.029	38.76	0.22	56.9	13.4
EM_z34	2.00	18.94	0.23	83.94	3588	0.0059858	0.052	0.03867	0.35	0.04687	0.32	0.510	38.526	0.030	38.52	0.13	41.6	7.8
EM_z41	1.79	10.89	0.17	62.27	2779	0.0059864	0.043	0.03848	0.42	0.04664	0.39	0.770	38.536	0.025	38.34	0.16	29.8	9.3
Quartz Monzonite Porphyry																		
QMP_z10_m2	0.73	18.94	0.20	94.60	5329	0.0059515	0.034	0.03857	0.22	0.04702	0.20	0.680	38.334	0.017	38.42	0.08	49.1	4.8
QMP_z9_m2	0.79	11.58	0.10	120.76	6690	0.0059496	0.036	0.03846	0.21	0.04690	0.19	0.682	38.321	0.017	38.32	0.08	43.2	4.5
QMP_z16	0.94	14.51	0.19	75.81	4062	0.0059468	0.054	0.03836	0.35	0.04680	0.31	0.779	38.303	0.023	38.22	0.13	38.1	7.4
QMP_z16_m2	0.88	7.48	0.09	81.44	4422	0.0059539	0.036	0.03850	0.33	0.04692	0.31	0.656	38.349	0.018	38.36	0.13	44.1	7.4
QMP_z21_m2	0.84	5.33	0.09	57.75	3173	0.0059496	0.051	0.03842	0.41	0.04686	0.38	0.685	38.322	0.022	38.28	0.16	40.8	9.1
QMP_z24	0.77	4.72	0.23	20.63	1165	0.0059508	0.059	0.03860	0.80	0.04707	0.77	0.583	38.329	0.025	38.46	0.30	51.8	18.3
QMP_z45	0.93	18.70	0.26	72.85	3912	0.0059527	0.057	0.03866	0.32	0.04713	0.29	0.716	38.341	0.024	38.52	0.12	54.7	6.8
QMP_z47[oc]	0.73	7.43	0.31	23.86	1358	0.0059522	0.049	0.03864	0.66	0.04710	0.64	0.301	38.338	0.022	38.50	0.25	53.4	15.4
QMP_z58[oc]	0.80	11.86	0.17	70.30	3896	0.0059438	0.055	0.03844	0.39	0.04693	0.34	0.853	38.284	0.024	38.30	0.15	44.6	8.2
QMP_z60	0.87	1.44	0.12	12.24	683	0.0059525	0.141	0.03834	2.17	0.04674	2.06	0.766	38.340	0.055	38.21	0.81	34.9	49.3
QMP_z63[oc]	0.82	5.59	0.23	24.45	1360	0.0059476	0.050	0.03854	0.70	0.04702	0.67	0.600	38.308	0.022	38.40	0.26	48.9	16.1
QMP_z74	0.79	4.60	0.14	33.54	1872	0.0059532	0.064	0.03837	0.57	0.04676	0.53	0.631	38.344	0.027	38.23	0.21	36.2	12.8
QMP_z78[oc]	0.76	3.46	0.15	22.79	1287	0.0059485	0.058	0.03871	0.81	0.04722	0.77	0.624	38.314	0.025	38.56	0.31	59.2	18.5
QMP_z83[oc]	0.83	6.53	0.27	24.19	1342	0.0059565	0.051	0.03876	0.68	0.04722	0.65	0.540	38.366	0.022	38.62	0.26	59.3	15.6
Latite Porphyry																		
LP_z2	0.52	85.90	0.62	138.69	8231	0.0059324	0.036	0.03843	0.13	0.04701	0.12	0.494	38.211	0.018	38.29	0.05	48.5	2.9
LP_z5	0.43	41.36	0.25	165.56	10061	0.0059811	0.039	0.03877	0.14	0.04703	0.11	0.784	38.523	0.018	38.62	0.05	49.6	2.8
LP_z6[oc]	0.64	14.36	0.17	82.96	4779	0.0059348	0.033	0.03851	0.24	0.04708	0.22	0.782	38.226	0.017	38.37	0.09	52.3	5.3
LP_z7[oc]	0.56	4.58	0.27	17.27	1031	0.0059308	0.048	0.03854	0.83	0.04715	0.81	0.506	38.201	0.021	38.40	0.31	55.9	19.3
LP_z23[oc]	0.88	6.91	0.13	51.76	2816	0.0059520	0.046	0.03852	0.40	0.04696	0.38	0.575	38.336	0.021	38.38	0.15	46.0	9.1
LP_z24	0.58	23.13	0.25	93.11	5440	0.0059414	0.034	0.03846	0.20	0.04697	0.18	0.594	38.268	0.017	38.32	0.07	46.5	4.3
LP_z25[oc]	0.75	7.34	0.12	62.46	3504	0.0059522	0.035	0.03872	0.32	0.04720	0.29	0.689	38.338	0.017	38.58	0.12	58.5	7.0
LP_z43	0.61	12.24	0.58	21.10	1239	0.0059240	0.049	0.03861	0.70	0.04729	0.68	0.525	38.157	0.021	38.46	0.27	62.7	16.2
LP_z79	0.57	27.23	0.09	299.22	17517	0.0059316	0.030	0.03840	0.14	0.04697	0.12	0.499	38.206	0.016	38.26	0.05	46.7	3.0
LP_z83	0.74	9.60	0.16	59.40	3338	0.0059599	0.039	0.03865	0.35	0.04706	0.32	0.672	38.387	0.019	38.51	0.13	51.0	7.7
LP_z88	0.57	11.45	0.07	164.55	9642	0.0059260	0.051	0.03821	0.26	0.04678	0.21	0.821	38.170	0.022	38.07	0.10	37.1	5.2
LP_z96	0.74	11.38	0.07	162.96	9129	0.0059438	0.033	0.03856	0.21	0.04708	0.20	0.379	38.284	0.016	38.42	0.08	52.1	4.7
LP_z99	0.84	9.21	0.08	112.27	6149	0.0059458	0.040	0.03851	0.28	0.04699	0.24	0.800	38.297	0.019	38.37	0.10	47.8	5.9

Bingham Canyon

Sample	Composition				Isotopic Ratios								Dates (Ma)					
	Th/U[1]	Pb* (pg)[2]	Pbc (pg)[3]	Pb*/ Pb_c[4]	$^{206}Pb/^{204}Pb$[5]	$^{206}Pb/^{238}U$[6]	±2σ (%)	$^{207}Pb/^{235}U$[6]	±2σ (%)	$^{207}Pb/^{206}Pb$[6]	±2σ (%)	Corr. coef.	$^{206}Pb/^{238}U<Th>$[7]	±2σ (abs)	$^{20}7Pb/^{235}U$[8]	±2σ (abs)	$^{207}Pb/^{206}Pb$[8]	±2σ (abs)
Quartz Latite Porphyry																		
QLP_z2[oc]	0.41	11.77	0.16	75.79	4644	0.0058628	0.031	0.03800	0.24	0.04702	0.22	0.644	37.765	0.016	37.87	0.09	49.4	5.2
QLP_z5[oc]	0.41	12.34	0.09	133.76	8186	0.0059032	0.050	0.03828	0.33	0.04705	0.28	0.942	38.024	0.022	38.14	0.12	50.6	6.8
QLP_z7	0.35	6.70	0.16	41.64	2602	0.0058648	0.041	0.03798	0.40	0.04698	0.38	0.606	37.778	0.019	37.85	0.15	47.4	9.0
QLP_z11	0.42	17.00	0.16	109.04	6643	0.0058950	0.035	0.03811	0.20	0.04691	0.18	0.691	37.971	0.017	37.98	0.08	43.4	4.4
QLP_z14	0.39	20.91	0.15	139.79	8593	0.0058809	0.040	0.03807	0.18	0.04697	0.16	0.567	37.881	0.018	37.93	0.07	46.5	3.9
QLP_z15	0.52	20.67	0.26	81.03	4822	0.0059223	0.057	0.03827	0.25	0.04688	0.23	0.498	38.146	0.024	38.13	0.09	42.2	5.4
QLP_z16m2	0.39	4.79	0.09	55.22	3408	0.0058763	0.047	0.03790	0.40	0.04680	0.37	0.683	37.851	0.021	37.77	0.15	37.9	8.9
QLP_z17	0.39	19.13	0.21	91.94	5657	0.0058763	0.047	0.03802	0.24	0.04695	0.21	0.623	37.851	0.021	37.89	0.09	45.5	5.1
QLP_z24	0.39	2.59	0.52	4.96	322	0.0058583	0.149	0.03869	2.89	0.04792	2.80	0.613	37.736	0.057	38.55	1.09	94.5	66.4
QLP_z35	0.47	6.69	0.15	44.69	2701	0.0058985	0.061	0.03795	0.49	0.04668	0.45	0.690	37.994	0.025	37.82	0.18	31.8	10.9
QLP_z36m2	0.38	11.11	0.07	162.99	10047	0.0058720	0.050	0.03784	0.32	0.04675	0.29	0.581	37.824	0.022	37.71	0.12	35.5	7.1
QLP_z38	0.40	17.16	0.12	141.94	8693	0.0058895	0.031	0.03811	0.16	0.04695	0.14	0.591	37.936	0.016	37.98	0.06	45.8	3.5

[1] Th contents calculated from radiogenic ^{208}Pb and ^{230}Th-corrected $^{206}Pb/^{238}U$ date of the sample, assuming concordance between U-Pb Th-Pb systems.

[2] Total mass of radiogenic Pb.

[3] Total mass of common Pb.

[4] Ratio of radiogenic Pb (including ^{208}Pb) to common Pb.

[5] Measured ratio corrected for fractionation and spike contribution only.

[6] Measured ratios corrected for fractionation, tracer and blank.

[7] Corrected for initial Th/U disequilibrium using radiogenic ^{208}Pb and Th/U[magma] specified.

[8] Isotopic dates calculated using λ238 = 1.55125E-10 (Jaffey et al. 1971) and λ235 = 9.8485E-10 (Jaffey et al. 1971).

[oc] online oxide correction was applied for U-analyses

Table S2:
LA-ICP-MS zircon trace element analyses

LA-ICP-MS signature	Zircon domain	ID-TIMS signature	Al (ppm)	P (ppm)	Zrc cryst. temp. (°C)[1]	Ti corr (ppm)	Ti (ppm)	Sr (ppm)	Y (ppm)	Zr (ppm)	Nb (ppm)	Ba (ppm)	La (ppm)	Ce (ppm)	Pr (ppm)	Nd (ppm)	Sm (ppm)	Eu (ppm)	Gd (ppm)	Tb (ppm)	Dy (ppm)	Ho (ppm)	Er (ppm)	Tm (ppm)	Yb (ppm)	Lu (ppm)	Hf (ppm)	Ta (ppm)	Th (ppm)	U (ppm)
Equigranular Monzonite																														
EM-z10-1-1	interior		-	112	889	19.0	17.5	-	372	440,900	1.28	0.064	0.025	36	0.186	2.28	3.22	0.95	12	3.4	36	12.2	53	11	101	19	8,520	0.78	507	377
EM-z10-1-2	exterior		-	128	883	18.2	16.7	-	991	441,300	8.24	0.478	0.060	115	0.380	5.51	7.54	2.20	30	8.7	92	32.8	141	31	280	50	9,940	3.40	2,251	1,583
EM-z10-1-3	exterior		-	123	828	11.2	10.3	0.18	511	447,000	4.62	0.330	0.018	70	0.182	2.77	3.93	1.12	16	4.3	46	16.6	75	17	163	30	12,610	3.09	1,249	1,762
EM-z1-1-1	interior		-	122	890	19.2	17.6	0.18	354	438,700	1.24	0.101	0.014	36	0.165	2.58	2.99	1.02	12	3.3	33	11.8	49	11	99	18	8,240	0.74	598	407
EM-z11-1-1	interior	EM-z11	-	138	900	20.8	19.1	0.19	838	444,200	4.20	0.225	0.054	56	0.276	4.00	5.08	1.53	20	5.8	68	26.8	122	26	240	45	7,740	1.48	1,197	905
EM-z11-1-2	exterior	EM-z11	-	159	899	20.7	19.0	0.18	1,582	440,700	18.28	0.694	0.086	197	0.587	7.76	10.70	3.01	41	12.2	136	51.4	225	49	446	79	9,200	4.57	3,740	2,566
EM-z1-1-2	exterior		-	123	900	20.9	19.2	-	423	442,100	1.63	0.179	0.020	45	0.213	3.04	3.59	1.05	14	3.8	40	14.2	60	13	117	21	8,710	0.97	985	597
EM-z12-1-1	interior		-	100	885	18.5	17.0	0.18	1,389	443,700	3.23	0.252	0.251	60	1.130	13.76	15.50	3.82	54	14.5	145	47.9	193	40	346	58	10,090	1.73	1,740	997
EM-z12-1-2	exterior		-	148	900	20.8	19.1	0.28	851	443,100	7.86	0.299	0.062	95	0.444	5.24	7.26	1.58	25	7.4	78	27.9	122	26	242	42	11,090	3.46	1,788	1,338
EM-z13-1-1	interior		-	173	909	22.3	20.5	0.21	1,482	438,200	22.42	0.960	0.137	272	0.861	11.83	17.48	4.37	60	15.7	152	49.7	205	43	390	65	10,930	9.24	6,480	4,600
EM-z13-1-2	exterior		-	92	855	14.3	13.2	-	398	435,800	4.29	0.230	0.030	53	0.166	2.42	3.03	0.92	12	3.5	37	12.6	56	12	116	21	11,040	2.18	972	1,037
EM-z14-1-2	exterior		-	87	888	18.9	17.4	-	687	438,100	1.40	0.085	0.098	36	0.553	6.93	7.76	2.33	26	7.0	69	23.0	96	20	180	33	8,820	0.84	666	449
EM-z15-1-2	exterior		-	103	867	15.8	14.6	0.19	635	437,600	5.88	0.285	0.031	90	0.275	4.24	5.01	1.52	21	5.9	61	21.3	91	20	181	32	10,700	3.26	2,010	1,735
EM-z16-1-2	exterior		-	106	898	20.4	18.8	-	1,235	449,000	2.24	0.196	0.257	52	1.055	12.64	13.44	4.09	50	13.3	127	42.6	173	35	310	55	8,760	1.24	1,558	869
EM-z17-1-2	exterior		-	113	877	17.3	15.9	0.22	707	434,100	5.48	0.393	0.045	84	0.333	4.66	5.75	1.65	23	6.1	66	23.2	101	22	202	37	9,050	2.30	1,312	999
EM-z18-1-1	interior		-	65	892	19.6	18.0	0.18	674	466,000	1.20	0.157	0.126	34	0.663	8.22	8.67	2.63	28	7.1	68	22.6	93	20	173	31	8,600	0.74	673	408
EM-z18-1-2	exterior		-	108	894	19.8	18.3	-	399	451,500	2.30	0.144	0.030	47	0.239	2.79	3.58	1.06	13	3.5	36	12.9	56	12	116	20	10,290	1.53	1,036	699
EM-z20-1-1	interior		-	167	928	26.0	23.9	-	768	448,100	3.21	0.217	0.130	79	0.531	6.57	8.78	2.68	31	8.1	78	25.7	107	22	194	34	8,020	1.61	2,690	1,142
EM-z20-1-2	exterior		-	123	878	17.4	16.0	0.20	891	444,600	8.22	0.190	0.044	84	0.304	4.67	5.88	1.66	22	6.6	73	28.7	131	29	274	52	9,480	3.41	1,411	1,287
EM-z2-1-1	interior	EM-z02	-	91	894	19.8	18.2	0.14	288	440,300	1.15	-	0.010	29	0.116	1.81	2.28	0.80	9	2.6	26	9.4	40	9	81	15	8,790	0.64	386	299
EM-z2-1-2	exterior	EM-z02	-	118	892	19.5	18.0	0.21	1,030	440,100	3.94	0.188	0.127	59	0.661	7.86	9.74	2.98	36	9.3	96	34.0	144	30	275	50	8,950	1.65	1,273	871
EM-z22-1-1	interior		-	222	901	21.0	19.3	0.26	3,190	443,600	9.25	0.549	0.467	170	2.270	33.90	47.70	13.69	154	36.8	339	106.1	407	82	710	118	8,090	2.34	5,060	1,928
EM-z22-1-2	exterior		-	135	902	21.2	19.5	0.19	876	453,700	5.87	0.311	0.048	70	0.342	4.58	5.54	1.62	22	6.7	74	27.9	129	28	262	48	8,920	2.29	1,256	1,003
EM-z23-1-1	interior		-	184	947	30.0	27.6	0.25	1,251	443,400	7.23	0.412	0.195	144	0.850	11.68	16.50	4.81	56	14.0	134	42.9	170	35	308	55	7,890	2.66	3,587	1,622
EM-z23-1-2	exterior		-	145	921	24.6	22.6	0.32	1,315	443,300	3.26	0.285	0.260	77	1.186	15.18	16.96	5.10	58	14.5	140	45.0	180	36	319	56	8,170	1.47	1,970	941
EM-z26-1-1	interior		-	101	895	20.0	18.4	-	320	448,700	1.09	-	0.016	33	0.134	2.27	2.75	0.96	10	2.9	30	10.5	44	9	87	16	8,770	0.63	484	346
EM-z26-1-2	exterior		-	166	912	22.9	21.1	-	750	443,300	2.80	0.190	0.051	60	0.360	4.66	5.92	1.76	22	6.4	67	24.3	105	22	200	37	8,270	1.42	1,684	916
EM-z27-1-1	interior		-	132	839	12.4	11.4	-	498	439,400	3.90	0.250	0.041	55	0.228	3.00	4.53	1.42	18	4.7	47	16.7	70	15	149	29	9,380	3.01	1,371	1,626
EM-z27-1-2	exterior		-	170	914	23.3	21.4	0.18	801	444,000	4.07	0.298	0.072	95	0.457	5.83	7.80	2.26	30	7.9	79	26.3	108	22	202	35	9,260	2.11	3,837	1,684
EM-z28-1-1	interior	EM-z28	-	166	923	25.0	23.0	-	934	450,000	3.92	0.216	0.085	68	0.476	6.19	7.37	2.32	30	8.4	86	30.5	129	27	239	43	8,210	1.45	1,454	842
EM-z28-1-2	exterior	EM-z28	-	117	870	16.2	14.9	0.23	1,090	442,200	6.23	0.318	0.080	81	0.534	6.34	7.84	2.28	30	8.8	96	35.0	155	33	303	55	9,620	2.50	1,691	1,204
EM-z29-1-1	interior		9.1	113	899	20.7	19.0	-	401	446,000	1.26	0.149	0.028	37	0.171	2.86	3.80	1.08	13	3.8	38	13.1	55	12	109	20	8,180	0.75	883	473
EM-z29-1-2	exterior		-	123	901	21.0	19.3	0.22	468	452,000	1.70	0.165	0.039	44	0.241	3.22	4.16	1.28	16	4.3	44	15.2	66	14	128	23	8,640	0.94	744	484
EM-z34-1-1	interior	EM_z34	-	179	940	28.5	26.2	-	947	442,300	5.40	0.436	0.108	114	0.636	7.76	10.20	3.28	38	10.0	97	31.5	130	26	233	40	7,940	2.23	3,701	1,608
EM-z34-1-2	exterior	EM_z34	-	113	872	16.5	15.2	0.39	894	447,000	5.50	0.314	0.085	96	0.532	7.04	7.93	2.18	31	8.6	87	29.5	126	26	235	41	10,370	2.74	2,749	1,579
EM-z36-1-1	interior		-	106	905	21.6	19.9	0.25	949	458,100	1.51	0.195	0.237	47	1.128	13.27	14.31	4.07	43	10.5	99	32.3	130	27	241	44	7,870	0.77	942	517
EM-z36-1-2	exterior		-	133	903	21.3	19.6	0.30	577	469,000	2.48	0.187	0.059	55	0.315	3.76	4.60	1.64	19	5.4	56	18.4	79	17	160	28	8,720	1.23	973	656
EM-z37-1-1	interior		-	161	914	23.3	21.4	0.21	1,549	444,000	2.77	0.303	0.306	76	1.341	18.45	22.96	6.96	76	17.9	168	53.2	208	41	356	60	8,360	1.20	2,111	922
EM-z38-1-1	interior		-	95	875	17.0	15.6	0.21	1,158	453,700	3.13	0.162	0.145	52	0.866	10.36	12.26	3.56	45	11.9	119	39.1	162	33	298	52	9,080	1.55	1,483	903
EM-z38-1-2	exterior		-	97	892	19.5	17.9	0.31	1,293	454,900	3.22	0.258	0.181	61	1.054	13.03	15.33	4.33	53	13.7	134	43.7	178	36	326	55	10,180	1.66	1,889	1,091
EM-z4-1-1	interior		-	178	930	26.4	24.3	0.14	965	438,800	3.93	0.396	0.102	95	0.687	8.96	12.19	3.67	43	10.7	100	32.9	132	27	236	41	7,820	1.82	2,940	1,306
EM-z4-1-2	exterior		-	87	805	9.1	8.4	-	408	445,300	5.15	0.211	0.022	52	0.129	1.96	2.59	0.85	11	3.2	36	12.9	58	13	128	24	12,060	3.33	851	1,291
EM-z41-1-1	interior	EM_z41	-	173	912	22.9	21.1	0.18	1,150	451,200	6.00	0.285	0.079	84	0.416	5.33	6.63	2.21	28	8.4	99	36.2	160	34	308	57	7,710	1.96	2,301	1,298
EM-z41-1-2	exterior	EM_z41	-	186	932	26.7	24.6	0.26	1,008	449,700	4.04	0.312	0.108	91	0.632	7.95	11.32	3.76	41	10.7	103	33.3	136	28	254	46	7,520	1.75	2,984	1,217
EM-z6-1-1	interior		-	159	913	23.2	21.3	-	641	449,200	2.58	0.180	0.059	61	0.308	4.65	6.59	1.98	24	6.4	64	21.4	90	19	170	31	8,020	1.26	1,041	637
EM-z6-1-2	exterior		-	142	890	19.1	17.6	0.29	1,246	443,200	11.15	0.386	0.065	132	0.443	5.85	8.29	2.34	34	9.9	107	40.1	179	38	353	62	9,630	3.79	2,697	1,746
EM-z7-1-1	interior		-	148	928	25.9	23.8	-	797	440,900	4.81	0.284	0.085	81	0.407	5.15	7.07	2.34	27	7.2	76	26.5	110	23	211	36	8,270	1.82	1,932	1,058
EM-z7-1-2	exterior		-	104	889	19.0	17.5	-	600	442,000	4.96	0.180	0.037	51	0.296	3.66	4.66	1.37	16	4.8	52	19.0	88	20	188	34	10,140	2.42	972	955
EM-z8-1-1	interior		-	144	920	24.5	22.5	0.21	842	449,500	5.50	0.448	0.094	113	0.486	6.66	7.71	2.48	32	8.5	84	28.4	116	24	215	38	9,380	2.46	2,550	1,434
EM-z8-1-2	exterior		-	123	874	16.8	15.5	0.23	715	463,000	5.95	0.328	0.072	91	0.431	5.27	6.28	1.81	24	6.7	67	22.9	100	22	199	35	11,160	2.91	1,800	1,332
EM-z9-1-2	exterior		-	115	890	19.2	17.7	-	757	449,000	5.10	0.213	0.042	62	0.253	3.77	5.06	1.45	19	5.5	63	24.0	110	25	232	44	8,830	1.98	1,034	854
Quartz Monzonite Porphyry																														
QMP-z1-1-1	interior		-	130	727	4.1	3.7	0.14	820	451,500	3.08	0.183	0.035	52	0.169	2.67	4.47	1.85	21	6.3	71	26.2	122	27	270	56	10,710	1.23	670	1,077
QMP-z7-1-1	interior		28.4	216	941	28.6	26.3	-	538	498,000	1.26	0.176	0.035	37	0.163	3.62	5.01	1.21	19	5.0	51	17.7	76	17	152	30	9,620	0.58	185	170
QMP-z7-1-2	exterior		11.7	154	872	16.5	15.2	-	302	449,700	1.21	0.111	-	27	0.063	1.32	2.33	0.72	10	2.8	28	9.8	41	9	87	17	9,560	0.60	190	221
QMP-z7-1-3	exterior		-	135	757	5.6	5.2	-	453	454,000	2.26	0.187	-	48	0.053	1.18	2.43	0.93	12	3.6	40	14.5	66	15	146	30	11,200	1.10	378	540
QMP-z9-1-1	interior		-	110	719	3.8	3.5	-	355	451,200	1.11	0.072	-	23	0.054	1.07	1.81	0.92	8	2.7	30	11.3	53	13	129	27	8,050	0.55	224	284
QMP-z9-1-2	exterior		-	136	724	3.9	3.6	-	440	470,000	1.13	0.155	0.016	40	0.119	1.76	3.00	1.43	13	3.9	40	14.2	64	14	146	29	8,420	0.66	540	494
QMP-z10-1-2	exterior		-	119	763	6.0	5.5	0.31	422	439,000	1.99	0.134	0.156	47	0.103	1.15	2.17	0.71	11	3.3	37	13.4	62	14	137	27	10,900	1.05	366	515
QMP-z22-1-1	interior		-	115	770	6.4	5.9	0.18	601	442,600	1.48	0.124	0.036	37	0.195	3.10	4.35	1.26	17	5.0	53	19.0	84	19	185	36	11,090	0.84	326	429
QMP-z22-1-2	exterior		-	135	760	5.8	5.4	0.25	561	446,000	2.92	0.179	-	64	0.092	1.94	3.82	1.15	16	4.5	50	18.4	82	18	176	35	11,000	1.33	601	723
QMP-z10-1-3	interior		-	144	833	11.8	10.9	-	596	439,700	1.06	0.114	0.023	32	0.258	4.37	6.18	2.06	23	6.1	59	19.8	82	17	162	31	9,220	0.53	294	284
QMP-z10-1-4	exterior		-	165	841	12.6	11.6	-	365	437,000	1.38	0.169	-	29	0.120	1.31	2.61	1.04	12	3.4	35	12.0	53	11	107	22	9,490	0.82	229	274
QMP-z17-1-2	exterior		-	95	757	5.7	5.2	-	378	436,700	2.42	0.170	-	51	0.103	1.41	2.52	0.78	10	3.0	33	12.1	55	13	127	27	10,960	1.12	538	758
QMP-z35-2	exterior		11.7	117	826	11.1	10.2	-	229	455,600	0.84	-	0.015	22	0.048	0.82	1.50	0.43	6	1.9	21	7.3	33	7	69	14	10,050	0.52	124	180

LA-ICP-MS signature	Zircon domain	ID-TIMS signature	Al (ppm)	P (ppm)	Zrc cryst. temp. (°C)[1]	Ti corr (ppm)	Ti (ppm)	Sr (ppm)	Y (ppm)	Zr (ppm)	Nb (ppm)	Ba (ppm)	La (ppm)	Ce (ppm)	Pr (ppm)	Nd (ppm)	Sm (ppm)	Eu (ppm)	Gd (ppm)	Tb (ppm)	Dy (ppm)	Ho (ppm)	Er (ppm)	Tm (ppm)	Yb (ppm)	Lu (ppm)	Hf (ppm)	Ta (ppm)	Th (ppm)	U (ppm)
QMP-z24-2	interior	QMP_z24	-	148	895	20.0	18.4	-	408	442,000	0.97	0.200	0.021	24	0.176	3.64	3.80	1.49	16	3.9	42	13.4	55	12	104	21	8,760	0.51	194	179
QMP-z24-1	exterior	QMP_z24	9.6	135	834	11.8	10.9	0.21	274	447,200	1.21	-	-	28	0.061	0.88	1.61	0.57	8	2.3	25	8.8	38	8	81	16	9,910	0.58	172	227
QMP-z15-1	interior		-	159	801	8.8	8.1	0.19	758	446,000	2.72	0.169	0.034	54	0.176	3.16	5.18	1.52	22	6.4	69	24.6	109	24	226	44	10,340	1.20	566	704
QMP-z15-2	exterior		-	140	834	11.8	10.9	0.18	262	453,600	1.08	0.105	-	26	0.036	0.97	1.97	0.62	8	2.2	24	8.5	38	8	81	16	10,120	0.62	165	225
QMP-z16-2	exterior	QMP_z16	-	134	784	7.4	6.8	-	441	452,000	2.27	0.212	-	47	0.070	1.36	2.42	0.79	11	3.6	38	14.4	63	15	140	28	10,770	1.08	409	540
QMP-z27-1	interior		-	114	787	7.6	7.0	0.50	1,480	470,000	4.60	0.390	0.053	90	0.420	7.00	9.60	4.07	44	12.3	132	47.1	213	46	472	94	10,790	1.61	1,560	2,200
QMP-z27-2	exterior		7.1	135	820	10.5	9.6	-	302	444,000	1.49	-	-	33	0.075	1.10	2.14	0.67	9	2.5	28	9.7	41	9	90	18	10,210	0.80	285	358
QMP-z43-1	interior		-	91	821	10.6	9.7	-	276	446,300	0.93	0.069	0.019	26	0.098	1.47	2.20	0.60	9	2.4	25	8.9	39	9	84	17	10,330	0.45	173	212
QMP-z40-1	interior		-	179	841	12.6	11.6	0.28	1,118	457,700	4.34	0.310	0.093	81	0.491	7.33	11.16	3.03	45	12.0	115	37.7	150	30	270	50	9,830	1.30	1,320	855
QMP-z40-2	exterior		-	126	776	6.8	6.3	-	628	472,900	3.45	0.156	-	63	0.157	2.75	3.66	1.23	16	5.0	53	19.5	88	20	194	38	11,530	1.40	730	1,010
QMP-z12-2	exterior		8.1	130	830	11.4	10.5	0.21	271	448,100	1.36	0.111	-	32	0.062	1.06	1.73	0.56	8	2.3	24	8.6	38	9	82	16	10,540	0.72	194	272
QMP-z45-1	interior	QMP_z45	-	302	896	20.2	18.6	0.24	2,374	457,700	4.94	0.184	0.288	63	1.270	15.37	21.00	6.74	98	25.4	250	77.7	313	61	547	102	8,800	1.64	1,933	1,245
QMP-z45-2	exterior	QMP_z45	-	114	747	5.0	4.6	0.34	644	434,000	4.03	0.193	0.070	73	0.131	2.44	4.02	1.23	20	5.5	58	20.9	92	20	191	38	10,530	1.73	813	1,041
QMP-z47-1	interior	QMP_z47oc	82	115	799	8.6	7.9	0.74	902	442,700	6.46	0.750	0.670	91	0.580	6.80	7.80	1.83	30	8.4	83	27.6	119	26	253	49	11,420	2.64	1,600	1,835
QMP-z47-2	exterior	QMP_z47oc	-	135	809	9.4	8.7	-	286	443,800	1.70	0.135	0.011	36	0.053	0.88	1.45	0.43	7	2.3	25	9.2	41	9	93	19	10,350	0.84	213	301
QMP-z47-3	exterior	QMP_z47oc	-	152	747	5.1	4.7	0.20	564	445,300	2.98	0.240	-	65	0.105	1.97	3.61	1.18	16	4.7	51	18.4	83	18	175	34	10,670	1.32	600	712
QMP-z50-1	interior		22.5	150	895	20.0	18.4	-	290	451,000	0.91	-	0.022	23	0.103	1.55	2.47	0.90	10	2.9	29	9.8	41	9	80	16	9,080	0.52	144	158
QMP-z50-2	exterior		-	156	894	19.9	18.3	-	809	458,400	1.13	0.129	0.099	31	0.544	7.41	9.72	2.48	34	8.6	85	27.2	108	22	199	39	9,180	0.57	520	341
QMP-z49-1	interior		-	111	752	5.3	4.9	0.29	894	445,200	5.94	0.293	0.084	72	0.186	2.68	4.67	1.41	20	5.9	70	26.6	131	31	326	70	11,780	2.16	1,067	2,095
QMP-z49-2	exterior		-	151	789	7.8	7.2	0.21	525	450,100	2.82	0.214	0.015	60	0.131	1.97	3.58	1.08	15	4.3	47	17.0	74	16	158	32	10,850	1.37	633	701
QMP-z60-1	interior	QMP_z60	9.8	142	870	16.2	14.9	-	447	462,000	0.86	-	0.030	24	0.231	3.58	4.83	1.32	18	4.4	43	14.2	62	13	121	24	9,820	0.48	192	199
QMP-z60-2	exterior	QMP_z60	8	133	848	13.4	12.3	0.22	267	436,700	1.35	-	-	28	0.069	0.97	1.79	0.55	8	2.3	23	8.5	36	8	80	16	9,670	0.66	196	265
QMP-z74-1	interior	QMP_z74	-	155	770	6.4	5.9	0.25	1,310	474,000	2.89	0.234	0.065	65	0.394	7.00	9.60	3.22	42	11.6	122	43.4	187	41	386	75	10,970	1.46	954	1,211
QMP-z74-2	exterior	QMP_z74	-	90	744	4.9	4.5	-	383	438,000	1.84	-	-	52	0.074	1.21	2.21	0.78	10	2.9	30	11.7	55	13	127	27	10,700	0.96	569	762
QMP-z72-1	interior		18.5	133	890	19.1	17.6	0.21	300	454,200	0.90	0.110	0.028	23	0.099	1.24	2.53	0.67	9	2.6	28	9.6	43	9	87	18	9,280	0.51	139	153
QMP-z72-2	exterior		20.3	130	868	16.0	14.7	-	204	450,300	0.68	0.098	-	21	0.049	0.81	1.36	0.42	6	1.8	19	6.5	29	6	61	12	9,810	0.47	114	158
QMP-z58-1	interior	QMP_z58oc	48	128	855	14.3	13.2	-	357	453,800	1.33	0.390	0.102	31	0.175	2.31	3.30	0.91	12	3.4	35	11.4	48	10	103	20	9,810	0.64	310	277
QMP-z58-2	exterior	QMP_z58oc	7.9	104	761	5.9	5.4	-	254	449,500	1.41	0.137	-	31	0.023	0.60	1.21	0.42	6	1.9	22	7.9	37	9	85	18	11,180	0.81	192	328
QMP-z76-1	interior		-	125	756	5.6	5.1	-	1,127	438,500	3.47	0.209	0.031	74	0.309	5.06	8.04	2.67	34	9.7	102	36.3	157	34	332	66	10,870	1.57	1,050	1,250
QMP-z88-1	interior		-	195	845	13.0	12.0	-	1,320	442,000	4.05	0.270	0.350	95	0.830	11.60	14.90	3.26	51	13.0	133	44.3	181	37	336	64	9,720	1.39	1,367	1,112
QMP-z83-1	interior	QMP_z83oc	17.2	177	884	18.3	16.8	-	373	450,200	0.78	-	0.013	21	0.185	2.81	3.64	1.27	14	3.7	36	12.2	50	10	99	19	8,770	0.46	142	146
QMP-z83-2	exterior	QMP_z83oc	16.7	138	870	16.3	15.0	-	229	451,000	1.00	0.099	-	22	0.048	1.12	1.57	0.54	7	2.0	21	7.1	32	7	67	14	9,680	0.52	131	186
QMP-z84-1	interior		-	175	816	10.1	9.3	0.27	607	434,000	1.65	0.093	0.030	44	0.219	4.04	5.33	1.51	22	5.8	56	18.9	79	18	164	33	9,920	0.85	418	411
QMP-z84-2	exterior		-	128	730	4.2	3.9	0.33	495	450,000	2.32	0.220	0.041	57	0.079	1.65	2.59	1.05	13	3.8	44	16.0	70	15	154	31	11,060	1.20	492	649
QMP-z69-2	exterior		11.7	142	843	12.8	11.8	0.18	310	449,300	1.75	0.122	-	31	0.056	1.07	1.94	0.65	9	2.6	28	9.9	44	10	95	19	10,120	0.74	252	371
QMP-z56-1	interior		-	126	839	12.4	11.4	-	309	449,400	0.96	-	0.019	24	0.089	1.19	1.79	0.80	10	2.8	28	9.8	43	9	93	19	9,910	0.44	178	211
QMP-z56-2	exterior		-	199	820	10.4	9.6	0.19	785	451,000	5.49	0.361	0.024	97	0.267	4.14	6.41	1.65	27	7.5	77	25.3	106	23	208	41	10,560	2.08	1,381	1,245
QMP-z78-1	interior	QMP_z78oc	-	199	852	13.9	12.8	0.28	1,008	447,100	1.81	0.216	0.470	48	0.750	9.58	12.50	3.42	43	11.3	105	33.5	137	28	252	48	9,450	0.90	728	545
QMP-z78-2	exterior	QMP_z78oc	8.5	123	830	11.4	10.5	-	322	472,900	1.80	0.215	-	34	0.052	1.27	2.05	0.74	10	2.7	30	9.8	46	10	98	20	10,920	0.82	226	310
QMP-z62-1	interior		-	141	829	11.3	10.4	-	594	461,000	1.51	-	0.034	41	0.249	4.01	5.40	1.51	21	5.5	56	19.1	83	17	166	32	10,340	0.85	412	404
QMP-z63-1	interior	QMP_z63oc	-	172	809	9.4	8.7	-	962	467,000	2.87	0.254	0.033	60	0.287	4.77	6.70	2.22	30	8.7	90	32.2	139	30	296	57	10,930	1.46	781	948
QMP-z63-2	exterior	QMP_z63oc	-	129	763	6.0	5.5	-	458	464,000	2.60	0.272	-	52	0.081	1.18	2.24	0.77	12	3.5	40	14.3	65	15	140	29	11,750	1.32	488	690
QMP-z03-1	interior		14.9	158	882	17.9	16.5	0.19	402	453,600	0.88	0.097	0.019	25	0.199	2.95	4.35	1.30	16	3.9	40	13.1	55	11	107	22	9,340	0.53	195	205
QMP-z51-2	exterior		-	164	768	6.3	5.8	0.25	577	434,700	2.95	0.236	0.051	59	0.151	2.25	3.49	1.13	15	4.5	49	17.7	81	18	177	36	11,030	1.33	692	902
QMP-z1-1m2	interior		-	52	677	2.3	2.1	-	416	407,900	0.99	-	0.028	31	0.059	1.22	2.74	1.02	10	3.2	33	12.8	56	14	141	28	10,630	0.55	314	439
QMP-z1-2m2	exterior		-	91	703	3.1	2.9	0.34	512	421,500	1.98	-	0.098	40	0.102	1.24	2.66	0.94	12	3.8	43	16.1	77	18	184	39	10,190	1.00	338	569
QMP-z2-1m2	interior		-	101	817	10.2	9.5	0.28	286	417,000	0.81	-	-	20	0.050	1.08	2.10	0.57	8	2.5	27	9.4	41	9	85	17	9,410	0.41	142	182
QMP-z2-2m2	exterior		-	87	831	11.6	10.8	-	159	421,000	0.53	-	-	18	0.055	0.36	0.73	0.30	4	1.4	14	5.0	24	5	55	11	9,510	0.35	72	117
QMP-z3-1m2	interior		-	139	742	4.8	4.5	-	660	424,000	2.99	0.290	-	52	0.123	1.93	3.70	1.20	19	4.8	60	19.3	92	21	209	41	10,590	1.28	500	640
QMP-z3-2m2	exterior		-	151	748	5.1	4.8	-	726	410,000	3.26	0.270	0.140	52	0.203	2.56	4.50	1.44	20	6.2	66	24.5	112	24	238	47	10,230	1.46	600	730
QMP-z5-1m2	interior		-	96	717	3.6	3.4	-	809	410,000	1.44	-	0.024	51	0.261	4.51	6.13	2.08	24	6.8	74	26.5	117	26	254	52	10,230	0.97	703	790
QMP-z5-2m2	exterior		-	75	746	5.0	4.7	-	560	431,000	3.29	-	-	51	0.091	1.45	2.49	0.85	11	3.6	44	17.0	81	19	198	42	10,400	1.48	462	727
QMP-z6-2m2	exterior		-	113	772	6.6	6.2	-	595	425,000	2.66	0.210	-	52	0.170	2.76	4.37	1.21	19	5.3	55	19.5	85	19	189	37	10,380	1.51	578	715
QMP-z7-1m2	interior		-	51	-	-	-	-	600	423,000	2.22	0.380	0.019	45	0.108	1.95	2.85	1.11	13	4.2	48	19.6	88	21	216	47	10,530	0.67	629	926
QMP-z8-1m2	interior		-	95	824	10.8	10.1	0.34	246	425,000	0.92	-	-	21	0.054	1.04	1.75	0.53	7	2.4	23	7.8	36	8	83	16	9,590	0.46	128	169
QMP-z9-1m2	interior	QMP_z9_m2	-	126	742	4.8	4.5	-	465	407,000	1.27	-	-	29	-	0.99	2.03	0.57	12	3.5	41	15.2	69	15	152	31	9,860	0.44	316	351
QMP-z9-2m2	exterior	QMP_z9_m2	-	93	782	7.3	6.8	-	609	435,000	1.59	-	0.053	46	0.197	2.91	4.67	1.35	18	5.1	55	20.2	84	20	196	40	10,910	0.78	650	720
QMP-z10-1m2	interior	QMP_z10_m2	-	202	805	9.1	8.5	-	159	433,000	0.76	-	0.100	21	0.075	0.72	0.79	0.30	5	1.2	14	5.2	23	5	54	11	10,060	0.43	88	141
QMP-z10-2m2	exterior	QMP_z10_m2	-	88	740	4.7	4.4	-	623	436,000	2.85	0.290	-	59	0.072	1.39	2.72	1.05	15	4.4	52	20.3	92	21	213	43	10,570	1.52	518	788
QMP-z11-2m2	exterior		-	118	791	7.9	7.4	-	266	441,000	2.00	0.200	-	37	0.077	1.06	1.29	0.66	7	2.2	23	7.9	39	9	90	19	10,580	0.84	352	433
QMP-z12-2m2	exterior		-	114	754	5.5	5.1	-	383	450,000	2.10	-	0.430	53	0.128	1.74	2.21	0.78	11	2.8	32	12.4	55	13	128	28	10,840	1.23	627	839
QMP-z13-1m2	interior		-	104	765	6.1	5.7	-	384	428,000	1.18	-	0.019	28	0.100	1.32	2.37	0.74	11	3.2	37	12.8	55	12	116	23	10,190	0.70	229	303
QMP-z15-1m2	interior		-	134	795	8.2	7.7	-	223	439,000	0.89	-	-	26	0.040	0.88	1.30	0.39	6	1.7	18	7.2	32	7	75	15	10,110	0.54	126	192
QMP-z16-1m2	interior	QMP_z16_m2	-	107	810	9.5	8.9	-	669	440,000	1.30	0.300	-	36	0.236	4.15	6.45	1.68	24	6.6	71	22.3	93	20	183	36	9,710	0.65	442	406
QMP-z16-2m2	exterior	QMP_z16_m2	-	145	778	7.0	6.5	-	495	415,000	2.42	0.370	-	50	0.113	1.63	3.74	0.79	14	3.9	46	15.2	72	16	142	30	9,970	1.22	618	649
QMP-z17-1m2	interior		-	136	811	9.6	9.0	0.37	258	430,000	1.51	-	-	31	0.034	1.05	1.37	0.54	7	2.2	23	8.1	36	8	83	16	10,130	0.64	223	294

LA-ICP-MS signature	Zircon domain	ID-TIMS signature	Al (ppm)	P (ppm)	Zrc cryst. temp. (°C)[1]	Ti corr (ppm)	Ti (ppm)	Sr (ppm)	Y (ppm)	Zr (ppm)	Nb (ppm)	Ba (ppm)	La (ppm)	Ce (ppm)	Pr (ppm)	Nd (ppm)	Sm (ppm)	Eu (ppm)	Gd (ppm)	Tb (ppm)	Dy (ppm)	Ho (ppm)	Er (ppm)	Tm (ppm)	Yb (ppm)	Lu (ppm)	Hf (ppm)	Ta (ppm)	Th (ppm)	U (ppm)
QMP-z17-2m2	exterior		-	131	801	8.8	8.2	-	636	427,000	1.40	-	0.034	39	0.291	4.86	6.21	1.68	24	6.6	60	20.5	85	19	169	35	9,510	0.62	391	381
QMP-z19-2m2	exterior		-	108	746	5.0	4.7	-	245	428,000	1.42	-	-	32	0.036	0.81	1.64	0.52	6	2.0	20	7.5	35	8	81	17	10,680	0.64	229	337
QMP-z20-1m2	interior		-	181	-	-	-	-	1,540	421,000	4.40	-	0.113	102	0.630	9.20	12.80	3.68	53	15.3	143	51.1	208	45	408	79	10,200	1.84	1,750	1,540
QMP-z21-2m2	exterior	QMP_z21_m2	-	197	804	9.0	8.4	-	1,002	439,000	2.80	0.290	0.060	56	0.480	6.90	9.60	2.53	35	9.3	91	32.5	136	29	279	55	10,820	1.19	860	992
QMP-z22-1m2	interior		-	194	756	5.6	5.2	-	886	438,000	2.13	-	0.024	51	0.187	3.52	6.21	2.02	27	7.8	82	29.4	126	28	265	51	10,210	1.08	569	613
QMP-z23-1m2	interior		-	92	727	4.1	3.8	-	916	432,000	1.69	-	0.027	55	0.316	5.13	7.80	2.39	29	8.4	81	28.9	129	28	274	59	10,130	0.84	840	940
QMP-z23-2m2	exterior		-	85	734	4.4	4.1	-	542	440,000	2.53	-	0.016	60	0.097	1.78	2.86	1.19	15	4.2	47	17.3	79	18	179	37	10,410	0.98	683	859
QMP-z24-1m2	interior		-	286	784	7.4	6.9	0.45	1,160	439,000	2.40	-	0.920	68	0.640	6.12	9.40	2.66	39	10.6	113	38.8	163	34	329	63	10,370	1.06	780	728
QMP-z25-2m2	exterior		-	138	768	6.3	5.9	-	1,087	430,000	7.40	0.370	0.048	116	0.287	5.55	9.10	2.39	36	10.3	102	35.3	151	33	319	59	10,080	2.63	2,120	1,783
QMP-z26-1m2	interior		-	127	748	5.1	4.8	-	721	436,000	2.30	-	-	51	0.169	2.59	4.35	1.47	21	6.1	64	22.9	104	23	226	45	9,900	1.22	507	606
QMP-z28-1m2	interior		-	63	-	-	-	-	650	435,000	1.18	0.240	0.018	39	0.220	4.20	4.50	1.89	20	4.8	61	20.4	94	21	227	50	10,740	0.60	680	1,070
QMP-z28-2m2	exterior		-	58	734	4.4	4.1	-	860	423,000	1.81	-	0.032	47	0.205	4.48	6.40	2.00	23	6.9	73	27.1	121	29	286	61	10,160	0.73	820	1,330
QMP-z30-1m2	interior		-	150	827	11.1	10.4	-	657	425,000	1.23	-	0.240	38	0.380	5.25	6.30	1.87	23	6.3	64	21.9	87	19	173	35	9,070	0.76	438	353
QMP-z31-1m2	interior		-	208	857	14.6	13.6	-	1,096	460,000	1.99	-	0.191	56	0.690	8.50	12.50	2.59	42	11.4	112	36.8	153	32	293	54	9,520	1.09	841	612
QMP-z32-1m2	interior		-	184	788	7.7	7.2	-	1,590	434,000	4.33	-	0.069	92	0.820	12.00	15.40	4.05	61	16.5	162	54.2	223	45	417	78	10,310	1.54	1,730	1,360
QMP-z34-1m2	interior		-	278	871	16.4	15.3	-	926	424,000	3.48	0.320	0.330	50	0.600	6.69	8.90	2.45	32	8.6	89	31.1	130	28	271	56	8,830	1.39	682	680
Latite Porphyry																														
LP-z01-1	interior		-	150	768	6.3	5.8	-	733	456,000	4.09	0.360	0.031	60	0.219	2.47	4.56	1.62	21	6.3	67	24.4	105	23	227	44	11,360	1.66	950	1,410
LP-z01-2	exterior		-	132	751	5.3	4.9	0.24	444	449,700	2.62	0.215	0.305	53	0.153	1.86	2.54	0.86	11	3.4	37	13.8	64	15	145	31	11,640	1.39	552	766
LP-z02-1	interior	LP_z2	8	121	827	11.1	10.2	-	305	457,000	1.28	0.103	0.009	29	0.057	0.85	1.83	0.65	9	2.3	27	9.6	42	10	96	19	10,550	0.63	185	252
LP-z02-2	exterior	LP_z2	-	70	680	2.4	2.2	0.20	610	451,200	2.88	0.154	-	43	0.076	1.29	2.75	1.22	14	4.5	50	19.1	91	21	214	46	11,600	1.02	932	1,588
LP-z03-1	interior		-	157	767	6.2	5.7	0.25	718	453,600	2.81	0.159	0.068	56	0.197	2.85	4.38	1.19	20	5.5	62	22.5	102	24	237	49	11,370	1.40	688	1,060
LP-z03-2	exterior		-	77	740	4.7	4.3	0.23	571	459,000	3.58	0.219	0.019	60	0.073	1.36	2.91	1.25	15	4.4	48	18.0	81	20	202	42	11,860	1.56	957	1,455
LP-z05-1	interior	LP_z5	-	67	716	3.6	3.3	0.25	847	455,400	3.93	0.161	0.037	43	0.134	2.01	3.37	1.36	17	5.3	62	24.4	124	30	330	76	12,080	1.52	734	2,077
LP-z05-2	exterior	LP_z5	-	119	828	11.2	10.3	0.16	224	443,600	0.98	-	-	25	0.050	0.83	1.15	0.42	6	1.8	20	7.1	32	7	70	14	10,130	0.53	143	202
LP-z06-1	interior	LP_z6oc	-	205	788	7.7	7.1	0.23	1,690	448,400	5.05	0.250	0.102	78	0.314	5.15	10.90	3.42	45	14.1	152	54.5	233	48	435	81	10,830	1.37	1,310	1,390
LP-z06-2	exterior	LP_z6oc	-	107	719	3.7	3.4	0.17	686	448,000	4.05	0.287	-	66	0.100	1.64	3.71	1.47	16	5.1	57	21.3	98	23	226	47	11,080	1.91	847	1,400
LP-z07-1	interior/r	LP_z7oc	-	167	774	6.7	6.1	0.16	682	446,700	1.92	-	0.017	37	0.185	2.77	4.12	1.47	19	5.4	60	21.8	96	22	209	43	9,560	1.02	366	461
LP-z31-1	interior		26	171	781	7.2	6.6	0.18	839	452,000	2.72	0.353	0.045	58	0.244	4.30	6.57	1.83	26	7.4	76	26.9	119	26	250	50	10,820	1.26	698	783
LP-z31-2	exterior		-	68	699	3.0	2.7	-	463	447,700	2.26	0.230	0.075	57	0.091	1.54	2.42	1.09	11	3.3	36	14.0	67	16	168	38	11,360	0.98	1,076	1,570
LP-z46-1	interior		-	156	807	9.2	8.5	-	940	437,500	1.71	0.253	0.090	46	0.506	7.29	9.91	2.68	35	9.7	94	30.7	129	27	250	49	9,880	0.85	720	627
LP-z46-2	exterior		-	70	682	2.4	2.2	-	573	436,000	3.09	0.174	-	56	0.077	1.51	3.03	1.27	15	4.4	46	17.6	82	19	198	43	11,130	1.10	1,110	1,757
LP-z43-1	interior	LP_z43	-	145	755	5.5	5.1	0.24	1,113	448,200	4.90	0.231	0.044	81	0.367	5.70	8.13	1.95	35	10.1	102	36.0	156	33	309	61	10,470	1.81	1,241	1,370
LP-z43-2	exterior	LP_z43	-	68	653	1.7	1.6	0.30	413	442,500	1.59	0.115	0.246	27	0.106	0.96	1.65	0.91	9	2.6	30	12.4	60	15	155	36	11,720	0.60	435	978
LP-z45-1	interior		-	91	765	6.1	5.6	-	723	501,000	3.49	0.190	0.036	50	0.192	1.96	3.86	1.28	16	5.0	56	21.8	106	25	264	54	12,580	1.62	706	1,267
LP-z45-2	exterior		-	167	803	8.9	8.2	-	768	477,000	5.55	0.320	0.201	88	0.301	3.85	5.19	1.49	24	6.3	70	24.5	106	23	223	44	11,430	2.21	1,241	1,422
LP-z39-1	interior		23.2	110	830	11.5	10.5	-	274	456,700	0.78	0.130	0.042	23	0.056	1.03	1.62	0.53	7	2.1	23	8.2	38	8	78	16	10,290	0.45	120	158
LP-z39-2	exterior		-	75	718	3.7	3.4	0.31	302	439,200	1.65	-	0.045	42	0.078	0.85	1.38	0.66	7	2.2	23	9.1	43	11	110	25	11,170	0.86	454	750
LP-z36-1	interior		-	85	754	5.4	5.0	0.20	377	461,000	1.54	0.125	-	32	0.057	0.99	1.94	0.72	9	2.8	31	11.8	52	12	126	26	12,000	0.94	243	422
LP-z23-1	interior	LP_z23oc	10	142	801	8.7	8.0	-	715	450,200	2.78	0.275	0.084	58	0.300	4.09	5.68	1.53	22	6.0	64	22.8	101	23	220	45	11,030	1.32	730	776
LP-z23-2	exterior	LP_z23oc	11.2	107	813	9.8	9.0	0.20	196	445,600	1.12	-	-	25	0.045	0.42	1.12	0.34	5	1.5	17	5.9	28	6	63	12	10,680	0.59	147	235
LP-z24-1	interior	LP_z24	-	110	739	4.7	4.3	-	1,131	441,600	2.78	0.237	0.034	70	0.331	5.52	7.94	2.51	33	9.7	101	36.0	160	36	346	70	11,080	1.20	977	1,390
LP-z24-2	exterior	LP_z24	-	64	709	3.3	3.1	0.26	565	441,200	3.76	0.181	0.063	42	0.077	1.28	2.81	1.20	13	4.3	47	17.4	80	19	193	42	11,710	1.17	911	1,632
LP-z25-1	interior	LP_z25oc	-	165	794	8.2	7.5	0.27	649	426,300	1.96	-	0.024	46	0.193	3.33	4.70	1.38	20	5.4	58	21.1	94	20	199	39	9,860	1.03	406	478
LP-z25-2	exterior	LP_z25oc	-	134	767	6.2	5.7	-	504	448,000	2.52	0.148	-	54	0.103	1.77	3.20	0.91	14	4.1	45	16.3	72	16	157	32	10,910	1.33	528	697
LP-z38-1	interior		13.4	171	806	9.1	8.4	-	1,320	491,000	5.25	0.450	0.112	104	0.500	7.27	11.15	3.27	45	12.6	129	44.0	189	40	375	71	11,100	2.15	1,497	1,486
LP-z38-2	exterior		-	94	735	4.4	4.1	0.22	433	440,900	2.07	0.153	-	48	0.094	1.17	2.31	0.91	11	3.3	37	13.4	62	14	145	31	11,370	1.17	605	893
LP-z35-1	interior		-	115	738	4.6	4.3	-	815	447,600	1.97	0.174	0.026	45	0.249	3.62	5.29	2.34	23	6.5	72	25.7	115	27	258	54	10,580	0.90	551	871
LP-z35-2	exterior		10.8	159	838	12.3	11.3	-	329	466,000	1.71	0.101	-	33	0.070	1.27	2.23	0.76	10	2.8	30	10.6	45	10	96	19	10,350	0.77	251	333
LP-z52-2	exterior		-	95	737	4.6	4.2	0.21	474	447,100	2.92	0.193	-	61	0.103	1.47	3.04	0.99	13	3.8	41	14.5	67	15	156	32	11,480	1.43	848	1,166
LP-z33-1	interior		-	136	879	17.5	16.1	-	487	446,200	0.70	-	0.036	33	0.263	4.33	5.54	1.69	20	5.3	52	16.3	65	14	124	24	9,620	0.40	251	197
LP-z33-2	exterior		13.2	147	842	12.7	11.7	-	279	449,000	1.53	0.153	-	36	0.091	1.48	2.00	0.63	9	2.4	24	8.6	38	8	81	17	10,260	0.80	252	316
LP-z19-1	interior		-	137	818	10.2	9.4	-	569	444,000	1.52	0.150	0.040	34	0.310	4.70	6.70	1.74	20	5.4	54	17.8	73	16	155	32	9,830	0.83	363	382
LP-z19-2	exterior		-	79	726	4.1	3.7	0.18	448	444,500	2.30	0.155	0.021	47	0.065	1.27	2.09	1.08	11	3.2	37	13.7	64	15	159	35	11,380	1.10	830	1,199
LP-z10-2	exterior		-	79	646	1.5	1.4	0.25	537	446,700	2.09	0.117	-	33	0.041	0.86	1.85	1.17	12	3.7	41	15.9	78	19	193	44	11,410	0.71	772	1,624
LP-z22-1	interior		-	139	853	14.0	12.9	-	567	452,300	0.97	0.102	0.046	28	0.187	2.99	5.76	1.82	22	6.0	57	19.3	77	16	146	28	9,690	0.41	274	232
LP-z22-2	exterior		-	80	720	3.8	3.5	-	395	450,300	1.85	0.161	-	45	0.072	1.11	1.96	0.81	9	2.7	32	11.9	59	14	143	31	11,270	0.97	509	807
LP-z41-1	interior		12	85	744	4.9	4.5	0.35	611	500,000	2.60	0.230	0.042	39	0.160	2.40	3.60	1.25	16	4.5	48	19.1	91	22	218	45	12,960	1.11	502	1,007
LP-z41-2	exterior		-	119	725	4.0	3.7	0.23	501	449,000	2.72	0.150	-	56	0.083	1.53	2.48	1.02	13	4.0	44	16.2	73	16	153	31	10,630	1.43	536	796
LP-z40-1	interior		15.1	169	896	20.2	18.6	0.29	445	443,400	0.99	0.132	0.026	25	0.278	4.01	4.58	1.52	18	4.5	43	14.5	59	12	117	24	8,900	0.53	224	218
LP-z40-2	exterior		-	71	718	3.7	3.4	-	432	447,000	2.02	0.149	-	43	0.064	1.10	2.19	0.82	9	3.0	34	13.6	64	15	158	34	11,430	0.98	494	861
LP-z42-2	exterior		28	89	739	4.7	4.3	0.37	402	446,200	2.01	0.570	0.237	49	0.096	1.34	2.40	0.86	10	3.0	33	12.3	58	13	141	31	11,230	1.01	719	1,064
LP-z59-2	exterior		-	86	720	3.8	3.5	-	477	445,400	2.02	0.216	0.023	57	0.091	1.63	2.74	1.13	12	3.6	40	14.7	69	16	160	34	10,820	1.11	830	1,145
LP-z58-2	exterior		-	64	702	3.1	2.8	0.19	447	444,900	1.92	0.090	-	36	0.046	0.90	1.86	0.99	10	3.0	35	13.5	65	15	162	36	11,160	0.77	643	1,182
LP-z71-2	exterior		23.2	76	737	4.6	4.2	0.20	540	441,300	2.26	0.306	0.047	54	0.092	1.49	2.59	1.16	13	4.0	44	16.7	78	18	184	39	10,830	1.26	802	1,168
LP-z83-1	interior	LP_z83	-	136	742	4.8	4.4	0.27	730	450,200	2.19	0.137	0.015	43	0.178	2.67	4.31	1.56	19	5.6	62	23.4	107	25	239	50	10,520	0.97	508	857

LA-ICP-MS signature	Zircon domain	ID-TIMS signature	Al (ppm)	P (ppm)	Zrc cryst. temp. (°C)[1]	Ti corr (ppm)	Ti (ppm)	Sr (ppm)	Y (ppm)	Zr (ppm)	Nb (ppm)	Ba (ppm)	La (ppm)	Ce (ppm)	Pr (ppm)	Nd (ppm)	Sm (ppm)	Eu (ppm)	Gd (ppm)	Tb (ppm)	Dy (ppm)	Ho (ppm)	Er (ppm)	Tm (ppm)	Yb (ppm)	Lu (ppm)	Hf (ppm)	Ta (ppm)	Th (ppm)	U (ppm)
LP-z83-2	exterior	LP_z83	-	146	779	7.1	6.5	-	486	454,200	1.96	0.131	-	43	0.110	1.53	2.78	0.95	12	4.1	44	15.3	68	15	148	30	10,490	1.11	422	563
LP-z99-1	interior	LP_z99	8	168	874	16.8	15.5	0.25	588	450,300	1.71	0.155	0.160	39	0.312	4.48	6.04	1.74	22	5.8	57	19.1	80	16	154	31	9,250	0.71	507	404
LP-z99-2	exterior	LP_z99	-	155	770	6.4	5.9	-	726	437,900	5.42	0.365	0.014	94	0.167	2.83	5.15	1.59	22	6.3	66	23.4	103	23	218	43	10,620	2.09	1,124	1,237
LP-z96-1	interior	LP_z96	8.8	156	864	15.5	14.3	-	382	446,900	0.93	0.101	0.026	24	0.144	2.33	3.54	1.02	13	3.6	36	12.3	52	11	105	22	8,990	0.57	173	184
LP-z96-2	exterior	LP_z96	-	117	746	5.0	4.6	-	429	456,100	2.34	0.150	-	51	0.078	1.32	2.33	0.86	12	3.4	38	14.0	61	14	134	27	11,310	1.12	460	589
LP-z90-1	interior		19.8	149	888	18.9	17.4	-	271	447,800	1.07	0.077	0.031	26	0.141	1.99	2.65	0.68	10	2.6	26	9.0	37	8	77	15	9,650	0.53	178	181
LP-z90-2	exterior		-	83	721	3.8	3.5	0.28	645	480,000	4.58	0.360	0.029	75	0.124	2.57	4.20	1.91	20	5.6	56	20.0	93	21	209	42	11,860	1.71	1,474	1,700
LP-z82-1	interior		-	150	759	5.7	5.3	0.19	884	446,800	4.07	0.209	-	80	0.176	2.96	5.51	1.95	24	7.2	78	28.4	126	28	270	54	10,500	1.72	767	882
LP-z82-2	exterior		-	79	694	2.8	2.6	0.25	689	442,100	3.28	0.188	0.020	46	0.067	1.54	2.98	1.49	14	4.7	51	20.1	97	23	252	57	11,990	0.99	1,314	2,898
LP-z79-1	interior	LP_z79	-	143	750	5.2	4.8	0.21	684	443,700	2.45	0.117	0.015	43	0.119	2.21	3.81	1.19	17	5.3	58	21.9	99	22	216	44	10,970	1.20	430	609
LP-z79-2	exterior	LP_z79	-	73	660	1.8	1.7	-	481	442,500	1.91	0.103	0.006	34	0.051	0.89	2.00	1.06	11	3.2	36	14.5	69	16	171	38	11,630	0.73	672	1,266
LP-z67-1	interior		-	96	728	4.1	3.8	0.37	561	438,200	3.86	0.146	0.120	53	0.119	1.84	3.01	1.02	13	4.0	46	16.9	80	19	195	41	11,590	1.69	762	1,302
LP-z67-2	exterior		-	108	774	6.7	6.2	0.29	541	451,100	3.18	0.243	-	58	0.074	1.62	2.71	0.98	13	4.0	47	16.7	77	17	168	34	11,130	1.60	679	939
LP-z66-2	exterior		-	70	654	1.7	1.6	0.21	497	446,100	2.19	-	-	32	0.043	0.70	1.76	1.01	11	3.1	37	14.6	72	18	184	42	11,820	0.93	692	1,533
LP-z78-1	interior		-	253	860	14.9	13.7	0.26	1,431	456,000	4.86	0.301	0.109	92	0.474	7.61	11.00	3.61	46	13.0	135	47.5	202	41	376	73	8,740	1.60	1,268	994
LP-z78-2	exterior		-	69	720	3.8	3.5	0.17	408	449,900	2.07	0.090	0.028	43	0.060	0.90	2.13	0.88	9	2.8	32	12.4	59	14	152	33	11,640	1.07	618	1,044
LP-z88-1	interior	LP_z88	5.9	265	788	7.7	7.1	0.22	1,234	443,400	5.75	0.322	0.184	87	0.367	5.92	8.59	2.59	36	10.4	111	39.8	176	38	361	71	10,010	2.04	1,173	1,219
LP-z88-2	exterior	LP_z88	-	76	703	3.1	2.9	0.24	659	448,000	3.03	0.126	0.035	48	0.055	1.08	2.49	1.16	13	4.2	49	19.8	99	24	252	56	11,320	1.11	735	1,298
LP-z73-1	interior		37.9	279	822	10.7	9.8	0.43	1,850	456,100	10.52	0.980	0.287	180	0.830	12.70	18.10	5.86	68	18.1	188	63.4	259	53	462	90	9,660	2.70	2,470	1,830
LP-z73-2	exterior		53.7	138	865	15.6	14.4	-	186	450,400	0.80	0.217	0.084	19	0.083	1.16	1.25	0.45	5	1.5	16	5.8	25	6	56	12	9,800	0.42	100	144
LP-z73-3	exterior		12.8	136	834	11.9	10.9	-	289	445,300	1.18	-	-	30	0.042	1.14	1.85	0.63	8	2.5	26	9.4	40	9	86	18	10,190	0.67	205	268
LP-z64-1	interior		-	96	748	5.1	4.7	0.20	512	444,100	1.54	-	-	37	0.080	1.61	3.09	1.03	14	4.1	44	16.1	74	17	169	35	11,160	0.79	367	526
LP-z64-2	exterior		-	64	692	2.7	2.5	-	410	435,400	1.43	-	-	29	0.058	0.82	1.83	0.79	9	2.8	32	12.8	62	14	151	34	11,230	0.68	545	1,104
LP-z90-3	interior		-	131	794	8.2	7.5	-	566	441,000	1.31	-	0.009	34	0.135	2.49	4.14	1.19	18	5.1	52	18.1	81	17	163	33	10,530	0.71	327	394
LP-z90-4	exterior		-	180	802	8.8	8.1	0.26	746	459,200	4.10	0.231	0.022	67	0.169	3.24	4.41	1.56	19	5.9	65	23.4	108	24	236	49	10,940	1.74	741	901
LP-z68-1	interior		18.4	139	771	6.5	6.0	0.22	750	449,000	2.92	0.326	0.127	54	0.218	3.25	5.04	1.46	21	6.2	67	23.7	105	24	230	45	10,890	1.34	628	763
LP-z68-2	exterior		-	136	764	6.1	5.6	0.20	511	442,000	2.55	0.200	-	57	0.066	1.80	2.91	1.03	13	4.1	43	16.0	73	17	160	33	11,030	1.28	490	658
LP-z70-1	interior		13.8	178	869	16.1	14.8	-	492	452,300	1.32	0.245	0.045	47	0.354	4.39	6.03	1.47	18	4.8	47	15.9	67	14	139	27	10,000	0.83	334	294
LP-z70-2	exterior		8.8	126	809	9.4	8.7	-	294	446,300	1.34	0.154	-	33	0.069	1.00	1.48	0.57	8	2.4	27	9.4	41	9	91	19	10,230	0.71	221	301
LP-z81-2	exterior		-	74	690	2.7	2.5	-	559	443,800	2.46	0.224	-	41	0.068	1.32	2.89	1.37	14	4.2	47	17.3	83	19	188	41	11,390	0.96	764	1,303
Quarz Latite Porphyry																														
QLP-z10-2	exterior		-	63	698	2.9	2.7	0.23	408	445,700	1.73	-	0.119	30	0.084	1.04	1.74	0.92	9	2.7	29	11.8	58	14	156	37	11,780	0.47	446	961
QLP-z2-1	interior	QLP_z2oc	-	51	677	2.3	2.1	0.13	389	448,700	1.13	0.079	0.086	18	0.048	0.70	1.14	0.58	7	2.1	26	11.1	57	15	169	42	11,880	0.31	191	576
QLP-z2-2	exterior	QLP_z2oc	-	63	710	3.4	3.1	0.16	552	432,000	2.11	0.126	0.127	28	0.076	0.81	1.58	0.91	10	3.2	38	15.8	78	19	211	49	11,400	0.55	285	753
QLP-z3-1	interior		24.2	55	691	2.7	2.5	0.19	336	405,200	1.14	0.239	0.234	19	0.104	0.72	1.29	0.57	7	2.0	23	9.4	50	12	138	34	10,970	0.37	217	556
QLP-z3-3	exterior		-	55	661	1.9	1.7	-	369	449,000	1.51	0.107	-	24	0.023	0.55	1.23	0.66	7	2.1	25	10.3	52	13	146	34	12,410	0.49	433	1,105
QLP-z11-1	interior	QLP_z11	148	91	757	5.6	5.2	0.81	1,113	444,600	4.67	1.190	0.334	54	0.253	3.03	4.64	1.97	22	6.9	80	32.1	157	37	396	90	11,840	0.92	2,300	3,480
QLP-z11-2	exterior	QLP_z11	-	52	703	3.1	2.9	0.26	555	449,100	2.79	-	0.244	31	0.089	0.97	2.11	1.07	11	3.2	38	15.2	77	19	212	51	12,670	0.67	549	1,335
QLP-z21-1	interior		16.9	53	696	2.9	2.6	0.32	554	447,400	1.49	0.131	0.116	20	0.078	0.81	1.69	0.93	10	3.2	38	16.0	83	20	227	54	11,860	0.51	316	882
QLP-z21-2	exterior		-	71	701	3.0	2.8	0.21	793	447,000	3.11	0.155	0.021	40	0.063	1.07	1.80	1.20	13	4.3	53	22.4	115	29	315	75	11,490	0.67	499	1,193
QLP-z35-1	interior	QLP_z35	7	107	732	4.3	4.0	0.28	720	444,700	3.22	0.290	0.114	69	0.165	2.46	4.13	1.59	18	5.4	59	22.3	105	24	249	53	10,670	1.37	1,042	1,320
QLP-z35-2	exterior	QLP_z35	-	138	706	3.2	3.0	0.74	615	453,200	2.39	0.094	0.360	44	0.196	2.14	2.98	1.57	15	4.2	46	18.2	89	21	222	50	11,520	0.68	709	1,392
QLP-z38-1	interior	QLP_z38	-	146	830	11.5	10.5	0.18	459	442,200	1.31	0.097	0.018	30	0.194	3.16	4.34	1.39	16	4.3	44	15.0	63	14	129	26	9,830	0.69	263	292
QLP-z38-2	exterior	QLP_z38	-	63	666	2.0	1.8	-	653	447,000	2.22	0.103	-	32	0.032	0.89	2.23	1.17	12	3.8	47	18.8	95	23	255	58	11,160	0.64	321	872
QLP-z24-1	interior	QLP_z24	98	79	726	4.0	3.7	0.71	698	448,000	2.81	0.540	0.227	41	0.139	1.94	3.24	1.47	16	4.7	54	21.2	102	24	257	58	11,570	0.80	746	1,474
QLP-z24-2	exterior	QLP_z24	-	36	647	1.6	1.4	-	274	450,000	1.00	0.102	-	16	0.014	0.39	0.62	0.45	4	1.5	18	7.9	42	10	118	29	12,630	0.40	178	623
QLP-z13-1	interior		80	539	806	9.2	8.4	0.73	3,610	437,600	13.48	0.930	0.198	139	0.325	5.74	15.25	6.43	88	28.7	322	119.9	510	105	934	171	9,990	2.74	2,210	2,026
QLP-z13-2	exterior		-	64	684	2.5	2.3	0.14	477	439,500	1.93	0.094	-	30	0.037	0.73	1.81	1.00	10	3.2	36	14.3	69	17	177	40	11,410	0.71	589	1,303
QLP-z25-1	interior		206	227	781	7.2	6.6	0.98	2,159	444,700	6.80	2.130	0.338	151	1.349	17.18	23.90	5.76	88	22.7	225	70.7	286	59	531	99	9,910	1.97	3,050	2,102
QLP-z25-2	exterior		-	56	681	2.4	2.2	0.35	501	441,700	2.68	0.080	-	29	0.057	0.57	1.63	0.90	9	2.9	34	14.4	72	18	204	48	12,220	0.68	535	1,398
QLP-z14-1	interior	QLP_z14	-	88	708	3.3	3.0	0.23	720	443,500	3.34	0.132	0.044	58	0.183	2.20	3.71	1.41	17	5.2	59	22.2	99	24	242	51	11,570	1.41	869	1,279
QLP-z14-2	exterior	QLP_z14	7.8	46	654	1.7	1.6	0.22	210	450,400	0.87	0.107	0.042	13	0.031	0.36	0.77	0.35	3	1.1	14	6.0	31	8	92	22	12,940	0.34	161	547
QLP-z5-1	interior	QLP_z5oc	-	72	726	4.0	3.7	0.22	667	489,000	3.01	-	0.020	51	0.052	1.25	2.60	1.24	13	4.2	50	20.5	100	25	262	57	11,890	0.97	781	1,426
QLP-z5-2	exterior	QLP_z5oc	-	40	701	3.0	2.8	0.21	293	445,600	1.15	0.098	-	17	0.018	0.49	1.07	0.58	6	1.7	20	8.8	43	11	120	28	11,710	0.48	256	748
QLP-z4-1	interior		64	77	724	4.0	3.6	0.47	558	440,900	1.32	0.450	0.214	23	0.082	1.18	2.28	1.10	11	3.3	37	16.5	80	20	221	53	11,250	0.39	266	739
QLP-z4-2	exterior		92	62	761	5.9	5.4	0.50	779	446,900	3.16	0.680	0.260	43	0.124	1.69	2.60	1.42	16	4.8	57	22.8	111	27	287	65	11,150	0.69	524	1,046
QLP-z12-2	exterior		26.4	47	687	2.6	2.4	0.30	578	454,400	2.69	0.251	0.156	21	0.068	0.64	1.02	0.69	7	2.7	34	15.4	85	22	262	65	13,280	0.64	262	939
QLP-z7-1	interior	QLP_z7	43	70	707	3.3	3.0	0.31	754	446,300	2.58	0.430	0.243	31	0.106	1.31	2.37	1.15	13	4.4	53	22.1	112	28	298	69	11,300	0.64	503	1,275
QLP-z7-2	exterior	QLP_z7	8.8	40	696	2.9	2.6	0.22	321	448,300	1.19	0.113	0.131	18	0.053	0.55	1.13	0.69	6	2.0	22	9.0	47	12	131	31	12,260	0.35	244	699
QLP-z15-1	interior	QLP_z15	-	147	793	8.1	7.4	0.26	783	448,600	1.96	0.209	0.024	48	0.199	3.91	6.18	1.79	25	6.9	74	25.6	110	24	229	46	10,740	0.94	527	543
QLP-z15-2	exterior	QLP_z15	-	83	693	2.8	2.5	0.38	448	452,000	1.93	0.096	0.110	32	0.086	1.12	1.95	0.95	10	3.0	34	13.6	64	15	164	38	11,690	0.74	604	1,248
QLP-z16-1	interior		208	111	752	5.3	4.9	0.80	895	435,800	1.77	1.370	0.258	38	0.244	3.07	5.10	2.24	23	6.7	76	28.1	127	29	299	65	10,680	0.54	588	1,034
QLP-z16-2	exterior		-	73	673	2.2	2.0	0.30	504	439,200	1.90	0.111	0.014	31	0.039	0.96	1.79	1.11	10	3.3	37	14.7	72	17	190	45	11,310	0.54	370	810
QLP-z17-1	interior	QLP_z17	10.3	77	711	3.4	3.1	0.36	607	447,000	1.63	0.143	0.065	23	0.096	1.17	2.22	1.16	12	3.9	45	18.2	91	22	238	56	11,360	0.45	340	876
QLP-z17-2	exterior	QLP_z17	-	53	678	2.3	2.1	0.29	572	443,000	2.08	0.107	-	32	0.058	0.83	1.84	1.05	11	3.4	40	16.5	83	20	227	52	11,330	0.54	378	974
QLP-z28-1	interior		13.9	447	818	10.2	9.4	0.52	3,440	450,800	8.65	0.600	0.310	165	0.713	11.71	19.90	8.40	99	30.2	328	119.0	493	95	809	146	9,590	1.36	1,490	782

LA-ICP-MS signature	Zircon domain	ID-TIMS signature	Al (ppm)	P (ppm)	Zrc cryst. temp. (°C)[1]	Ti corr (ppm)	Ti (ppm)	Sr (ppm)	Y (ppm)	Zr (ppm)	Nb (ppm)	Ba (ppm)	La (ppm)	Ce (ppm)	Pr (ppm)	Nd (ppm)	Sm (ppm)	Eu (ppm)	Gd (ppm)	Tb (ppm)	Dy (ppm)	Ho (ppm)	Er (ppm)	Tm (ppm)	Yb (ppm)	Lu (ppm)	Hf (ppm)	Ta (ppm)	Th (ppm)	U (ppm)
QLP-z28-2	exterior		-	80	702	3.1	2.8	0.24	586	447,400	2.56	0.167	0.024	44	0.053	1.54	2.69	1.30	13	4.1	47	17.5	84	20	208	46	11,410	0.75	1,046	1,761
QLP-z54-2	exterior		51.3	69	737	4.6	4.2	0.43	599	446,500	2.97	0.370	0.400	44	0.197	1.95	2.82	1.35	14	4.3	47	18.0	85	20	208	47	12,180	0.65	604	1,083
QLP-z40-1	interior		-	102	710	3.4	3.1	0.26	643	436,600	2.40	0.179	0.017	49	0.135	2.32	3.33	1.34	15	4.6	50	19.5	93	22	225	50	10,850	1.09	634	1,002
QLP-z40-2	exterior		-	56	695	2.8	2.6	0.19	563	441,900	2.24	0.118	-	27	0.036	0.82	1.69	0.98	10	3.3	40	16.6	84	21	230	53	11,640	0.72	398	1,107
QLP-z41-1	interior		-	179	721	3.8	3.5	-	786	439,700	3.21	0.180	0.039	58	0.171	2.77	4.85	1.86	23	6.8	72	25.4	111	24	231	46	10,990	1.44	607	704
QLP-z41-2	exterior		-	49	681	2.4	2.2	0.18	415	449,300	1.34	-	0.012	20	0.023	0.47	1.29	0.71	7	2.5	28	11.8	60	15	170	40	12,010	0.42	224	672
QLP-z30-1	interior		94	139	771	6.5	6.0	0.58	838	444,400	3.65	0.760	0.244	78	0.411	4.90	6.81	2.34	25	7.2	77	27.5	116	26	251	51	10,780	1.51	1,175	1,387
QLP-z29_-2	exterior		8.3	95	781	7.2	6.6	0.18	186	452,200	1.04	0.124	-	24	0.026	0.68	0.96	0.32	4	1.4	15	5.8	26	6	65	14	10,870	0.62	153	290
QLP-z31-1	interior		20.8	60	673	2.2	2.0	-	444	447,200	1.61	0.250	0.059	26	0.048	0.85	1.36	0.76	8	2.6	31	13.0	64	16	177	41	11,780	0.54	394	995
QLP-z57-1	interior		-	133	775	6.8	6.3	0.23	601	446,800	2.57	0.084	0.016	44	0.119	1.83	3.30	1.23	16	4.7	53	19.6	89	20	195	40	10,160	1.20	372	555
QLP-z57-2	exterior		-	42	688	2.6	2.4	0.20	494	452,400	1.93	0.120	-	27	0.037	0.75	1.78	0.90	9	2.8	35	14.2	72	18	196	46	11,950	0.63	442	1,178
QLP-z43-1	interior		-	62	725	4.0	3.7	0.25	743	447,800	2.86	0.129	-	37	0.043	1.05	2.51	1.24	14	4.5	55	22.0	110	27	288	67	11,450	0.66	502	1,236
QLP-z43-2	exterior		29.6	44	743	4.9	4.5	0.25	381	444,800	1.62	0.270	0.182	27	0.102	0.89	1.41	0.85	8	2.3	27	10.8	54	14	152	37	11,990	0.53	420	996
QLP-z66-2	exterior		6.9	78	676	2.3	2.1	0.17	517	446,300	2.18	-	-	20	0.014	0.63	1.60	0.89	10	3.2	38	15.1	74	18	201	48	12,130	0.53	190	622
QLP-z67-1	interior		12.2	359	781	7.2	6.6	0.52	4,190	445,000	12.45	0.980	0.572	269	2.200	32.30	50.30	14.27	193	48.7	446	139.6	523	103	883	162	9,330	2.56	6,300	3,000
QLP-z67-2	exterior		-	63	697	2.9	2.7	0.25	533	439,700	2.19	0.226	-	35	0.055	0.97	2.59	1.09	12	3.7	41	15.8	76	18	194	43	11,600	0.74	824	1,645
QLP-z69-2	exterior		-	64	671	2.1	2.0	0.28	539	438,300	3.87	0.088	0.019	32	0.055	0.86	2.01	0.90	12	3.6	42	16.1	77	19	205	47	13,920	1.46	908	2,250
QLP-z60-2	exterior		-	96	752	5.3	4.9	0.19	508	442,500	2.59	0.213	0.038	64	0.101	1.88	2.52	1.09	13	3.7	41	15.5	72	17	170	37	10,690	1.18	699	954
QLP-z59-1	interior		-	76	680	2.4	2.2	0.26	684	445,400	1.33	0.077	0.023	22	0.101	1.93	3.00	1.46	14	4.3	50	20.1	98	24	256	61	11,530	0.43	378	981
QLP-z59-2	exterior		-	62	677	2.3	2.1	0.18	380	444,700	1.48	-	-	27	0.034	0.63	1.56	0.82	8	2.4	28	11.3	55	13	146	33	11,780	0.45	436	1,038
QLP-z49-2	exterior		-	55	664	1.9	1.8	0.18	530	436,000	2.01	0.085	0.014	26	0.034	0.74	1.79	0.91	10	3.2	38	15.2	76	19	209	50	11,870	0.56	336	886
QLP-z51-1	interior		175	94	788	7.7	7.1	0.70	754	436,000	5.25	1.410	0.560	45	0.440	4.21	4.45	1.07	18	5.2	59	22.8	109	26	259	54	12,120	2.37	2,030	2,015
QLP-z51-2	exterior		6.2	113	809	9.5	8.7	0.17	212	446,700	1.18	0.117	-	30	0.042	0.67	1.29	0.37	6	1.6	17	6.5	29	7	72	15	10,760	0.69	210	309
QLP-z62-2	exterior		-	88	733	4.4	4.0	-	391	442,000	1.90	0.140	0.010	46	0.059	1.23	2.20	0.77	10	2.9	32	11.9	57	13	131	27	10,830	1.01	454	653
QLP-z71-1	interior		13.1	67	691	2.7	2.5	0.20	599	437,200	2.34	0.274	0.049	36	0.078	1.03	2.27	1.02	12	3.7	43	17.6	87	21	228	53	11,170	0.61	437	1,006
QLP-z71-2	exterior		-	67	704	3.2	2.9	-	526	437,400	2.02	-	-	32	0.049	1.00	1.90	0.97	10	3.2	38	15.1	77	19	213	48	11,460	0.53	398	965
QLP-z65-1	interior		7.9	122	731	4.3	3.9	0.28	795	449,900	2.97	0.227	0.035	74	0.225	3.16	4.74	1.91	20	6.0	67	25.1	113	26	266	57	10,690	1.39	1,093	1,307
QLP-z65-2	exterior		-	74	679	2.3	2.1	-	499	444,800	2.08	0.106	-	33	0.039	0.91	2.04	1.00	11	3.4	39	15.0	71	17	186	42	11,470	0.73	759	1,545
QLP-z74-1	interior		-	47	688	2.6	2.4	0.25	527	437,700	1.52	0.135	0.036	22	0.031	0.83	1.76	0.89	9	3.2	37	15.4	76	19	205	47	11,530	0.48	289	784
QLP-z74-2	exterior		8.7	61	712	3.5	3.2	0.25	481	440,500	2.01	0.121	0.100	32	0.066	1.06	2.01	1.13	11	3.2	35	13.8	69	17	181	41	11,510	0.64	538	1,195
QLP-z73-1	interior		-	50	669	2.1	1.9	0.17	337	442,800	1.32	0.095	-	17	-	0.50	1.14	0.71	7	2.1	25	10.3	49	12	124	28	12,040	0.49	194	489
QLP-z78-1	interior		-	166	753	5.4	5.0	0.24	969	447,700	2.20	0.201	0.036	56	0.333	4.88	7.93	2.44	32	9.0	91	32.2	139	29	278	55	10,450	1.06	720	696
QLP-z78-2	exterior		-	64	696	2.9	2.6	0.31	553	434,200	2.44	0.078	-	33	0.051	0.81	2.18	1.03	10	3.4	42	17.0	82	20	209	48	11,530	0.78	616	1,505
QLP-z1-1m2	interior		-	426	752	5.4	5.0	0.62	4,230	422,000	10.00	1.140	0.245	336	2.220	35.30	46.60	14.90	180	47.6	477	152.9	589	113	941	167	8,910	2.20	3,420	1,997
QLP-z1-2m2	exterior		-	-	-	-	-	-	710	512,000	1.44	0.530	-	25	0.131	2.80	4.30	1.83	16	4.9	49	22.2	100	23	263	51	13,630	0.53	440	910
QLP-z2-1m2	exterior		-	85	672	2.1	2.0	-	413	432,000	1.28	-	-	16	0.052	0.40	1.10	0.59	7	2.0	28	11.9	63	16	183	45	11,290	0.25	171	581
QLP-z2-2m2	interior		-	58	-	-	-	-	453	443,000	1.70	-	-	26	-	0.91	1.69	0.72	9	2.8	34	13.5	66	16	179	41	10,930	0.53	314	703
QLP-z3-1m2	interior		-	117	853	14.0	13.1	-	307	447,000	1.05	-	-	25	0.056	1.42	2.85	0.72	11	2.7	30	10.1	43	9	86	17	9,310	0.49	173	181
QLP-z3-2m2	exterior		-	145	808	9.3	8.7	-	526	442,000	2.33	-	0.025	45	0.102	1.46	2.50	1.06	14	4.3	45	17.1	75	17	165	32	9,970	1.07	421	544
QLP-z4-1m2	interior		-	35	-	-	-	-	386	432,000	1.85	-	-	25	0.037	0.66	1.68	0.66	8	2.7	28	11.5	56	14	153	37	12,090	0.57	589	1,240
QLP-z5-1m2	interior		-	194	843	12.8	12.0	-	560	467,000	1.76	-	0.031	46	0.199	3.49	4.99	1.47	19	5.2	54	18.3	79	18	174	33	9,690	1.10	406	434
QLP-z6-1m2	interior		28	42	731	4.3	4.0	-	524	438,000	1.83	0.320	0.107	25	0.035	0.70	1.50	0.76	8	2.8	34	14.7	77	19	222	54	11,240	0.43	307	778
QLP-z6-2m2	exterior		-	43	-	-	-	-	516	439,000	2.62	-	0.054	32	0.061	0.64	2.40	0.74	9	3.2	36	15.0	75	19	203	47	11,040	0.44	381	878
QLP-z7-1m2	interior		-	143	750	5.2	4.9	-	1,350	460,000	3.75	0.290	0.053	80	0.219	3.80	7.60	3.68	45	11.6	125	43.9	192	42	404	85	10,150	0.99	1,080	1,500
QLP-z7-2m2	exterior		-	68	722	3.9	3.6	0.47	872	458,000	3.63	-	-	52	0.053	1.35	2.74	1.86	17	5.7	67	25.9	129	30	311	71	11,180	0.97	860	1,534
QLP-z8-1m2	interior		-	51	-	-	-	-	501	437,000	2.16	-	-	37	0.066	0.85	2.22	1.03	12	3.6	39	14.8	72	17	187	42	10,620	0.61	635	1,280
QLP-z9-1m2	interior		-	58	669	2.1	1.9	-	400	455,000	1.66	-	-	19	0.014	0.43	1.12	0.74	7	2.1	26	11.4	59	16	178	42	11,790	0.34	243	706
QLP-z9-2m2	exterior		-	62	-	-	-	-	395	426,000	1.07	-	-	14	-	0.44	0.99	0.49	6	1.9	25	11.2	59	16	187	46	11,580	0.31	172	620
QLP-z10-1m2	interior		-	94	697	2.9	2.7	-	657	440,000	2.12	-	-	32	0.105	1.14	1.98	1.24	12	4.1	48	18.9	99	24	259	58	10,700	0.50	347	790
QLP-z11-1m2	interior		-	67	703	3.1	2.9	-	450	443,000	1.31	-	-	15	-	-	1.05	0.50	7	2.3	29	12.7	68	18	202	49	11,350	0.42	234	769
QLP-z11-2m2	exterior		-	60	680	2.4	2.2	-	416	418,000	1.80	-	-	30	0.066	0.87	1.76	1.00	10	2.5	32	12.1	59	14	148	34	10,870	0.47	491	999
QLP-z12-1m2	interior		-	35	677	2.3	2.1	-	423	440,000	2.18	-	0.103	29	0.042	0.86	1.38	0.72	8	2.7	32	12.3	61	15	169	38	11,730	0.50	431	937
QLP-z13-1m2	interior		-	106	687	2.6	2.4	-	970	440,000	3.30	0.250	0.112	38	0.179	2.92	4.53	1.77	23	6.5	76	27.5	142	34	362	79	11,590	1.00	1,400	2,060
QLP-z14-1m2	interior		-	-	738	4.6	4.3	-	767	412,000	2.61	0.750	0.350	34	0.270	2.36	3.74	1.89	16	5.3	57	23.4	112	26	286	62	10,840	0.57	522	1,024
QLP-z14-2m2	exterior		-	-	-	-	-	-	432	443,000	2.20	0.340	-	23	0.044	0.83	1.28	0.70	8	2.7	33	13.0	62	16	168	39	11,750	0.58	456	1,067
QLP-z15-2m2	exterior		-	204	851	13.8	12.9	-	2,990	424,000	33.90	1.270	0.090	357	1.010	18.40	29.90	11.30	107	30.0	299	97.4	388	75	663	111	9,360	4.72	9,000	4,900
QLP-z16-1m2	interior	QLP-z16m2	-	57	744	4.9	4.6	-	621	438,000	1.46	-	0.208	20	0.175	1.76	2.73	1.20	13	3.8	44	18.0	88	22	240	56	11,610	0.44	322	827
QLP-z16-2m2	exterior	QLP-z16m2	-	59	-	-	-	-	264	436,000	1.10	-	0.119	15	0.046	0.45	0.40	0.46	4	1.5	15	7.4	38	10	119	30	12,350	0.35	180	590
QLP-z17-1m2	interior		91	51	730	4.2	3.9	0.55	321	444,000	1.61	1.000	0.185	19	0.058	0.59	1.23	0.68	6	1.9	23	9.6	47	12	126	29	11,410	0.34	216	547
QLP-z20-1m2	exterior		-	-	-	-	-	-	365	430,000	1.37	-	-	12	-	-	0.51	0.51	5	1.8	23	9.7	55	15	185	45	11,660	0.38	126	527
QLP-z20-2m2	interior		-	-	-	-	-	-	735	417,000	1.40	-	-	22	0.082	2.01	2.56	1.46	14	4.4	52	21.3	101	26	287	68	11,360	0.38	432	1,012
QLP-z21-1m2	interior		-	60	697	2.9	2.7	-	419	436,900	1.22	-	-	15	0.036	0.46	0.92	0.72	7	2.3	29	11.8	63	16	181	44	11,250	0.36	170	594
QLP-z21-2m2	exterior		-	63	-	-	-	-	515	439,000	1.75	-	0.055	20	0.016	0.44	1.62	0.63	9	3.0	37	15.7	77	20	216	53	11,190	0.52	273	716
QLP-z22-1m2	interior		-	152	750	5.2	4.9	-	715	438,000	3.07	0.440	-	45	0.077	1.22	2.58	1.01	16	4.9	61	22.9	109	26	254	53	11,290	1.28	583	1,039
QLP-z23-1m2	interior		18.2	67	-	-	-	-	536	444,000	1.49	-	0.034	20	0.043	0.50	1.48	0.50	8	2.7	35	14.4	76	20	232	55	11,690	0.40	258	809
QLP-z24-1m2	interior		-	74	-	-	-	-	624	450,000	2.38	-	0.050	26	0.052	0.78	1.88	0.93	10	3.4	44	18.1	93	24	253	60	11,210	0.51	395	976

LA-ICP-MS signature	Zircon domain	ID-TIMS signature	Al (ppm)	P (ppm)	Zrc cryst. temp. (°C)[1]	Ti corr (ppm)	Ti (ppm)	Sr (ppm)	Y (ppm)	Zr (ppm)	Nb (ppm)	Ba (ppm)	La (ppm)	Ce (ppm)	Pr (ppm)	Nd (ppm)	Sm (ppm)	Eu (ppm)	Gd (ppm)	Tb (ppm)	Dy (ppm)	Ho (ppm)	Er (ppm)	Tm (ppm)	Yb (ppm)	Lu (ppm)	Hf (ppm)	Ta (ppm)	Th (ppm)	U (ppm)
QLP-z24-2m2	exterior		-	89	-	-	-	-	668	452,000	2.19	-	-	27	-	0.83	1.81	1.06	11	3.9	47	20.1	101	25	276	63	11,220	0.48	372	986
QLP-z25-2m2	exterior		-	86	-	-	-	-	1,209	462,000	5.86	-	-	54	0.080	0.90	3.82	1.68	20	7.3	90	36.6	178	44	457	102	11,820	1.02	715	1,590
QLP-z26-2m2	exterior		-	53	-	-	-	-	609	447,000	2.30	0.440	0.050	30	-	0.79	1.68	0.98	11	3.7	47	17.8	91	22	239	56	11,820	0.61	357	814
QLP-z28-1m2	interior		-	72	-	-	-	-	588	440,000	1.80	-	0.127	40	0.179	1.96	2.18	1.04	13	3.5	42	15.9	83	20	211	50	11,070	0.45	600	775
QLP-z29-1m2	interior		-	135	700	3.0	2.8	-	922	440,000	3.30	0.320	0.038	64	0.147	2.87	4.95	2.04	22	6.7	75	28.3	132	30	302	64	9,920	1.08	1,001	1,232
QLP-z30-1m2	interior		27	105	-	-	-	-	609	444,000	2.12	-	-	25	-	0.81	1.10	0.73	10	3.4	42	17.7	89	23	248	59	10,740	0.62	371	938
QLP-z33-1m2	interior		67	62	754	5.5	5.1	-	476	443,000	1.75	0.380	0.441	30	0.135	1.41	1.86	0.85	9	2.8	35	14.2	71	18	199	45	11,320	0.43	378	789
QLP-z34-2m2	exterior		-	57	-	-	-	-	286	439,000	1.20	-	-	14	-	0.44	0.94	0.52	5	1.6	20	8.3	43	11	121	28	11,630	0.37	183	532
QLP-z36-1m2	interior	QLP-z36_m2	-	71	672	2.1	2.0	-	396	453,000	1.04	-	-	17	-	0.49	0.94	0.58	6	2.1	26	11.5	60	16	187	44	11,210	0.31	172	529
QLP-z36-2m2	exterior	QLP-z36_m2	48	33	-	-	-	-	530	440,000	2.25	-	0.073	22	0.046	0.60	1.15	0.66	8	2.4	33	14.8	79	21	231	57	11,530	0.52	266	772
QLP-z37-1m2	interior		-	54	717	3.6	3.4	-	537	438,000	1.20	-	-	21	0.090	1.50	2.24	1.23	13	3.7	38	16.2	80	20	227	51	10,970	0.26	277	717
QLP-z37-2m2	exterior		-	-	706	3.2	3.0	-	260	442,000	0.40	-	-	10	-	-	0.40	0.32	4	1.1	17	7.6	39	11	128	32	12,170	0.25	89	383
QLP-z38-1m2	interior		-	42	-	-	-	-	400	448,000	1.75	-	-	27	0.066	0.50	1.29	0.84	8	2.4	30	11.8	58	14	156	37	11,380	0.55	440	1,067
QLP-z38-2m2	exterior		-	87	-	-	-	-	726	460,000	1.50	-	0.046	24	0.119	2.54	2.99	1.72	16	4.4	55	21.2	107	27	278	65	11,210	0.43	401	954
QLP-z39-1m2	interior		-	85	734	4.4	4.1	-	656	449,000	3.26	0.220	-	53	0.080	2.01	3.50	1.28	17	4.8	56	21.1	97	22	234	49	10,500	1.16	763	953
QLP-z39-2m2	exterior		-	40	-	-	-	0.51	734	440,000	3.33	-	-	39	0.064	0.85	1.57	1.23	14	4.5	53	22.1	108	26	280	64	11,410	0.92	708	1,397

[1] Zircon crystallisation temperature calculated applying the Ti-in-zircon thermometer by Ferry and Watson (2007)

Table S3:
LA-ICP-MS zircon geochronology (1st session)

Identifier	Integ. length (s)	Final 207/235	Final 207/235 prop2σ	Final 206/238	Final 206/238 prop2σ	Error Corr. 6/38 vs. 7/35	Final 207/206	Final 207/206 prop2σ	Final 208/232	Final 208/232 prop2σ	207/235 Age	207/235 Age prop2σ	206/238 Age	206/238 Age prop2σ	208/232 Age	208/232 Age prop2σ	Pb206 CPS	Pb207 CPS	U238 CPS
Equigranular Monzonite																			
EM-z10-1-1	26.0	0.0380	0.003	0.00602	0.00010	0.0818	0.0460	0.00320	0.00194	0.00032	37.9	2.6	38.66	0.64	39.2	6.4	350	31	2.37E+06
EM-z10-1-2	26.0	0.0400	0.002	0.00603	0.00007	0.2413	0.0482	0.00170	0.00206	0.00032	39.8	1.5	38.77	0.47	41.6	6.4	1.20E+03	86	9.95E+06
EM-z10-1-3	26.0	0.0390	0.001	0.00593	0.00008	-0.1864	0.0482	0.00160	0.00211	0.00033	38.9	1.3	38.11	0.48	42.5	6.6	1.10E+03	73	1.10E+07
EM-z1-1-1	26.1	0.0403	0.003	0.00605	0.00011	-0.1625	0.0471	0.00310	0.00193	0.00031	40.1	2.7	38.9	0.69	39	6.3	240	35	2.59E+06
EM-z11-1-1	26.0	0.0373	0.003	0.00599	0.00008	0.2547	0.0454	0.00280	0.00206	0.00032	37.1	2.4	38.49	0.51	41.7	6.5	1.30E+03	74	4.08E+06
EM-z11-1-2	26.1	0.0385	0.002	0.00592	0.00010	0.2225	0.0473	0.00210	0.00198	0.00031	38.3	1.7	38.06	0.61	40.1	6.3	390	51	5.82E+06
EM-z1-1-2	26.1	0.0390	0.001	0.00598	0.00007	0.1187	0.0470	0.00160	0.00207	0.00032	38.9	1.3	38.45	0.47	41.7	6.4	2.00E+03	110	1.66E+07
EM-z12-1-1	26.1	0.0384	0.002	0.00595	0.00008	-0.1540	0.0476	0.00220	0.00200	0.00031	38.2	1.5	38.24	0.52	40.4	6.3	700	46	6.44E+06
EM-z12-1-2	26.1	0.0369	0.002	0.00584	0.00008	0.3094	0.0463	0.00190	0.00201	0.00031	36.8	1.6	37.51	0.51	40.5	6.3	770	69	8.50E+06
EM-z13-1-1	26.1	0.0393	0.001	0.00604	0.00007	0.2732	0.0473	0.00120	0.00205	0.00031	39.11	1.1	38.83	0.43	41.31	6.3	3.70E+03	250	2.99E+07
EM-z13-1-2	26.1	0.0456	0.002	0.00671	0.00015	0.4872	0.0501	0.00190	0.00218	0.00034	45.2	1.9	43.13	0.98	44	6.9	2.30E+03	110	7.13E+06
EM-z14-1-2	26.0	0.0379	0.003	0.00607	0.00010	0.1423	0.0461	0.00290	0.00200	0.00032	37.7	2.4	38.99	0.66	40.3	6.5	170	30	2.78E+06
EM-z15-1-2	26.1	0.0386	0.001	0.00591	0.00008	0.1562	0.0473	0.00150	0.00201	0.00031	38.5	1.3	37.99	0.49	40.5	6.3	1.40E+03	80	1.10E+07
EM-z16-1-2	26.1	0.0395	0.002	0.00602	0.00009	0.2867	0.0474	0.00200	0.00215	0.00034	39.4	1.7	38.7	0.55	43.3	6.8	930	61	5.40E+06
EM-z17-1-2	26.1	0.0396	0.002	0.00606	0.00009	0.2084	0.0472	0.00200	0.00215	0.00034	39.4	1.6	38.96	0.57	43.4	6.8	1.40E+03	88	6.44E+06
EM-z18-1-1	14.0	0.0423	0.004	0.00599	0.00010	-0.1635	0.0513	0.00480	0.00186	0.00032	42	3.5	38.52	0.63	37.6	6.5	370	50	2.71E+06
EM-z18-1-2	26.1	0.0395	0.002	0.00609	0.00009	-0.0655	0.0473	0.00250	0.00200	0.00032	39.3	2.0	39.12	0.54	40.4	6.4	570	47	4.33E+06
EM-z20-1-1	26.1	0.0359	0.002	0.00584	0.00008	0.1169	0.0448	0.00200	0.00200	0.00031	35.8	1.6	37.56	0.53	40.4	6.3	410	50	7.12E+06
EM-z20-1-2	26.1	0.0381	0.002	0.00596	0.00007	0.0076	0.0466	0.00190	0.00216	0.00034	37.9	1.4	38.32	0.44	43.7	6.8	880	68	8.01E+06
EM-z2-1-1	26.3	0.0397	0.003	0.00611	0.00011	-0.0311	0.0467	0.00340	0.00202	0.00032	39.5	2.6	39.25	0.69	40.8	6.5	250	23	1.98E+06
EM-z2-1-2	25.3	0.0389	0.002	0.00596	0.00009	-0.0726	0.0474	0.00230	0.00199	0.00031	38.7	1.8	38.3	0.6	40.2	6.3	540	51	5.51E+06
EM-z22-1-1	26.0	0.0376	0.002	0.00592	0.00007	0.1454	0.0456	0.00160	0.00201	0.00031	37.4	1.5	38.06	0.47	40.61	6.2	3.00E+03	150	1.21E+07
EM-z22-1-2	26.0	0.0373	0.002	0.00596	0.00009	0.0315	0.0453	0.00210	0.00208	0.00032	37.2	1.7	38.29	0.54	42	6.5	970	68	6.32E+06
EM-z23-1-1	26.1	0.0399	0.001	0.00589	0.00009	-0.1990	0.0494	0.00200	0.00206	0.00032	39.7	1.4	37.83	0.55	41.52	6.4	1.50E+03	76	1.01E+07
EM-z23-1-2	26.8	0.0429	0.002	0.00620	0.00010	0.1163	0.0506	0.00210	0.00218	0.00034	42.6	1.8	39.81	0.63	44	6.8	850	64	5.82E+06
EM-z26-1-1	26.0	0.0382	0.003	0.00605	0.00013	0.2091	0.0451	0.00330	0.00194	0.00033	38.1	2.9	38.87	0.81	39.1	6.6	360	33	2.16E+06
EM-z26-1-2	26.1	0.0387	0.002	0.00590	0.00008	0.3201	0.0479	0.00190	0.00208	0.00032	38.5	1.8	37.9	0.52	42	6.5	820	65	5.80E+06
EM-z27-1-1	26.1	0.0391	0.001	0.00587	0.00007	-0.0295	0.0485	0.00160	0.00207	0.00032	38.9	1.4	37.75	0.47	41.7	6.5	1.70E+03	94	1.03E+07
EM-z27-1-2	26.1	0.0384	0.002	0.00587	0.00008	0.0037	0.0476	0.00200	0.00201	0.00031	38.3	1.6	37.72	0.5	40.49	6.2	1.30E+03	87	1.06E+07
EM-z28-1-1	26.1	0.0381	0.002	0.00579	0.00008	0.1320	0.0482	0.00200	0.00199	0.00031	37.9	1.5	37.21	0.48	40.2	6.2	490	48	5.20E+06
EM-z28-1-2	26.1	0.0400	0.002	0.00600	0.00009	0.2277	0.0480	0.00190	0.00215	0.00033	39.8	1.6	38.55	0.59	43.4	6.7	1.10E+03	76	7.43E+06
EM-z29-1-1	16.4	0.0374	0.003	0.00604	0.00014	0.1908	0.0447	0.00310	0.00208	0.00034	37.3	2.6	38.84	0.9	41.9	6.8	220	40	3.15E+06
EM-z29-1-2	26.1	0.0383	0.002	0.00605	0.00011	0.2481	0.0454	0.00220	0.00201	0.00032	38.1	1.7	38.88	0.67	40.5	6.5	290	23	3.00E+06
EM-z34-1-1	26.1	0.0394	0.001	0.00595	0.00007	0.2387	0.0483	0.00150	0.00212	0.00033	39.2	1.3	38.26	0.47	42.8	6.6	1.40E+03	83	1.02E+07
EM-z34-1-2	26.1	0.0399	0.001	0.00600	0.00008	0.0079	0.0484	0.00160	0.00219	0.00034	39.75	1.2	38.54	0.51	44.2	6.8	1.50E+03	70	9.97E+06
EM-z36-1-1	26.0	0.0407	0.002	0.00607	0.00009	0.0131	0.0495	0.00230	0.00193	0.00031	40.5	1.8	39.02	0.56	39	6.2	240	30	3.13E+06
EM-z36-1-2	13.5	0.0371	0.002	0.00581	0.00010	0.1209	0.0465	0.00260	0.00188	0.00031	36.9	1.8	37.35	0.66	38	6.3	370	37	4.44E+06

Identifier	Integ. length (s)	Final 207/235	Final 207/235 prop2σ	Final 206/238	Final 206/238 prop2σ	Error Corr. 6/38 vs. 7/35	Final 207/206	Final 207/206 prop2σ	Final 208/232	Final 208/232 prop2σ	207/235 Age	207/235 Age prop2σ	206/238 Age	206/238 Age prop2σ	208/232 Age	208/232 Age prop2σ	Pb206 CPS	Pb207 CPS	U238 CPS
EM-z37-1-1	26.0	0.0393	0.002	0.00614	0.00009	0.1759	0.0473	0.00200	0.00211	0.00033	39.2	1.5	39.48	0.55	42.6	6.6	970	58	5.80E+06
EM-z38-1-1	26.1	0.0394	0.001	0.00601	0.00008	-0.0908	0.0482	0.00180	0.00200	0.00031	39.2	1.3	38.6	0.48	40.3	6.3	320	36	5.49E+06
EM-z38-1-2	26.1	0.0379	0.001	0.00595	0.00008	0.0044	0.0461	0.00200	0.00201	0.00032	37.7	1.4	38.21	0.52	40.5	6.4	700	45	6.72E+06
EM-z4-1-1	26.0	0.0376	0.001	0.00584	0.00009	0.1869	0.0465	0.00150	0.00208	0.00032	37.4	1.2	37.54	0.56	42.03	6.4	1.50E+03	76	8.26E+06
EM-z4-1-2	26.1	0.0379	0.001	0.00584	0.00009	0.2864	0.0472	0.00150	0.00196	0.00031	37.8	1.2	37.51	0.6	39.5	6.3	670	47	8.11E+06
EM-z41-1-1	26.1	0.0382	0.001	0.00588	0.00009	0.3276	0.0469	0.00150	0.00211	0.00033	38	1.3	37.81	0.55	42.6	6.6	960	58	8.00E+06
EM-z41-1-2	26.1	0.0376	0.002	0.00581	0.00007	0.1393	0.0465	0.00200	0.00204	0.00032	37.4	1.6	37.36	0.47	41.2	6.4	910	70	7.58E+06
EM-z6-1-1	24.9	0.0435	0.002	0.00625	0.00010	0.1024	0.0504	0.00220	0.00213	0.00034	43.2	1.8	40.16	0.64	43	6.8	510	37	3.98E+06
EM-z6-1-2	26.0	0.0384	0.001	0.00588	0.00007	-0.2047	0.0474	0.00160	0.00199	0.00030	38.2	1.2	37.79	0.47	40.12	6.2	1.20E+03	76	1.11E+07
EM-z7-1-1	26.0	0.0399	0.002	0.00598	0.00008	-0.0986	0.0480	0.00220	0.00204	0.00032	39.7	1.7	38.42	0.54	41.2	6.4	820	66	6.73E+06
EM-z7-1-2	26.1	0.0382	0.002	0.00605	0.00008	0.2895	0.0460	0.00200	0.00197	0.00031	38	1.7	38.89	0.54	39.7	6.2	780	54	5.99E+06
EM-z8-1-1	26.1	0.0378	0.002	0.00584	0.00007	0.2503	0.0469	0.00180	0.00197	0.00030	37.6	1.5	37.53	0.47	39.78	6.1	1.70E+03	88	9.02E+06
EM-z8-1-2	19.0	0.0383	0.002	0.00590	0.00008	0.1145	0.0470	0.00240	0.00213	0.00033	38.1	2.0	37.95	0.53	43	6.6	1.20E+03	100	8.76E+06
EM-z9-1-2	26.1	0.0386	0.002	0.00598	0.00008	-0.0531	0.0471	0.00230	0.00200	0.00032	38.4	1.8	38.41	0.49	40.3	6.4	930	52	5.39E+06
Quartz Monzonite Porphyry																			
QMP-z1-1-1	26.1	0.0373	0.002	0.00589	0.00009	0.0432	0.0454	0.00220	0.00182	0.00029	37.2	1.8	37.83	0.56	36.8	5.9	1.30E+03	84	6.40E+06
QMP-z7-1-1	8.7	0.0365	0.004	0.00564	0.00019	0.1839	0.0470	0.00480	0.00169	0.00040	36.4	3.5	36.3	1.2	34	8.1	140	18	1.14E+06
QMP-z7-1-2	26.0	0.0374	0.003	0.00592	0.00012	-0.2098	0.0462	0.00410	0.00187	0.00032	37.8	3.0	38.04	0.75	37.7	6.5	200	16	1.36E+06
QMP-z7-1-3	26.1	0.0398	0.003	0.00601	0.00010	-0.1033	0.0477	0.00320	0.00193	0.00034	39.6	2.5	38.59	0.63	39	6.9	480	45	3.27E+06
QMP-z9-1-1	26.0	0.0387	0.003	0.00608	0.00011	-0.0193	0.0464	0.00370	0.00175	0.00029	38.6	3.0	39.06	0.72	35.4	5.9	160	24	1.71E+06
QMP-z9-1-2	14.7	0.0376	0.004	0.00605	0.00018	-0.1285	0.0449	0.00470	0.00216	0.00037	37.5	3.6	38.9	1.1	43.7	7.5	520	42	3.22E+06
QMP-z10-1-2	10.4	0.0433	0.003	0.00587	0.00019	0.3708	0.0537	0.00330	0.00196	0.00036	43	2.5	37.8	1.2	39.5	7.3	410	41	3.03E+06
QMP-z22-1-1	26.0	0.0397	0.003	0.00616	0.00014	0.2309	0.0465	0.00300	0.00209	0.00035	39.5	2.6	39.58	0.87	42.2	7.1	630	33	2.55E+06
QMP-z22-1-2	26.1	0.0370	0.002	0.00601	0.00009	0.1161	0.0449	0.00230	0.00183	0.00030	36.9	1.9	38.6	0.55	37	6	590	40	4.44E+06
QMP-z10-1-3	26.0	0.0399	0.003	0.00605	0.00013	-0.1405	0.0487	0.00390	0.00202	0.00034	39.7	2.8	38.87	0.86	40.9	6.9	810	46	1.70E+06
QMP-z10-1-4	10.8	0.0388	0.006	0.00609	0.00019	0.3685	0.0461	0.00680	0.00153	0.00029	38.6	5.8	39.2	1.2	30.9	5.8	200	43	1.51E+06
QMP-z17-1-2	23.8	0.0375	0.002	0.00545	0.00009	0.5372	0.0502	0.00210	0.00181	0.00029	37.4	1.8	35.03	0.56	36.6	5.8	1.80E+03	100	1.36E+07
QMP-z35-2	26.1	0.0397	0.005	0.00621	0.00013	0.2537	0.0459	0.00510	0.00166	0.00035	39.4	4.4	39.9	0.84	33.5	7	120	23	1.13E+06
QMP-z24-2	7.2	0.0500	0.011	0.00617	0.00015	0.6279	0.0580	0.01100	0.00253	0.00064	49	10.0	39.67	0.98	51	13	120	51	9.42E+05
QMP-z24-1	26.0	0.0425	0.003	0.00606	0.00013	-0.0985	0.0516	0.00350	0.00185	0.00033	42.3	2.7	38.94	0.86	37.4	6.7	190	23	1.44E+06
QMP-z15-1	26.1	0.0392	0.002	0.00585	0.00008	0.1554	0.0488	0.00210	0.00188	0.00030	39	1.7	37.62	0.53	37.9	6.1	360	32	4.39E+06
QMP-z15-2	26.1	0.0412	0.004	0.00585	0.00014	-0.0788	0.0506	0.00430	0.00172	0.00034	40.9	3.4	37.61	0.87	34.7	6.8	180	22	1.41E+06
QMP-z16-2	26.0	0.0395	0.002	0.00616	0.00010	-0.1331	0.0468	0.00280	0.00190	0.00032	39.3	2.1	39.6	0.62	38.5	6.4	190	33	3.26E+06
QMP-z27-1	7.3	0.0384	0.002	0.00578	0.00009	0.3165	0.0467	0.00310	0.00195	0.00034	38.2	2.2	37.13	0.56	39.5	6.8	4.70E+03	290	1.51E+07
QMP-z27-2	26.1	0.0381	0.003	0.00594	0.00009	0.0856	0.0471	0.00370	0.00185	0.00031	37.9	2.9	38.21	0.59	37.4	6.2	320	35	2.27E+06
QMP-z43-1	26.1	0.0408	0.003	0.00636	0.00014	0.1039	0.0455	0.00340	0.00227	0.00042	40.6	3.2	40.87	0.92	45.8	8.5	120	18	1.32E+06
QMP-z40-1	26.1	0.0412	0.002	0.00638	0.00016	0.5672	0.0473	0.00230	0.00220	0.00035	41	2.4	40.99	1	44.3	7.1	850	53	5.20E+06

Identifier	Integ. length (s)	Final 207/235	Final 207/235 prop2σ	Final 206/238	Final 206/238 prop2σ	Error Corr. 6/38 vs. 7/35	Final 207/206	Final 207/206 prop2σ	Final 208/232	Final 208/232 prop2σ	207/235 Age	207/235 Age prop2σ	206/238 Age	206/238 Age prop2σ	208/232 Age	208/232 Age prop2σ	Pb206 CPS	Pb207 CPS	U238 CPS
QMP-z40-2	5.0	0.0415	0.004	0.00585	0.00011	-0.0191	0.0512	0.00520	0.00195	0.00039	41.3	4.2	37.6	0.7	39.3	7.9	650	140	7.21E+06
QMP-z12-2	26.1	0.0398	0.004	0.00607	0.00009	0.0597	0.0477	0.00440	0.00193	0.00036	39.6	3.5	38.99	0.6	38.9	7.2	170	27	1.65E+06
QMP-z45-1	26.0	0.0359	0.002	0.00586	0.00009	-0.1050	0.0446	0.00190	0.00193	0.00030	35.8	1.5	37.64	0.57	39	6	410	53	7.61E+06
QMP-z45-2	11.1	0.0378	0.002	0.00600	0.00013	0.0984	0.0466	0.00270	0.00196	0.00033	37.7	2.2	38.57	0.85	39.5	6.7	520	72	5.77E+06
QMP-z47-1	26.0	0.0400	0.002	0.00583	0.00008	0.1560	0.0496	0.00180	0.00194	0.00030	39.9	1.5	37.45	0.51	39.2	6.1	1.70E+03	87	1.13E+07
QMP-z47-2	26.0	0.0391	0.003	0.00590	0.00011	0.4854	0.0481	0.00380	0.00193	0.00034	38.9	3.2	37.91	0.73	39	6.9	240	23	1.85E+06
QMP-z47-3	26.1	0.0377	0.002	0.00606	0.00008	0.0301	0.0450	0.00250	0.00180	0.00029	37.9	2.1	38.92	0.53	36.3	5.8	590	42	4.29E+06
QMP-z50-1	26.1	0.0407	0.004	0.00596	0.00016	0.2405	0.0500	0.00470	0.00186	0.00035	40.5	3.9	38.3	1.1	37.6	7.1	91	18	9.66E+05
QMP-z50-2	26.0	0.0363	0.003	0.00581	0.00010	0.0792	0.0456	0.00370	0.00186	0.00031	36.1	2.9	37.32	0.64	37.6	6.2	180	28	2.09E+06
QMP-z49-1	22.7	0.0369	0.001	0.00586	0.00008	-0.0036	0.0459	0.00150	0.00196	0.00031	36.74	1.1	37.65	0.53	39.6	6.3	1.80E+03	97	1.31E+07
QMP-z49-2	26.1	0.0393	0.002	0.00609	0.00009	-0.0500	0.0471	0.00230	0.00193	0.00032	39.1	1.9	39.1	0.6	39	6.5	580	46	4.36E+06
QMP-z60-1	20.5	0.0368	0.004	0.00597	0.00016	0.2025	0.0455	0.00480	0.00181	0.00037	36.6	3.8	38.4	1	36.5	7.4	270	26	1.28E+06
QMP-z60-2	26.1	0.0384	0.003	0.00595	0.00012	-0.0941	0.0469	0.00420	0.00173	0.00031	38.3	3.3	38.26	0.75	35	6.3	280	27	1.66E+06
QMP-z74-1	8.9	0.0399	0.004	0.00582	0.00013	-0.0282	0.0500	0.00500	0.00195	0.00032	39.7	3.7	37.39	0.8	39.4	6.5	1.70E+03	190	8.21E+06
QMP-z74-2	12.8	0.0390	0.004	0.00589	0.00010	-0.1632	0.0474	0.00470	0.00187	0.00032	38.8	3.8	37.83	0.66	37.8	6.5	570	78	4.18E+06
QMP-z72-1	26.1	0.0412	0.003	0.00587	0.00014	0.0358	0.0502	0.00460	0.00176	0.00032	41	3.3	37.75	0.88	35.6	6.5	110	14	9.33E+05
QMP-z72-2	26.1	0.0399	0.003	0.00604	0.00014	-0.0397	0.0479	0.00400	0.00190	0.00039	39.7	3.4	38.84	0.9	38.4	7.9	100	15	9.37E+05
QMP-z58-1	24.8	0.0394	0.004	0.00575	0.00012	-0.0946	0.0496	0.00520	0.00196	0.00036	39.2	4.0	36.98	0.8	40.3	7.5	1.10E+03	74	1.69E+06
QMP-z58-2	26.1	0.0423	0.003	0.00610	0.00011	0.0458	0.0501	0.00350	0.00190	0.00033	42.1	2.7	39.18	0.73	38.5	6.7	450	37	2.07E+06
QMP-z76-1	17.9	0.0369	0.002	0.00573	0.00008	-0.0350	0.0468	0.00240	0.00181	0.00031	36.7	1.9	36.85	0.53	36.6	6.2	2.90E+03	160	7.45E+06
QMP-z88-1	5.3	0.0394	0.003	0.00562	0.00014	-0.4775	0.0508	0.00400	0.00187	0.00030	39.2	2.5	36.14	0.89	37.8	6.1	1.40E+03	95	7.13E+06
QMP-z83-1	26.1	0.0406	0.004	0.00591	0.00015	0.0050	0.0503	0.00540	0.00201	0.00040	40.3	4.2	37.98	0.99	40.7	8	210	18	9.05E+05
QMP-z83-2	26.1	0.0389	0.003	0.00608	0.00013	-0.0809	0.0447	0.00430	0.00206	0.00040	38.7	3.2	39.07	0.84	41.6	8.1	350	24	1.13E+06
QMP-z84-1	7.0	0.0407	0.005	0.00621	0.00011	-0.2665	0.0473	0.00570	0.00191	0.00036	40.5	4.6	39.89	0.68	38.5	7.2	640	67	2.68E+06
QMP-z84-2	9.2	0.0420	0.003	0.00601	0.00012	-0.0856	0.0503	0.00390	0.00191	0.00032	41.8	3.1	38.63	0.75	38.5	6.5	320	58	4.09E+06
QMP-z69-2	26.0	0.0384	0.003	0.00616	0.00013	0.1213	0.0453	0.00320	0.00184	0.00031	38.2	2.6	39.59	0.83	37.2	6.2	800	43	2.35E+06
QMP-z56-1	20.0	0.0429	0.005	0.00613	0.00014	0.2065	0.0497	0.00510	0.00189	0.00034	42.6	4.6	39.37	0.9	38.1	6.9	210	27	1.21E+06
QMP-z56-2	26.0	0.0368	0.001	0.00587	0.00009	-0.0555	0.0457	0.00190	0.00205	0.00032	36.7	1.3	37.7	0.6	41.4	6.4	1.50E+03	94	7.68E+06
QMP-z78-1	26.1	0.0370	0.002	0.00571	0.00009	-0.1761	0.0470	0.00280	0.00179	0.00029	36.8	2.1	36.68	0.6	36.2	5.8	720	54	3.29E+06
QMP-z78-2	9.6	0.0388	0.004	0.00606	0.00020	0.2830	0.0457	0.00480	0.00212	0.00044	38.7	4.3	38.9	1.3	42.8	8.9	230	38	2.05E+06
QMP-z62-1	15.5	0.0433	0.003	0.00622	0.00014	0.2690	0.0508	0.00310	0.00193	0.00033	43	2.7	39.97	0.92	39.1	6.6	910	53	2.74E+06
QMP-z63-1	12.6	0.0355	0.002	0.00584	0.00011	0.2457	0.0437	0.00270	0.00185	0.00030	35.4	2.2	37.52	0.72	37.4	6.1	1.20E+03	83	6.26E+06
QMP-z63-2	12.1	0.0410	0.003	0.00584	0.00012	-0.1985	0.0510	0.00380	0.00199	0.00032	40.8	2.8	37.56	0.8	40.2	6.4	330	64	4.62E+06
QMP-z03-1	26.1	0.0389	0.003	0.00584	0.00014	0.0071	0.0477	0.00400	0.00176	0.00031	38.7	3.2	37.51	0.92	35.6	6.3	190	20	1.26E+06
QMP-z51-2	16.4	0.0382	0.002	0.00579	0.00011	0.2980	0.0481	0.00270	0.00182	0.00030	38	2.2	37.22	0.73	36.7	6.1	270	50	5.13E+06
Latite Porphyry																			
LP-z01-1	12.8	0.0462	0.002	0.00585	0.00009	0.0201	0.0573	0.00290	0.00212	0.00036	45.9	2.2	37.62	0.56	42.9	7.3	5.60E+03	340	9.20E+06

Identifier	Integ. length (s)	Final 207/235	Final 207/235 prop2σ	Final 206/238	Final 206/238 prop2σ	Error Corr. 6/38 vs. 7/35	Final 207/206	Final 207/206 prop2σ	Final 208/232	Final 208/232 prop2σ	207/235 Age	207/235 Age prop2σ	206/238 Age	206/238 Age prop2σ	208/232 Age	208/232 Age prop2σ	Pb206 CPS	Pb207 CPS	U238 CPS
LP-z01-2	26.1	0.0391	0.002	0.00601	0.00008	-0.0127	0.0472	0.00180	0.00199	0.00032	39	1.5	38.62	0.5	40.3	6.5	1.00E+03	57	4.63E+06
LP-z02-1	26.1	0.0378	0.003	0.00617	0.00012	0.2953	0.0448	0.00280	0.00178	0.00034	37.7	2.4	39.63	0.75	35.9	6.9	410	23	1.51E+06
LP-z02-2	26.0	0.0377	0.002	0.00574	0.00008	0.2646	0.0474	0.00180	0.00195	0.00031	37.5	1.5	36.88	0.5	39.3	6.4	920	65	9.74E+06
LP-z03-1	26.1	0.0403	0.002	0.00620	0.00011	0.1861	0.0472	0.00210	0.00205	0.00033	40.1	1.8	39.86	0.68	41.4	6.6	3.20E+03	160	6.55E+06
LP-z03-2	8.7	0.0364	0.002	0.00580	0.00012	0.2334	0.0453	0.00230	0.00201	0.00033	36.3	2.0	37.27	0.75	40.6	6.6	820	94	1.01E+07
LP-z05-1	26.0	0.0375	0.001	0.00594	0.00007	0.3035	0.0464	0.00170	0.00189	0.00030	37.3	1.3	38.17	0.45	38.2	6.1	1.20E+03	100	1.26E+07
LP-z05-2	26.0	0.0377	0.003	0.00614	0.00012	0.0442	0.0451	0.00400	0.00176	0.00035	37.5	3.2	39.46	0.76	35.5	7.1	320	25	1.28E+06
LP-z06-1	6.8	0.0399	0.005	0.00574	0.00024	0.3103	0.0506	0.00540	0.00207	0.00035	39.7	4.6	36.9	1.6	41.9	7	4.00E+03	230	8.00E+06
LP-z06-2	26.0	0.0374	0.002	0.00598	0.00008	0.1635	0.0463	0.00190	0.00185	0.00030	37.2	1.6	38.46	0.53	37.3	6	1.20E+03	91	8.24E+06
LP-z07-1	26.1	0.0392	0.003	0.00610	0.00011	-0.2047	0.0461	0.00330	0.00181	0.00030	39	2.7	39.19	0.68	36.5	6.1	270	35	2.73E+06
LP-z31-1	26.0	0.0381	0.002	0.00601	0.00010	0.1861	0.0464	0.00210	0.00197	0.00032	37.9	1.6	38.64	0.66	39.7	6.4	1.10E+03	52	4.81E+06
LP-z31-2	26.0	0.0384	0.001	0.00599	0.00008	0.2272	0.0463	0.00150	0.00192	0.00030	38.2	1.4	38.46	0.49	38.7	6.1	1.30E+03	79	9.37E+06
LP-z46-1	17.1	0.0397	0.002	0.00594	0.00015	0.0990	0.0478	0.00290	0.00190	0.00030	40	2.2	38.18	0.98	38.4	6.1	240	37	3.60E+06
LP-z46-2	12.0	0.0374	0.003	0.00576	0.00008	0.4234	0.0473	0.00320	0.00193	0.00031	37.2	2.5	37.02	0.53	38.9	6.3	880	120	9.58E+06
LP-z43-1	26.1	0.0367	0.001	0.00578	0.00008	0.0038	0.0462	0.00160	0.00191	0.00031	36.57	1.1	37.14	0.53	38.6	6.2	1.10E+03	57	8.36E+06
LP-z43-2	26.0	0.0360	0.002	0.00584	0.00009	-0.2599	0.0451	0.00230	0.00187	0.00031	35.9	1.6	37.53	0.56	37.7	6.4	670	55	5.91E+06
LP-z45-1	3.1	0.0373	0.005	0.00583	0.00026	0.6454	0.0463	0.00540	0.00185	0.00064	37.2	5.2	37.5	1.6	37	13	1.60E+03	180	8.32E+06
LP-z45-2	10.3	0.0381	0.002	0.00569	0.00011	-0.0112	0.0483	0.00200	0.00190	0.00031	38	1.4	36.58	0.71	38.3	6.4	460	58	9.67E+06
LP-z39-1	26.0	0.0465	0.004	0.00605	0.00018	0.1118	0.0565	0.00550	0.00186	0.00039	46.1	4.3	38.9	1.1	37.6	7.8	370	27	9.50E+05
LP-z39-2	26.1	0.0361	0.002	0.00596	0.00011	0.2526	0.0439	0.00220	0.00192	0.00031	36	1.9	38.28	0.68	38.7	6.3	890	54	4.55E+06
LP-z36-1	19.0	0.0385	0.002	0.00617	0.00015	0.3318	0.0459	0.00270	0.00192	0.00033	38.4	2.3	39.62	0.99	38.8	6.6	1.20E+03	63	2.60E+06
LP-z23-1	26.0	0.0390	0.002	0.00585	0.00010	0.3546	0.0484	0.00260	0.00191	0.00031	38.8	2.1	37.61	0.66	38.6	6.2	1.60E+03	67	4.83E+06
LP-z23-2	26.1	0.0380	0.003	0.00639	0.00013	0.0911	0.0434	0.00380	0.00218	0.00040	37.9	3.3	41.08	0.84	43.9	8.1	430	30	1.45E+06
LP-z24-1	26.1	0.0380	0.002	0.00601	0.00009	0.0899	0.0461	0.00210	0.00187	0.00029	37.9	1.7	38.63	0.6	37.7	5.9	3.70E+03	180	8.70E+06
LP-z24-2	26.0	0.0365	0.002	0.00587	0.00009	0.1983	0.0452	0.00170	0.00194	0.00030	36.4	1.5	37.74	0.54	39.1	6.1	1.10E+03	74	9.79E+06
LP-z25-1	10.1	0.0402	0.005	0.00602	0.00015	-0.0178	0.0491	0.00640	0.00196	0.00038	40	5.2	38.71	0.95	39.6	7.6	1.00E+03	42	2.63E+06
LP-z25-2	26.1	0.0398	0.002	0.00614	0.00010	0.3557	0.0474	0.00250	0.00197	0.00032	39.6	2.2	39.45	0.63	39.7	6.4	750	53	4.30E+06
LP-z38-1	7.5	0.0389	0.004	0.00584	0.00017	0.6910	0.0480	0.00350	0.00189	0.00035	38.7	3.5	37.5	1.1	38.2	7	780	140	9.76E+06
LP-z38-2	26.0	0.0381	0.002	0.00602	0.00008	0.1726	0.0466	0.00220	0.00181	0.00029	37.9	1.9	38.71	0.51	36.4	5.9	1.20E+03	69	5.36E+06
LP-z35-1	26.1	0.0375	0.002	0.00586	0.00010	0.3993	0.0469	0.00220	0.00180	0.00029	37.4	1.9	37.64	0.64	36.4	5.9	1.80E+03	73	5.44E+06
LP-z35-2	18.3	0.0404	0.003	0.00611	0.00013	0.0994	0.0482	0.00370	0.00184	0.00037	40.2	3.0	39.29	0.86	37.2	7.4	520	40	2.10E+06
LP-z52-2	26.1	0.0378	0.002	0.00584	0.00008	0.0758	0.0471	0.00190	0.00184	0.00030	37.7	1.5	37.53	0.5	37.2	6	800	53	6.99E+06
LP-z33-1	26.1	0.0384	0.004	0.00593	0.00015	0.1985	0.0470	0.00470	0.00178	0.00031	38.2	3.8	38.11	0.95	36	6.3	360	24	1.19E+06
LP-z33-2	26.0	0.0379	0.003	0.00593	0.00013	0.0051	0.0457	0.00300	0.00191	0.00033	37.7	2.4	38.14	0.82	38.6	6.7	240	20	1.88E+06
LP-z19-1	3.6	0.0370	0.013	0.00599	0.00032	0.4797	0.0450	0.01500	0.00181	0.00051	37	13.0	38.5	2.1	36.6	10	360	110	1.88E+06
LP-z19-2	26.1	0.0366	0.001	0.00588	0.00009	0.2042	0.0454	0.00160	0.00174	0.00028	36.5	1.4	37.78	0.6	35.2	5.6	560	45	7.26E+06
LP-z10-2	26.1	0.0388	0.001	0.00584	0.00008	0.4496	0.0480	0.00150	0.00181	0.00029	38.7	1.4	37.56	0.5	36.6	5.9	710	60	9.76E+06

Identifier	Integ. length (s)	Final 207/235	Final 207/235 prop2σ	Final 206/238	Final 206/238 prop2σ	Error Corr. 6/38 vs. 7/35	Final 207/206	Final 207/206 prop2σ	Final 208/232	Final 208/232 prop2σ	207/235 Age	207/235 Age prop2σ	206/238 Age	206/238 Age prop2σ	208/232 Age	208/232 Age prop2σ	Pb206 CPS	Pb207 CPS	U238 CPS
LP-z22-1	26.1	0.0416	0.004	0.00607	0.00013	0.0088	0.0520	0.00490	0.00192	0.00031	41.3	3.6	39.02	0.86	38.8	6.3	180	26	1.36E+06
LP-z22-2	26.0	0.0391	0.002	0.00599	0.00008	0.4146	0.0476	0.00210	0.00188	0.00030	38.9	2.0	38.51	0.53	38	6.1	950	51	4.78E+06
LP-z41-1	5.5	0.0374	0.004	0.00615	0.00019	-0.0287	0.0441	0.00480	0.00214	0.00048	37.3	4.1	39.5	1.2	43.1	9.8	820	96	6.48E+06
LP-z41-2	26.1	0.0405	0.003	0.00615	0.00009	0.2242	0.0482	0.00270	0.00202	0.00033	40.2	2.4	39.53	0.59	40.8	6.6	250	48	4.71E+06
LP-z40-1	26.0	0.0372	0.003	0.00604	0.00012	-0.1264	0.0459	0.00460	0.00173	0.00030	37	3.4	38.82	0.74	34.9	6.1	150	19	1.24E+06
LP-z40-2	26.1	0.0402	0.002	0.00603	0.00009	0.1118	0.0482	0.00170	0.00188	0.00030	40.1	1.4	38.76	0.6	38	6.1	660	37	4.97E+06
LP-z42-2	26.1	0.0384	0.002	0.00593	0.00008	0.1958	0.0466	0.00220	0.00199	0.00032	38.2	1.9	38.1	0.54	40.1	6.5	740	68	6.42E+06
LP-z59-2	26.0	0.0363	0.002	0.00582	0.00008	0.0202	0.0456	0.00220	0.00186	0.00030	36.2	1.6	37.43	0.48	37.6	6.1	990	60	6.94E+06
LP-z58-2	26.1	0.0360	0.002	0.00584	0.00008	0.0658	0.0448	0.00200	0.00186	0.00030	35.9	1.6	37.53	0.53	37.6	6.2	1.70E+03	88	7.30E+06
LP-z71-2	26.1	0.0400	0.001	0.00581	0.00009	0.0398	0.0505	0.00170	0.00195	0.00031	39.8	1.3	37.36	0.55	39.3	6.3	790	49	7.06E+06
LP-z83-1	26.1	0.0385	0.002	0.00571	0.00010	0.0913	0.0485	0.00240	0.00200	0.00033	38.4	1.9	36.71	0.61	40.5	6.7	1.50E+03	87	5.18E+06
LP-z83-2	26.1	0.0376	0.002	0.00588	0.00008	0.1278	0.0454	0.00240	0.00189	0.00031	37.4	2.0	37.89	0.53	38.1	6.2	420	35	3.38E+06
LP-z99-1	26.1	0.0376	0.003	0.00593	0.00013	-0.0204	0.0459	0.00330	0.00214	0.00035	37.4	2.5	38.11	0.8	43.2	7	700	44	2.47E+06
LP-z99-2	26.1	0.0364	0.001	0.00564	0.00007	0.1233	0.0473	0.00170	0.00191	0.00030	36.3	1.3	36.25	0.47	38.5	6.1	510	42	7.55E+06
LP-z96-1	26.1	0.0411	0.004	0.00608	0.00014	-0.0875	0.0486	0.00460	0.00187	0.00035	40.9	3.7	39.08	0.91	37.7	7	190	21	1.11E+06
LP-z96-2	26.1	0.0361	0.002	0.00587	0.00010	0.0915	0.0456	0.00290	0.00171	0.00029	36	2.2	37.73	0.65	34.5	5.8	340	45	3.51E+06
LP-z90-1	26.1	0.0398	0.004	0.00602	0.00015	0.1553	0.0477	0.00420	0.00182	0.00035	39.6	3.6	38.7	0.93	36.7	7.2	360	22	1.09E+06
LP-z90-2	4.3	0.0387	0.003	0.00603	0.00005	-0.2752	0.0460	0.00410	0.00192	0.00037	38.6	3.1	38.774	0.32	38.8	7.4	1.10E+03	160	1.12E+07
LP-z82-1	26.0	0.0366	0.002	0.00592	0.00009	0.2111	0.0452	0.00210	0.00194	0.00031	36.5	1.8	38.04	0.55	39.1	6.2	990	62	5.37E+06
LP-z82-2	17.6	0.0354	0.001	0.00555	0.00007	0.1800	0.0469	0.00180	0.00188	0.00030	35.3	1.3	35.7	0.45	38	6	1.70E+03	150	1.61E+07
LP-z79-1	26.0	0.0370	0.002	0.00594	0.00010	-0.1475	0.0452	0.00310	0.00189	0.00032	36.8	2.3	38.15	0.65	38.1	6.5	370	43	3.53E+06
LP-z79-2	26.1	0.0368	0.001	0.00589	0.00007	0.2130	0.0454	0.00150	0.00190	0.00031	36.7	1.3	37.84	0.47	38.3	6.2	1.10E+03	60	7.59E+06
LP-z67-1	26.0	0.0382	0.002	0.00594	0.00010	0.2752	0.0468	0.00200	0.00206	0.00033	38.1	1.6	38.2	0.61	41.6	6.7	570	65	7.58E+06
LP-z67-2	26.0	0.0370	0.002	0.00576	0.00008	0.0416	0.0469	0.00250	0.00195	0.00032	36.9	1.9	37.05	0.51	39.5	6.4	270	51	5.50E+06
LP-z66-2	26.1	0.0364	0.001	0.00586	0.00008	-0.0186	0.0456	0.00170	0.00193	0.00031	36.3	1.4	37.64	0.52	38.9	6.3	440	55	9.28E+06
LP-z78-1	20.0	0.0376	0.002	0.00570	0.00008	0.2558	0.0481	0.00210	0.00198	0.00031	37.4	1.6	36.64	0.54	39.9	6.2	400	52	6.23E+06
LP-z78-2	26.1	0.0378	0.002	0.00577	0.00007	-0.0084	0.0480	0.00210	0.00202	0.00033	37.7	1.6	37.08	0.46	40.9	6.6	380	48	6.29E+06
LP-z88-1	26.1	0.0381	0.002	0.00587	0.00008	0.1007	0.0469	0.00200	0.00202	0.00031	37.9	1.6	37.72	0.48	40.8	6.3	1.60E+03	100	7.43E+06
LP-z88-2	26.1	0.0387	0.001	0.00588	0.00008	-0.1983	0.0468	0.00190	0.00192	0.00031	38.5	1.4	37.8	0.51	38.9	6.4	1.00E+03	76	7.71E+06
LP-z73-1	26.0	0.0426	0.002	0.00627	0.00010	0.1246	0.0491	0.00160	0.00251	0.00039	42.4	1.4	40.31	0.64	50.7	7.8	2.10E+03	130	1.04E+07
LP-z73-2	26.1	0.0429	0.004	0.00585	0.00015	-0.0869	0.0531	0.00520	0.00212	0.00040	42.6	4.1	37.63	0.93	42.8	8.2	110	16	8.25E+05
LP-z73-3	26.1	0.0353	0.003	0.00597	0.00014	0.3462	0.0437	0.00380	0.00196	0.00036	35.2	3.0	38.38	0.87	39.5	7.2	270	24	1.59E+06
LP-z64-1	26.1	0.0407	0.003	0.00605	0.00011	0.2432	0.0486	0.00320	0.00195	0.00033	40.5	2.6	38.9	0.69	39.5	6.6	260	38	3.11E+06
LP-z64-2	16.2	0.0388	0.002	0.00588	0.00011	0.1210	0.0482	0.00230	0.00205	0.00036	38.7	1.8	37.8	0.7	41.5	7.2	670	33	6.11E+06
LP-z90-3	26.1	0.0394	0.003	0.00602	0.00013	0.2731	0.0470	0.00360	0.00202	0.00035	39.2	3.0	38.71	0.83	40.7	7.1	650	44	2.36E+06
LP-z90-4	26.1	0.0380	0.002	0.00576	0.00008	0.1148	0.0478	0.00230	0.00195	0.00031	37.9	1.9	37.02	0.54	39.4	6.3	1.50E+03	73	5.44E+06
LP-z68-1	26.0	0.0393	0.002	0.00592	0.00010	0.0735	0.0497	0.00240	0.00201	0.00033	39.1	2.0	38.05	0.61	40.6	6.6	630	41	4.49E+06

Identifier	Integ. length (s)	Final 207/235	Final 207/235 prop2σ	Final 206/238	Final 206/238 prop2σ	Error Corr. 6/38 vs. 7/35	Final 207/206	Final 207/206 prop2σ	Final 208/232	Final 208/232 prop2σ	207/235 Age	207/235 Age prop2σ	206/238 Age	206/238 Age prop2σ	208/232 Age	208/232 Age prop2σ	Pb206 CPS	Pb207 CPS	U238 CPS
LP-z68-2	26.1	0.0370	0.002	0.00609	0.00010	0.1973	0.0452	0.00300	0.00199	0.00033	36.9	2.4	39.13	0.66	40.2	6.8	380	46	3.91E+06
LP-z70-1	26.0	0.0370	0.003	0.00605	0.00013	0.3491	0.0444	0.00380	0.00193	0.00033	36.8	3.3	38.9	0.8	39	6.6	150	27	1.72E+06
LP-z70-2	26.1	0.0373	0.003	0.00587	0.00010	0.1484	0.0450	0.00340	0.00195	0.00039	37.1	2.9	37.75	0.64	39.3	7.9	120	22	1.75E+06
LP-z81-2	26.1	0.0371	0.002	0.00578	0.00007	0.2948	0.0467	0.00230	0.00193	0.00031	37	1.8	37.12	0.42	38.9	6.2	1.20E+03	75	7.65E+06
Quarz Latite Porphyry																			
QLP-z10-2	26.1	0.0371	0.002	0.00589	0.00009	0.2115	0.0460	0.00180	0.00194	0.00032	37	1.4	37.88	0.56	39.1	6.5	450	34	5.64E+06
QLP-z2-1	26.1	0.0400	0.002	0.00594	0.00011	0.2467	0.0485	0.00220	0.00225	0.00041	39.8	2.0	38.18	0.69	45.4	8.4	530	33	3.44E+06
QLP-z2-2	16.4	0.0362	0.002	0.00574	0.00009	0.2268	0.0458	0.00250	0.00200	0.00037	36.5	1.8	36.88	0.58	40.5	7.4	1.00E+03	54	4.32E+06
QLP-z3-1	26.0	0.0459	0.003	0.00662	0.00013	0.0436	0.0501	0.00340	0.00208	0.00037	45.5	3.0	42.52	0.84	42	7.5	430	40	2.28E+06
QLP-z3-3	26.1	0.0360	0.001	0.00568	0.00008	0.1137	0.0463	0.00160	0.00189	0.00032	35.9	1.3	36.48	0.54	38.2	6.4	430	39	6.61E+06
QLP-z11-1	26.1	0.0378	0.001	0.00537	0.00009	0.5228	0.0512	0.00170	0.00189	0.00031	37.7	1.4	34.52	0.57	38.2	6.2	2.50E+03	150	1.99E+07
QLP-z11-2	26.0	0.0349	0.001	0.00542	0.00008	0.3438	0.0466	0.00170	0.00186	0.00031	34.8	1.3	34.87	0.5	37.5	6.3	2.20E+03	110	7.84E+06
QLP-z21-1	26.1	0.0393	0.002	0.00594	0.00010	0.1297	0.0488	0.00250	0.00208	0.00034	39.1	1.9	38.18	0.61	41.9	6.9	590	50	5.10E+06
QLP-z21-2	26.0	0.0371	0.002	0.00579	0.00007	0.0899	0.0464	0.00180	0.00182	0.00031	37	1.5	37.21	0.47	36.8	6.2	590	55	6.92E+06
QLP-z35-1	26.1	0.0393	0.002	0.00573	0.00007	0.0106	0.0497	0.00200	0.00193	0.00030	39.1	1.6	36.81	0.47	38.9	6.1	1.30E+03	73	7.99E+06
QLP-z35-2	26.0	0.0364	0.002	0.00574	0.00008	0.5030	0.0460	0.00170	0.00190	0.00030	36.3	1.5	36.89	0.51	38.4	6.1	1.10E+03	64	8.24E+06
QLP-z38-1	26.0	0.0388	0.003	0.00630	0.00012	-0.0594	0.0446	0.00340	0.00207	0.00035	38.6	2.8	40.5	0.79	41.9	7	320	26	1.63E+06
QLP-z38-2	26.1	0.0370	0.002	0.00575	0.00008	-0.0617	0.0464	0.00210	0.00190	0.00034	36.9	1.5	36.94	0.53	38.4	6.8	460	42	5.13E+06
QLP-z24-1	26.1	0.0385	0.001	0.00579	0.00008	0.0516	0.0484	0.00150	0.00193	0.00031	38.4	1.2	37.19	0.51	39	6.3	710	44	8.57E+06
QLP-z24-2	26.1	0.0390	0.002	0.00609	0.00010	-0.0470	0.0465	0.00270	0.00197	0.00036	39.2	2.2	39.13	0.62	39.7	7.3	380	36	3.53E+06
QLP-z13-1	26.1	0.0431	0.002	0.00595	0.00007	0.1109	0.0530	0.00190	0.00217	0.00033	42.9	1.5	38.25	0.43	43.7	6.8	830	78	1.16E+07
QLP-z13-2	26.1	0.0369	0.002	0.00573	0.00008	0.3452	0.0468	0.00190	0.00181	0.00030	36.8	1.5	36.81	0.49	36.5	6.1	890	60	7.67E+06
QLP-z25-1	25.5	0.0359	0.002	0.00535	0.00008	0.4677	0.0483	0.00180	0.00185	0.00029	35.8	1.5	34.41	0.54	37.3	5.8	1.40E+03	110	1.23E+07
QLP-z25-2	26.1	0.0370	0.002	0.00556	0.00007	0.3255	0.0479	0.00180	0.00179	0.00029	36.8	1.5	35.72	0.47	36.1	5.9	1.10E+03	78	8.19E+06
QLP-z14-1	14.4	0.0384	0.002	0.00582	0.00013	0.3470	0.0478	0.00250	0.00174	0.00028	38.3	2.1	37.39	0.82	35.1	5.7	1.80E+03	100	7.34E+06
QLP-z14-2	26.1	0.0389	0.002	0.00584	0.00008	-0.1278	0.0481	0.00260	0.00174	0.00032	38.8	2.0	37.57	0.53	35.1	6.5	490	41	3.25E+06
QLP-z5-1	5.5	0.0359	0.003	0.00590	0.00015	0.2081	0.0439	0.00350	0.00183	0.00035	35.8	2.8	37.92	0.98	37	7.1	600	100	9.14E+06
QLP-z5-2	26.0	0.0375	0.002	0.00610	0.00012	0.3306	0.0448	0.00200	0.00183	0.00033	37.4	1.7	39.22	0.78	37	6.6	450	36	4.30E+06
QLP-z4-1	26.1	0.0461	0.004	0.00593	0.00010	0.3600	0.0566	0.00510	0.00228	0.00043	45.7	3.9	38.09	0.61	46.1	8.7	2.40E+03	160	4.52E+06
QLP-z4-2	26.1	0.0408	0.002	0.00565	0.00008	0.1827	0.0519	0.00200	0.00196	0.00032	40.6	1.6	36.3	0.5	39.7	6.5	1.30E+03	85	6.20E+06
QLP-z12-2	26.0	0.0405	0.002	0.00573	0.00008	0.3041	0.0508	0.00220	0.00184	0.00035	40.3	1.7	36.86	0.53	37.1	7	1.00E+03	66	5.14E+06
QLP-z7-1	26.1	0.0373	0.002	0.00592	0.00007	0.0425	0.0454	0.00200	0.00190	0.00031	37.1	1.7	38.05	0.48	38.4	6.3	620	62	7.43E+06
QLP-z7-2	26.1	0.0395	0.002	0.00591	0.00010	0.1563	0.0475	0.00280	0.00205	0.00036	39.3	2.3	38	0.62	41.3	7.2	480	47	4.07E+06
QLP-z15-1	26.0	0.0378	0.002	0.00587	0.00008	-0.0173	0.0473	0.00250	0.00167	0.00027	37.6	1.8	37.72	0.49	33.8	5.4	210	28	3.12E+06
QLP-z15-2	26.1	0.0386	0.002	0.00590	0.00008	0.1478	0.0473	0.00200	0.00173	0.00028	38.5	1.7	37.92	0.52	34.9	5.7	1.20E+03	65	7.22E+06
QLP-z16-1	26.1	0.0426	0.002	0.00576	0.00009	-0.1371	0.0542	0.00300	0.00196	0.00032	42.3	2.1	37.04	0.55	39.5	6.4	880	91	6.23E+06
QLP-z16-2	26.0	0.0364	0.002	0.00580	0.00010	-0.3381	0.0457	0.00260	0.00171	0.00029	36.3	1.8	37.31	0.61	34.6	5.8	600	50	4.70E+06

Identifier	Integ. length (s)	Final 207/235	Final 207/235 prop2σ	Final 206/238	Final 206/238 prop2σ	Error Corr. 6/38 vs. 7/35	Final 207/206	Final 207/206 prop2σ	Final 208/232	Final 208/232 prop2σ	207/235 Age	207/235 Age prop2σ	206/238 Age	206/238 Age prop2σ	208/232 Age	208/232 Age prop2σ	Pb206 CPS	Pb207 CPS	U238 CPS
QLP-z17-1	26.1	0.0411	0.002	0.00598	0.00011	-0.0374	0.0499	0.00230	0.00207	0.00035	40.9	1.8	38.41	0.67	41.7	7	570	46	5.14E+06
QLP-z17-2	26.1	0.0403	0.002	0.00578	0.00009	0.2529	0.0502	0.00240	0.00179	0.00029	40.1	1.9	37.16	0.56	36.2	5.9	590	60	5.67E+06
QLP-z28-1	26.1	0.0372	0.002	0.00567	0.00008	0.3437	0.0478	0.00250	0.00176	0.00028	37	2.0	36.47	0.54	35.5	5.6	1.10E+03	62	4.42E+06
QLP-z28-2	26.1	0.0354	0.001	0.00573	0.00007	0.1614	0.0448	0.00160	0.00177	0.00028	35.3	1.4	36.8	0.42	35.7	5.6	1.20E+03	87	1.04E+07
QLP-z54-2	26.0	0.0384	0.001	0.00559	0.00008	0.0757	0.0496	0.00190	0.00171	0.00028	38.3	1.4	35.92	0.49	34.4	5.6	440	47	6.50E+06
QLP-z40-1	9.6	0.0419	0.003	0.00631	0.00019	0.3585	0.0489	0.00350	0.00173	0.00030	41.6	2.9	40.6	1.2	34.9	6.1	810	69	5.19E+06
QLP-z40-2	26.0	0.0347	0.002	0.00575	0.00010	0.3506	0.0436	0.00170	0.00178	0.00030	34.6	1.6	36.93	0.61	36	6	890	59	6.50E+06
QLP-z41-1	26.0	0.0494	0.003	0.00628	0.00010	0.3390	0.0586	0.00320	0.00212	0.00035	48.9	2.8	40.33	0.62	42.7	7	520	52	3.97E+06
QLP-z41-2	26.0	0.0374	0.002	0.00606	0.00009	0.2774	0.0443	0.00200	0.00202	0.00035	37.3	1.9	38.93	0.59	40.8	7	460	39	3.92E+06
QLP-z30-1	26.0	0.0396	0.002	0.00582	0.00009	-0.1039	0.0497	0.00200	0.00186	0.00029	39.5	1.6	37.44	0.59	37.6	5.9	1.70E+03	110	8.20E+06
QLP-z29_-2	26.0	0.0408	0.003	0.00595	0.00013	-0.0570	0.0515	0.00390	0.00198	0.00035	40.6	3.1	38.21	0.83	39.9	7	240	31	1.71E+06
QLP-z31-1	26.1	0.0367	0.002	0.00573	0.00009	0.1330	0.0479	0.00260	0.00187	0.00031	36.6	2.0	36.85	0.57	37.8	6.3	1.50E+03	100	5.73E+06
QLP-z57-1	26.0	0.0380	0.002	0.00576	0.00010	-0.0264	0.0483	0.00290	0.00184	0.00031	37.8	2.1	37.04	0.62	37.1	6.3	670	42	3.30E+06
QLP-z57-2	26.0	0.0370	0.002	0.00559	0.00008	0.1514	0.0482	0.00210	0.00170	0.00028	36.9	1.6	35.96	0.52	34.4	5.6	1.20E+03	55	7.03E+06
QLP-z43-1	26.1	0.0377	0.001	0.00579	0.00009	0.0755	0.0481	0.00190	0.00170	0.00028	37.8	1.5	37.2	0.58	34.3	5.7	320	50	7.34E+06
QLP-z43-2	26.1	0.0373	0.002	0.00567	0.00008	-0.0455	0.0485	0.00230	0.00172	0.00028	37.2	1.7	36.43	0.5	34.7	5.7	770	52	5.94E+06
QLP-z66-2	26.0	0.0398	0.003	0.00597	0.00012	-0.0380	0.0490	0.00320	0.00183	0.00033	39.6	2.6	38.4	0.76	36.9	6.6	1.10E+03	66	3.68E+06
QLP-z67-1	13.5	0.0371	0.001	0.00565	0.00008	-0.2810	0.0473	0.00160	0.00182	0.00028	37	1.4	36.34	0.51	36.69	5.6	3.90E+03	170	1.86E+07
QLP-z67-2	26.1	0.0364	0.001	0.00569	0.00007	0.3135	0.0462	0.00150	0.00183	0.00029	36.3	1.3	36.58	0.43	37	5.8	1.20E+03	65	9.81E+06
QLP-z69-2	26.1	0.0380	0.001	0.00582	0.00007	0.2759	0.0473	0.00160	0.00196	0.00031	37.8	1.4	37.4	0.43	39.5	6.2	3.60E+03	200	1.37E+07
QLP-z60-2	24.3	0.0417	0.002	0.00608	0.00012	0.3965	0.0490	0.00200	0.00197	0.00031	41.5	1.8	39.08	0.76	39.7	6.2	410	48	5.65E+06
QLP-z59-1	26.0	0.0364	0.002	0.00564	0.00008	0.3260	0.0468	0.00180	0.00178	0.00031	36.3	1.5	36.28	0.54	36	6.3	660	37	5.66E+06
QLP-z59-2	26.1	0.0373	0.001	0.00565	0.00009	0.1284	0.0475	0.00170	0.00180	0.00029	37.2	1.4	36.31	0.55	36.4	5.9	750	43	5.96E+06
QLP-z49-2	26.1	0.0387	0.002	0.00576	0.00010	0.1676	0.0485	0.00250	0.00179	0.00030	38.6	1.9	37.01	0.61	36.2	6	820	49	5.25E+06
QLP-z51-1	26.1	0.0400	0.002	0.00571	0.00010	0.5791	0.0519	0.00220	0.00169	0.00030	39.8	1.8	36.72	0.67	34.2	6	940	110	1.18E+07
QLP-z51-2	26.0	0.0374	0.002	0.00603	0.00011	0.1131	0.0458	0.00300	0.00210	0.00036	37.2	2.4	38.76	0.72	42.5	7.3	170	22	1.78E+06
QLP-z62-2	26.0	0.0411	0.002	0.00623	0.00011	-0.0786	0.0480	0.00240	0.00203	0.00033	40.9	2.0	40.01	0.72	40.9	6.7	390	40	3.82E+06
QLP-z71-1	15.7	0.0357	0.002	0.00552	0.00011	-0.0470	0.0474	0.00280	0.00186	0.00034	35.6	2.1	35.49	0.73	37.6	6.9	700	52	5.41E+06
QLP-z71-2	26.1	0.0383	0.002	0.00601	0.00010	-0.0239	0.0467	0.00250	0.00196	0.00032	38.1	1.9	38.63	0.62	39.5	6.4	600	54	5.60E+06
QLP-z65-1	26.0	0.0365	0.002	0.00574	0.00007	-0.0403	0.0458	0.00230	0.00177	0.00028	36.4	1.9	36.93	0.45	35.8	5.6	670	67	7.54E+06
QLP-z65-2	26.1	0.0382	0.002	0.00581	0.00008	-0.0447	0.0478	0.00190	0.00190	0.00030	38.1	1.4	37.31	0.48	38.3	6.1	1.30E+03	78	9.34E+06
QLP-z74-1	26.0	0.0380	0.002	0.00595	0.00010	-0.1925	0.0465	0.00260	0.00178	0.00033	37.9	2.0	38.24	0.63	36	6.7	1.10E+03	73	4.63E+06
QLP-z74-2	26.1	0.0377	0.001	0.00564	0.00009	-0.1722	0.0482	0.00170	0.00188	0.00030	37.54	1.1	36.28	0.58	37.9	6.1	520	35	6.93E+06
QLP-z73-1	26.0	0.0397	0.002	0.00625	0.00011	0.3604	0.0465	0.00260	0.00212	0.00039	39.5	2.3	40.17	0.67	42.8	7.9	1.00E+03	48	2.98E+06
QLP-z78-1	26.1	0.0380	0.002	0.00589	0.00008	-0.0559	0.0475	0.00290	0.00187	0.00030	37.8	2.4	37.85	0.53	37.8	6.1	910	62	3.98E+06

Identifier	Integ. length (s)	Final 207/235	Final 207/235 prop2σ	Final 206/238	Final 206/238 prop2σ	Error Corr. 6/38 vs. 7/35	Final 207/206	Final 207/206 prop2σ	Final 208/232	Final 208/232 prop2σ	207/235 Age	207/235 Age prop2σ	206/238 Age	206/238 Age prop2σ	208/232 Age	208/232 Age prop2σ	Pb206 CPS	Pb207 CPS	U238 CPS
AUSZ7_1_1	26.1	0.0393	0.006	0.00601	0.00019	0.0039	0.0472	0.00650	0.00158	0.00048	39	5.4	38.6	1.2	31.9	9.6	110	16	5.96E+05
AUSZ7_1_2	26.1	0.0373	0.005	0.00595	0.00020	0.1081	0.0440	0.00570	0.00153	0.00040	37.1	5.0	38.3	1.3	30.9	8	110	17	7.30E+05
AUSZ7_1_3	26.1	0.0353	0.004	0.00620	0.00025	-0.0138	0.0421	0.00580	0.00174	0.00048	35.1	4.2	39.8	1.6	35.1	9.8	160	17	7.29E+05
AUSZ7_1_4	26.1	0.0421	0.004	0.00599	0.00017	0.0896	0.0506	0.00530	0.00162	0.00049	41.8	4.2	38.5	1.1	32.6	9.9	120	14	6.99E+05
AUSZ7_1_5	26.1	0.0405	0.005	0.00612	0.00018	0.0469	0.0486	0.00540	0.00240	0.00100	40.3	4.4	39.3	1.1	48	20	130	16	7.13E+05
AUSZ7_1_6	26.1	0.0350	0.005	0.00589	0.00013	0.0098	0.0408	0.00540	0.00180	0.00050	34.9	4.7	37.85	0.84	36.3	10	120	16	7.02E+05
AUSZ7_1_7	26.1	0.0406	0.006	0.00593	0.00017	-0.2862	0.0502	0.00770	0.00231	0.00068	40.3	5.7	38.1	1.1	47	14	110	20	7.18E+05
AUSZ7_1_8	26.1	0.0420	0.005	0.00591	0.00019	-0.0383	0.0525	0.00660	0.00161	0.00049	42.6	4.7	38	1.2	32.4	9.8	97	15	6.58E+05
AUSZ7_1_9	26.1	0.0342	0.005	0.00588	0.00018	-0.1383	0.0431	0.00680	0.00159	0.00048	34	4.9	37.8	1.2	32.1	9.7	100	13	5.90E+05
AUSZ7_1_10	26.1	0.0373	0.006	0.00599	0.00017	0.0404	0.0453	0.00700	0.00182	0.00053	37	5.5	38.5	1.1	36.8	11	86	15	5.59E+05
AUSZ7_5_1	26.1	0.0034	0.002	0.00037	0.00004	0.1916	0.0640	0.03100	0.00007	0.00005	3.4	1.6	2.36	0.26	1.4	1.1	17	3.9	5.92E+05
AUSZ7_5_2	26.1	0.0049	0.002	0.00033	0.00005	-0.1457	0.1500	0.08000	0.00003	0.00005	4.9	2.1	2.15	0.3	0.65	0.91	13	4	4.09E+05
AUSZ7_5_3	26.1	0.0045	0.002	0.00038	0.00005	-0.2465	0.1080	0.04700	0.00026	0.00014	4.5	1.9	2.47	0.29	5.3	2.9	14	3.4	4.37E+05
AUSZ7_5_4	26.1	0.0020	0.002	0.00046	0.00007	0.1334	0.0410	0.04500	0.00012	0.00015	2	1.9	2.97	0.43	2.4	2.9	14	2.7	2.94E+05
AUSZ7_5_5	26.1	0.0043	0.002	0.00033	0.00004	0.0291	0.0860	0.03700	0.00009	0.00007	4.3	1.7	2.13	0.24	1.9	1.3	18	5.4	6.93E+05
AUSZ7_5_6	26.1	0.0022	0.001	0.00040	0.00004	-0.2806	0.0450	0.02700	0.00014	0.00008	2.3	1.2	2.57	0.26	2.8	1.6	19	4.2	7.19E+05
AUSZ7_5_7	26.1	0.0030	0.002	0.00033	0.00004	-0.0185	0.0660	0.03400	0.00012	0.00006	3	1.5	2.13	0.24	2.5	1.2	18	4.5	6.72E+05
AUSZ7_5_8	26.1	0.0029	0.002	0.00035	0.00004	0.0055	0.0570	0.03800	0.00015	0.00010	2.9	1.8	2.23	0.25	3	1.9	14	4.9	5.65E+05
AUSZ7_5_9	26.1	0.0017	0.002	0.00038	0.00005	0.2250	0.0020	0.02900	0.00002	0.00005	1.7	1.7	2.44	0.31	0.32	0.99	17	3.8	5.30E+05
AUSZ7_5_10	26.1	0.0027	0.001	0.00038	0.00005	-0.1990	0.0600	0.03100	0.00008	0.00006	2.7	1.3	2.44	0.3	1.6	1.3	16	3	5.15E+05
GJ_1_1	26.1	0.8220	0.020	0.09874	0.00110	0.2948	0.0607	0.00130	0.03120	0.00540	608.9	11.0	607	6.7	621	110	4.10E+03	250	2.10E+06
GJ_1_2	26.1	0.8160	0.020	0.09791	0.00110	0.4639	0.0606	0.00130	0.02940	0.00510	605.6	11.0	602.1	6.5	585	100	4.50E+03	260	2.15E+06
GJ_1_3	26.1	0.8210	0.020	0.09735	0.00100	0.4677	0.0611	0.00120	0.02930	0.00510	608.6	11.0	598.8	6.1	584	100	4.10E+03	250	2.18E+06
GJ_1_4	26.1	0.7890	0.020	0.09770	0.00098	0.1518	0.0586	0.00140	0.03100	0.00520	590.5	11.0	600.9	5.8	617	100	4.10E+03	300	2.11E+06
GJ_1_5	26.1	0.8090	0.018	0.09769	0.00110	0.0589	0.0600	0.00130	0.03000	0.00590	601.8	10.0	600.9	6.5	608	120	4.00E+03	290	2.13E+06
GJ_1_6	26.1	0.8150	0.021	0.09822	0.00110	0.5443	0.0602	0.00130	0.03020	0.00550	604.7	12.0	604	6.7	602	110	4.40E+03	240	2.10E+06
GJ_1_7	26.1	0.8080	0.019	0.09837	0.00100	0.4056	0.0599	0.00120	0.03240	0.00590	601.3	11.0	604.8	6.1	643	120	4.40E+03	260	2.10E+06
GJ_1_8	26.1	0.8080	0.019	0.09760	0.00100	0.1157	0.0596	0.00120	0.03090	0.00550	600.8	11.0	600.3	5.9	614	110	3.90E+03	280	2.15E+06
GJ_1_9	26.1	0.8100	0.020	0.09793	0.00100	0.1431	0.0601	0.00130	0.02550	0.00490	602.3	11.0	602.3	5.9	508	95	4.40E+03	290	2.07E+06
GJ_1_10	26.1	0.8090	0.022	0.09831	0.00110	0.3173	0.0599	0.00150	0.03030	0.00510	601.6	13.0	604.5	6.7	603	100	4.30E+03	320	2.07E+06
GJ_1_11	26.1	0.8180	0.020	0.09856	0.00120	0.3161	0.0600	0.00130	0.03080	0.00530	606.9	11.0	606	7	612	100	4.60E+03	260	2.04E+06

Identifier	Integ. length (s)	Final 207/235	Final 207/235 prop2σ	Final 206/238	Final 206/238 prop2σ	Error Corr. 6/38 vs. 7/35	Final 207/206	Final 207/206 prop2σ	Final 208/232	Final 208/232 prop2σ	207/235 Age	207/235 Age prop2σ	206/238 Age	206/238 Age prop2σ	208/232 Age	208/232 Age prop2σ	Pb206 CPS	Pb207 CPS	U238 CPS
GJ_1_12	26.1	0.8060	0.021	0.09711	0.00100	0.4829	0.0598	0.00130	0.02960	0.00520	599.8	12.0	597.4	5.9	589	100	4.00E+03	260	2.08E+06
GJ_1_13	26.1	0.8140	0.023	0.09753	0.00110	0.5256	0.0608	0.00140	0.03260	0.00610	604	13.0	599.9	6.5	659	120	4.00E+03	270	2.11E+06
GJ_1_14	26.1	0.8160	0.019	0.09853	0.00110	0.5491	0.0600	0.00120	0.02790	0.00520	605.5	11.0	605.8	6.2	556	100	4.10E+03	240	2.06E+06
GJ_1_15	26.1	0.8010	0.019	0.09736	0.00100	0.1144	0.0600	0.00130	0.03100	0.00520	597.4	11.0	598.9	6.1	617	100	4.10E+03	250	2.10E+06
GJ_1_16	26.1	0.8250	0.020	0.09861	0.00100	0.0240	0.0605	0.00130	0.02880	0.00540	610.8	11.0	606.2	6.1	574	110	4.60E+03	250	2.05E+06
GJ_1_17	26.1	0.8170	0.019	0.09810	0.00110	0.1999	0.0606	0.00130	0.03100	0.00540	606.3	11.0	603.3	6.4	616	110	4.40E+03	260	2.08E+06
GJ_1_18	26.1	0.7990	0.020	0.09726	0.00100	0.3181	0.0595	0.00130	0.02760	0.00510	595.9	12.0	598.3	5.9	550	100	4.40E+03	310	2.09E+06
GJ_1_19	26.1	0.8230	0.020	0.09781	0.00110	0.5977	0.0614	0.00110	0.03160	0.00570	609.4	11.0	601.5	6.3	629	110	4.10E+03	270	2.08E+06
GJ_1_20	26.1	0.8030	0.020	0.09732	0.00110	0.2736	0.0599	0.00130	0.02940	0.00550	598.2	11.0	598.7	6.4	585	110	4.00E+03	260	2.05E+06
GJ_1_21	26.1	0.8030	0.020	0.09745	0.00110	0.2368	0.0605	0.00140	0.03270	0.00560	599.9	12.0	599.4	6.6	649	110	3.90E+03	270	2.03E+06
GJ_1_22	26.1	0.8140	0.020	0.09844	0.00120	0.3731	0.0601	0.00140	0.03230	0.00590	604.3	11.0	605.2	7.1	643	120	4.30E+03	280	2.00E+06
GJ_1_23	26.1	0.8090	0.022	0.09875	0.00110	0.5087	0.0594	0.00130	0.02990	0.00560	601.7	12.0	607.1	6.7	595	110	4.00E+03	200	2.01E+06
GJ_1_24	26.1	0.8290	0.019	0.09840	0.00100	0.0453	0.0608	0.00140	0.02490	0.00470	612.8	10.0	605	6.1	496	94	4.10E+03	270	1.96E+06
GJ_1_25	26.1	0.8010	0.021	0.09741	0.00100	0.3561	0.0598	0.00140	0.02970	0.00550	597	12.0	599.2	6.1	591	110	3.70E+03	260	2.04E+06
GJ_1_26	26.1	0.8080	0.021	0.09838	0.00120	0.2107	0.0595	0.00130	0.03050	0.00540	601.2	12.0	604.9	6.8	606	110	4.10E+03	220	2.01E+06
GJ_1_27	26.1	0.8030	0.020	0.09739	0.00120	0.3169	0.0600	0.00130	0.03150	0.00570	598.2	11.0	599.1	6.9	625	110	3.60E+03	220	2.01E+06
GJ_1_28	26.1	0.8040	0.018	0.09777	0.00110	0.3764	0.0595	0.00120	0.03070	0.00520	599.1	10.0	601.3	6.7	611	100	3.90E+03	230	1.97E+06
GJ_1_29	26.1	0.8110	0.019	0.09755	0.00100	0.4119	0.0604	0.00140	0.03070	0.00580	602.8	11.0	600	6.1	609	110	3.80E+03	250	2.02E+06
GJ_1_30	26.1	0.8210	0.020	0.09797	0.00110	0.1323	0.0611	0.00130	0.03010	0.00540	608.4	11.0	602.5	6.3	599	110	3.80E+03	220	2.02E+06
GJ_1_31	26.1	0.8120	0.020	0.09822	0.00110	0.3900	0.0602	0.00130	0.02660	0.00510	603.3	11.0	604	6.7	529	100	4.00E+03	240	2.02E+06
GJ_1_32	26.1	0.8200	0.022	0.09792	0.00100	0.3549	0.0607	0.00140	0.03040	0.00550	607.5	12.0	602.2	6.1	604	110	3.50E+03	260	1.99E+06
GJ_1_33	26.1	0.8090	0.021	0.09773	0.00100	0.3473	0.0597	0.00130	0.03250	0.00580	601.3	12.0	601.1	6	645	110	3.90E+03	280	2.04E+06
Temora2_1	26.1	0.4980	0.017	0.06544	0.00072	-0.1036	0.0555	0.00200	0.02089	0.00330	410	12.0	408.6	4.4	418	65	1.10E+03	100	9.91E+05
Temora2_2	26.1	0.5040	0.016	0.06578	0.00079	0.1573	0.0558	0.00160	0.02070	0.00340	413.7	11.0	410.6	4.8	414	68	1.40E+03	120	1.16E+06
Temora2_3	26.1	0.4980	0.017	0.06601	0.00080	0.2843	0.0552	0.00180	0.02131	0.00340	411.7	11.0	412.1	4.8	426	67	1.20E+03	90	8.77E+05
Temora2_4	26.1	0.5030	0.019	0.06522	0.00084	0.2237	0.0551	0.00200	0.02120	0.00350	413	13.0	407.3	5.1	425	69	500	67	8.54E+05
Temora2_5	26.1	0.5100	0.017	0.06593	0.00081	0.1868	0.0565	0.00180	0.02110	0.00340	418.2	11.0	411.6	4.9	422	67	1.50E+03	110	1.09E+06
Temora2_6	26.1	0.4970	0.018	0.06697	0.00079	0.1015	0.0539	0.00180	0.02150	0.00370	409	12.0	417.9	4.8	431	72	2.10E+03	130	9.25E+05
Temora2_7	26.1	0.5136	0.012	0.06712	0.00085	0.2970	0.0552	0.00120	0.02050	0.00310	420.7	8.2	418.8	5.1	410	62	6.00E+03	400	4.12E+06
Temora2_8	26.1	0.5150	0.016	0.06761	0.00088	-0.0376	0.0559	0.00160	0.02071	0.00320	421.6	11.0	421.7	5.3	414	64	2.00E+03	130	1.58E+06
Temora2_9	26.1	0.5380	0.017	0.06688	0.00077	0.2594	0.0578	0.00160	0.02260	0.00350	438.3	11.0	417.3	4.7	452	70	2.10E+03	120	1.78E+06
Temora2_10	26.1	0.5040	0.022	0.06685	0.00110	0.1551	0.0544	0.00210	0.02060	0.00360	413	15.0	417.1	6.8	412	72	710	55	4.45E+05
Temora2_11	26.1	0.5050	0.015	0.06604	0.00076	0.2704	0.0556	0.00150	0.01979	0.00310	414.9	10.0	412.3	4.6	396	62	970	74	9.19E+05
Temora2_12	26.1	0.4980	0.016	0.06548	0.00095	0.2248	0.0561	0.00170	0.02078	0.00330	409.9	11.0	408.8	5.8	416	65	1.50E+03	100	9.41E+05
Temora2_13	26.1	0.5190	0.022	0.06673	0.00085	0.1840	0.0562	0.00240	0.02270	0.00370	424	15.0	416.4	5.1	454	73	300	62	6.18E+05
Temora2_14	26.1	0.5180	0.019	0.06615	0.00088	0.2168	0.0575	0.00210	0.02170	0.00350	426	13.0	412.9	5.3	434	69	1.20E+03	72	9.56E+05
Temora2_15	25.6	0.4940	0.017	0.06629	0.00082	0.2064	0.0538	0.00170	0.02069	0.00320	406.9	11.0	413.8	5	414	64	2.30E+03	130	1.26E+06
Temora2_16	26.1	0.5090	0.021	0.06710	0.00092	-0.0677	0.0552	0.00230	0.01930	0.00330	417	14.0	418.7	5.6	387	64	1.30E+03	96	7.50E+05
Temora2_17	26.1	0.5100	0.018	0.06655	0.00083	0.1450	0.0560	0.00180	0.01896	0.00300	420	12.0	415.3	5	380	60	2.10E+03	140	1.19E+06
Temora2_18	26.1	0.5110	0.016	0.06678	0.00091	-0.0283	0.0561	0.00190	0.02080	0.00330	418.5	11.0	416.7	5.5	415	66	1.10E+03	87	1.08E+06

Identifier	Integ. length (s)	Final 207/235	Final 207/235 prop2σ	Final 206/238	Final 206/238 prop2σ	Error Corr. 6/38 vs. 7/35	Final 207/206	Final 207/206 prop2σ	Final 208/232	Final 208/232 prop2σ	207/235 Age	207/235 Age prop2σ	206/238 Age	206/238 Age prop2σ	208/232 Age	208/232 Age prop2σ	Pb206 CPS	Pb207 CPS	U238 CPS
Temora2_19	26.1	0.5110	0.019	0.06609	0.00088	-0.1198	0.0554	0.00240	0.02160	0.00350	418	13.0	412.6	5.3	433	70	1.20E+03	97	7.69E+05
91500_1	26.1	1.8430	0.046	0.17770	0.00210	0.2403	0.0756	0.00170	0.05560	0.00890	1060	16.0	1054.5	11	1104	160	1.80E+03	140	5.02E+05
91500_2	26.1	1.8410	0.054	0.17900	0.00220	0.2148	0.0751	0.00220	0.05370	0.00880	1059	19.0	1063.5	12	1057	170	1.50E+03	120	4.25E+05
91500_3	26.1	1.8790	0.058	0.17950	0.00230	0.3303	0.0755	0.00230	0.05360	0.00850	1072	21.0	1064.4	13	1056	160	1.50E+03	150	4.15E+05
91500_4	26.1	1.8730	0.050	0.17790	0.00260	0.2028	0.0764	0.00180	0.05500	0.00890	1071	18.0	1055	15	1081	170	1.20E+03	100	4.11E+05
91500_5	26.1	1.8540	0.053	0.17860	0.00210	-0.0172	0.0757	0.00200	0.05310	0.00850	1066	18.0	1059.4	12	1046	160	1.50E+03	110	4.14E+05
91500_6	26.1	1.8480	0.051	0.17780	0.00230	0.0923	0.0750	0.00210	0.05470	0.00890	1065	19.0	1056.6	12	1076	170	1.50E+03	120	4.18E+05
91500_7	26.1	1.8130	0.059	0.18010	0.00220	0.3236	0.0734	0.00230	0.05800	0.00930	1056	21.0	1067.3	12	1139	180	1.60E+03	140	4.05E+05
91500_8	26.1	1.8060	0.057	0.17850	0.00260	0.3794	0.0735	0.00230	0.05520	0.00880	1046	21.0	1059	14	1085	170	890	96	3.19E+05
91500_9	26.1	1.8930	0.056	0.18370	0.00230	-0.0271	0.0754	0.00220	0.05170	0.00840	1083	18.0	1086.9	13	1019	160	1.70E+03	140	4.34E+05
91500_10	26.1	1.8320	0.058	0.17770	0.00230	0.2955	0.0759	0.00220	0.05340	0.00850	1058	20.0	1054.4	12	1052	160	1.60E+03	150	4.64E+05

Table S4:
LA-ICP-MS zircon geochronology (2nd session)

Identifier	Integ. length (s)	Final 207/ 235	Final 207/235 prop2σ	Final 206/238	Final 206/238 prop2σ	Error Corr. 6/38 vs. 7/35	Final 207/ 206	Final 207/206 prop2σ	Final 208/232	Final 208/232 prop2σ	207/235 Age	207/235 Age prop2σ	206/238 Age	206/238 Age prop2σ	208/232 Age	208/232 Age prop2σ	Pb206 CPS	Pb207 CPS	U238 CPS
Quartz Monzonite Porphyry																			
QMP-z1-1m2	26.411	0.0396	0.0032	0.00612	0.00018	-0.054552	0.0468	0.0044	0.00167	0.00034	39.4	3.1	39.3	1.2	33.8	6.9	1.10E+03	58	2.10E+05
QMP-z1-2m2	26.411	0.0395	0.0038	0.00607	0.00011	-0.055555	0.0469	0.0046	0.00198	0.00039	39.2	3.7	39.03	0.7	40	7.8	370	31	7.70E+04
QMP-z2-1m2	26.396	0.0332	0.0055	0.006	0.00025	-0.14882	0.0413	0.0075	0.00209	0.00047	34.2	5.8	38.6	1.6	42.2	9.6	200	15	2.60E+04
QMP-z2-2m2	26.617	0.0276	0.0071	0.00596	0.00023	-0.21463	0.0357	0.0097	0.00171	0.00049	27.4	7.1	38.3	1.5	34.5	10	130	11	2.60E+04
QMP-z3-1m2	26.796	0.0438	0.0034	0.00626	0.00016	0.061071	0.0496	0.0038	0.00214	0.00037	43.5	3.3	40.3	1	43.1	7.4	1.40E+03	69	2.80E+05
QMP-z3-2m2	26.396	0.0396	0.0024	0.00622	0.00016	0.14605	0.0479	0.0032	0.00204	0.00035	39.4	2.4	40	1	41.2	7	1.30E+03	67	2.50E+05
QMP-z5-1m2	26.396	0.0419	0.0031	0.00638	0.00021	0.50117	0.0471	0.003	0.00207	0.00035	41.6	3	41	1.3	41.7	7	630	30	1.70E+05
QMP-z5-2m2	26.396	0.0376	0.0035	0.0063	0.00017	0.054172	0.0449	0.004	0.00198	0.00033	37.5	3.4	40.5	1.1	40	6.7	620	39	1.70E+05
QMP-z6-2m2	26.396	0.0375	0.0029	0.00606	0.00014	-0.070873	0.0448	0.0035	0.00228	0.00041	37.4	2.8	38.97	0.9	45.9	8.2	490	29	1.10E+05
QMP-z7-1m2	26.396	0.0371	0.0026	0.00591	0.00011	0.062465	0.0467	0.0034	0.00194	0.00032	36.9	2.5	37.97	0.7	39.2	6.4	490	29	6.50E+04
QMP-z8-1m2	26.796	0.0353	0.0067	0.00617	0.00019	0.40132	0.0409	0.0076	0.00169	0.00042	35	6.6	39.7	1.2	34.1	8.4	320	22	5.10E+04
QMP-z9-1m2	12.798	0.0419	0.0045	0.00572	0.0003	0.20153	0.0542	0.0064	0.00213	0.00052	41.7	4.4	36.8	1.9	42.9	10	300	27	5.20E+04
QMP-z9-2m2	26.396	0.0388	0.0034	0.00595	0.00012	0.17726	0.0477	0.0042	0.002	0.00031	38.6	3.3	38.22	0.77	40.4	6.4	1.30E+03	72	2.60E+05
QMP-z10-1m2	26.396	0.0466	0.0074	0.00584	0.00018	0.063326	0.0578	0.0094	0.00221	0.00052	46	7.2	37.5	1.2	44.6	11	92	11	2.00E+04
QMP-z10-2m2	26.396	0.0345	0.0027	0.00585	0.00013	0.23285	0.0436	0.0033	0.0019	0.00032	34.4	2.6	37.59	0.82	38.4	6.5	560	37	1.30E+05
QMP-z11-2m2	26.796	0.0434	0.0034	0.00633	0.00013	0.16329	0.0492	0.0038	0.00206	0.00036	43.1	3.3	40.69	0.85	41.6	7.3	500	23	1.10E+05
QMP-z12-2m2	26.396	0.0457	0.0033	0.00597	0.00013	0.22459	0.056	0.0042	0.00216	0.00036	45.3	3.2	38.37	0.84	43.7	7.3	1.20E+03	69	2.30E+05
QMP-z13-1m2	26.796	0.0371	0.0053	0.00627	0.0002	0.11455	0.0417	0.0057	0.0022	0.00041	36.8	5.2	40.3	1.2	44.4	8.3	300	21	6.10E+04
QMP-z15-1m2	26.796	0.0398	0.0046	0.00613	0.0002	-0.1759	0.0474	0.006	0.00235	0.00051	39.6	4.5	39.4	1.3	47.5	10	160	13	3.00E+04
QMP-z16-1m2	26.396	0.0403	0.0044	0.00582	0.00014	-0.045457	0.0506	0.0057	0.00173	0.00034	40.1	4.3	37.42	0.87	35	7	470	30	1.10E+05
QMP-z16-2m2	17.597	0.0375	0.004	0.00591	0.00016	0.25094	0.0465	0.0049	0.00211	0.0004	37.3	3.9	38	1	42.7	8.1	420	28	8.90E+04
QMP-z17-1m2	26.396	0.0366	0.0049	0.00599	0.00015	-0.067137	0.0449	0.0061	0.00194	0.00039	36.4	4.8	38.49	0.94	39.2	7.9	230	18	5.20E+04
QMP-z17-2m2	26.396	0.0377	0.0044	0.00588	0.00018	-0.087771	0.0473	0.006	0.00171	0.00033	37.5	4.4	37.8	1.2	34.6	6.6	610	32	1.20E+05
QMP-z19-2m2	26.594	0.0382	0.0047	0.00616	0.00019	0.10227	0.0471	0.0054	0.0019	0.00036	38.7	4.4	39.6	1.2	38.3	7.3	340	21	6.90E+04
QMP-z20-1m2	19.597	0.0364	0.0024	0.00588	0.00016	0.02698	0.0458	0.0032	0.002	0.00034	36.3	2.3	37.8	1	40.4	6.8	1.10E+03	59	2.00E+05
QMP-z21-2m2	26.578	0.037	0.0027	0.00587	0.00015	0.15055	0.0448	0.0034	0.00193	0.00032	36.8	2.6	37.7	0.97	39	6.5	420	30	9.00E+04
QMP-z22-1m2	26.396	0.0388	0.0038	0.00592	0.00013	0.061095	0.0473	0.0047	0.00192	0.00035	38.6	3.7	38.03	0.86	38.7	7.1	140	23	2.10E+04
QMP-z23-1m2	26.396	0.0411	0.0031	0.0063	0.0002	0.48996	0.0472	0.0035	0.00189	0.00033	40.9	3.1	40.5	1.3	38.1	6.7	1.10E+03	63	2.30E+05
QMP-z23-2m2	26.396	0.0426	0.0026	0.00606	0.00011	0.047171	0.051	0.0033	0.00207	0.00033	42.3	2.5	38.98	0.68	41.8	6.7	910	47	2.00E+05
QMP-z24-1m2	26.396	0.0396	0.0033	0.00586	0.00015	-0.21097	0.0498	0.0048	0.00199	0.00034	39.4	3.3	37.66	0.95	40.2	6.9	810	37	1.50E+05
QMP-z25-2m2	26.796	0.0385	0.0019	0.005688	0.00008	0.22787	0.0484	0.0024	0.00185	0.00028	38.3	1.9	36.56	0.51	37.4	5.7	1.00E+03	56	2.50E+05
QMP-z26-1m2	26.396	0.0379	0.0028	0.00609	0.00012	-0.2426	0.0454	0.0037	0.00201	0.00038	37.7	2.7	39.16	0.75	40.5	7.6	500	34	1.10E+05
QMP-z28-1m2	26.796	0.0392	0.0022	0.00602	0.00017	0.13999	0.0482	0.0032	0.00195	0.00036	39	2.1	38.7	1.1	39.3	7.2	1.10E+03	58	1.90E+05
QMP-z28-2m2	26.396	0.0378	0.0025	0.00585	0.00013	0.1848	0.048	0.0032	0.00179	0.00029	37.7	2.5	37.62	0.84	36.1	5.9	1.20E+03	69	2.00E+05
QMP-z30-1m2	17.597	0.0419	0.0054	0.00586	0.00023	-0.080895	0.0507	0.0069	0.00164	0.00032	41.6	5.3	37.7	1.5	33.2	6.4	150	20	2.10E+04
QMP-z31-1m2	16.797	0.0371	0.0028	0.00586	0.00013	-0.13655	0.0458	0.0034	0.00188	0.00031	36.9	2.7	37.65	0.86	37.9	6.4	170	18	3.90E+04
QMP-z32-1m2	26.396	0.0395	0.0021	0.00601	0.00012	0.071579	0.048	0.0026	0.00199	0.0003	39.6	2.2	38.64	0.74	40.2	6.1	610	37	7.50E+04

Identifier	Integ. length (s)	Final 207/ 235	Final 207/235 prop2σ	Final 206/238	Final 206/238 prop2σ	Error Corr. 6/38 vs. 7/35	Final 207/ 206	Final 207/206 prop2σ	Final 208/232	Final 208/232 prop2σ	207/235 Age	207/235 Age prop2σ	206/238 Age	206/238 Age prop2σ	208/232 Age	208/232 Age prop2σ	Pb206 CPS	Pb207 CPS	U238 CPS
QMP-z34-1m2	26.568	0.0369	0.0032	0.0058	0.00011	0.11779	0.0463	0.004	0.0018	0.00032	36.7	3.1	37.28	0.68	36.4	6.4	180	23	2.80E+04
Quarz Latite Porphyry																			
QLP-z1-1m2	26.796	0.0413	0.0022	0.00595	0.00012	0.35052	0.0509	0.0024	0.001979	0.00029	41.1	2.1	38.23	0.77	40	5.9	570	63	1.50E+05
QLP-z1-2m2	7.4281	0.0423	0.004	0.00612	0.00019	-0.22609	0.0507	0.0057	0.00232	0.00048	42.1	3.9	39.3	1.2	46.8	9.6	870	44	2.30E+05
QLP-z2-1m2	26.796	0.041	0.0037	0.005854	0.000098	0.15186	0.0519	0.0048	0.00177	0.00041	40.7	3.6	37.63	0.63	35.7	8.3	280	25	7.80E+04
QLP-z2-2m2	26.796	0.0385	0.0023	0.00588	0.00011	-0.17423	0.0477	0.0034	0.00165	0.00034	38.3	2.3	37.81	0.7	33.4	6.9	120	18	2.70E+04
QLP-z3-1m2	26.396	0.0407	0.0071	0.006	0.00018	0.0842	0.049	0.0085	0.00159	0.00034	40.3	6.9	38.6	1.1	32.1	6.9	85	13	2.10E+04
QLP-z3-2m2	26.396	0.0383	0.0054	0.00584	0.00013	0.2144	0.0486	0.007	0.00202	0.0004	38	5.3	37.55	0.86	40.9	8.1	120	28	1.90E+04
QLP-z4-1m2	26.396	0.0396	0.0022	0.00602	0.00011	0.032144	0.0477	0.0027	0.00211	0.00036	39.4	2.2	38.67	0.71	42.6	7.2	1.10E+03	57	2.30E+05
QLP-z5-1m2	16.796	0.0396	0.0047	0.0063	0.0002	-0.18035	0.0456	0.0055	0.00181	0.00036	39.4	4.6	40.5	1.3	36.5	7.2	360	32	8.40E+04
QLP-z6-1m2	22.796	0.0392	0.0041	0.00605	0.00015	0.38609	0.0466	0.0044	0.00229	0.00055	39	4	38.88	0.98	46.2	11	740	31	1.70E+05
QLP-z6-2m2	26.396	0.0381	0.0024	0.00581	0.00013	0.12045	0.047	0.003	0.00178	0.00032	37.9	2.3	37.34	0.82	36	6.5	330	24	7.90E+04
QLP-z7-1m2	17.597	0.0386	0.0023	0.00598	0.00012	0.2246	0.0467	0.0027	0.00197	0.00036	38.4	2.2	38.44	0.74	39.9	7.2	1.10E+03	49	2.10E+05
QLP-z7-2m2	26.396	0.0361	0.0021	0.00574	0.00011	0.185	0.0457	0.0026	0.00179	0.00031	35.9	2	36.93	0.73	36.1	6.2	540	34	6.60E+04
QLP-z8-1m2	26.396	0.0394	0.0022	0.005749	0.000092	-0.029967	0.0501	0.003	0.00179	0.00029	39.3	2.1	36.95	0.59	36.1	5.8	600	42	1.70E+05
QLP-z9-1m2	26.796	0.04	0.0029	0.006	0.00016	0.11527	0.0483	0.0035	0.00198	0.0004	39.8	2.8	38.6	1	40	8	150	22	3.80E+04
QLP-z9-2m2	26.396	0.0372	0.0026	0.00599	0.00012	0.030572	0.0466	0.0039	0.00187	0.0005	37.1	2.5	38.49	0.75	37.8	10	420	29	1.10E+05
QLP-z10-1m2	26.796	0.0397	0.0032	0.00589	0.00015	0.32309	0.0477	0.0036	0.00177	0.00032	39.4	3.1	37.86	0.94	35.7	6.4	310	21	5.50E+04
QLP-z11-1m2	26.796	0.0378	0.0032	0.006	0.00016	-0.1005	0.0447	0.0038	0.00183	0.00039	37.6	3.2	38.74	0.96	37	7.8	300	25	8.20E+04
QLP-z11-2m2	26.396	0.0394	0.0025	0.00593	0.00011	0.2648	0.048	0.0032	0.00187	0.00033	39.2	2.4	38.12	0.71	37.8	6.6	230	25	6.80E+04
QLP-z12-1m2	26.396	0.0407	0.0027	0.00608	0.00011	0.017432	0.0498	0.0034	0.00209	0.00035	40.5	2.6	39.07	0.73	42.2	7	390	31	9.90E+04
QLP-z13-1m2	26.396	0.0403	0.0021	0.00599	0.00011	0.046384	0.0493	0.0028	0.00181	0.00031	40.5	2.2	38.49	0.73	36.6	6.2	940	61	1.40E+05
QLP-z14-1m2	14.398	0.0366	0.0032	0.00548	0.00018	-0.053093	0.0492	0.0045	0.00177	0.00033	36.5	3.1	35.2	1.2	35.7	6.6	380	28	6.10E+04
QLP-z14-2m2	26.796	0.0391	0.0018	0.0058	0.00012	0.12135	0.0498	0.0026	0.00165	0.00033	38.9	1.8	37.3	0.77	33.2	6.8	370	25	1.00E+05
QLP-z15-2m2	26.796	0.0408	0.0016	0.00574	0.00012	0.54038	0.0513	0.0019	0.001848	0.00027	40.6	1.5	36.93	0.77	37.3	5.4	4.20E+03	240	8.70E+05
QLP-z16-1m2	26.396	0.039	0.0026	0.00605	0.00013	0.19054	0.0464	0.003	0.00184	0.00037	38.8	2.5	38.86	0.8	37.1	7.5	360	28	8.10E+04
QLP-z16-2m2	26.796	0.0374	0.0036	0.00608	0.00015	-0.084951	0.0451	0.0045	0.00228	0.00051	37.2	3.5	39.09	0.94	46	10	250	28	7.20E+04
QLP-z17-1m2	26.796	0.0466	0.0061	0.00622	0.0001	0.31842	0.0543	0.007	0.00295	0.00055	46.1	5.9	39.95	0.66	59.6	11	300	26	6.60E+04
QLP-z20-1m2	26.396	0.0377	0.0037	0.0059	0.00013	-0.0242	0.0466	0.0046	0.00211	0.00059	37.5	3.6	37.93	0.83	42	12	390	25	8.40E+04
QLP-z20-2m2	26.396	0.0356	0.0032	0.00595	0.00011	0.35757	0.0448	0.0038	0.00208	0.00036	35.5	3.1	38.25	0.73	42	7.2	320	31	4.90E+04
QLP-z21-1m2	26.396	0.0406	0.0031	0.00586	0.00014	0.029025	0.0502	0.0041	0.00172	0.00038	40.4	3	37.64	0.87	34.8	7.6	240	18	5.00E+04
QLP-z21-2m2	26.396	0.0386	0.0038	0.00592	0.00014	-0.083911	0.0472	0.0048	0.0021	0.00044	38.4	3.7	38.04	0.93	42.3	8.9	400	31	7.30E+04
QLP-z22-1m2	26.396	0.0414	0.0025	0.00604	0.00016	-0.079092	0.0495	0.0033	0.00182	0.00034	41.2	2.4	38.8	1	36.8	6.8	730	42	1.80E+05
QLP-z23-1m2	26.796	0.04	0.0033	0.00586	0.00012	-0.11587	0.0496	0.0042	0.0021	0.00041	39.7	3.2	37.69	0.75	42.3	8.3	390	32	9.50E+04
QLP-z24-1m2	26.396	0.0384	0.0027	0.00612	0.0001	-0.067728	0.0461	0.0034	0.00194	0.00036	38.2	2.6	39.31	0.65	39.2	7.3	300	30	2.30E+04
QLP-z24-2m2	26.796	0.0372	0.0024	0.00585	0.00011	0.05472	0.047	0.0034	0.00196	0.00039	37	2.4	37.61	0.71	39.6	7.8	230	25	5.00E+04
QLP-z25-2m2	14.949	0.0374	0.0028	0.00591	0.00015	0.12083	0.0468	0.0037	0.0018	0.0003	37.3	2.7	38.01	0.98	36.3	6.1	1.10E+03	69	2.80E+05

Identifier	Integ. length (s)	Final 207/235	Final 207/235 prop2σ	Final 206/238	Final 206/238 prop2σ	Error Corr. 6/38 vs. 7/35	Final 207/206	Final 207/206 prop2σ	Final 208/232	Final 208/232 prop2σ	207/235 Age	207/235 Age prop2σ	206/238 Age	206/238 Age prop2σ	208/232 Age	208/232 Age prop2σ	Pb206 CPS	Pb207 CPS	U238 CPS
QMP-z40-2	5.0	0.0415	0.004	0.00585	0.00011	-0.0191	0.0512	0.00520	0.00195	0.00039	41.3	4.2	37.6	0.7	39.3	7.9	650	140	7.21E+06
QMP-z12-2	26.1	0.0398	0.004	0.00607	0.00009	0.0597	0.0477	0.00440	0.00193	0.00036	39.6	3.5	38.99	0.6	38.9	7.2	170	27	1.65E+06
QMP-z45-1	26.0	0.0359	0.002	0.00586	0.00009	-0.1050	0.0446	0.00190	0.00193	0.00030	35.8	1.5	37.64	0.57	39	6	410	53	7.61E+06
QMP-z45-2	11.1	0.0378	0.002	0.00600	0.00013	0.0984	0.0466	0.00270	0.00196	0.00033	37.7	2.2	38.57	0.85	39.5	6.7	520	72	5.77E+06
QMP-z47-1	26.0	0.0400	0.002	0.00583	0.00008	0.1560	0.0496	0.00180	0.00194	0.00030	39.9	1.5	37.45	0.51	39.2	6.1	1.70E+03	87	1.13E+07
QMP-z47-2	26.0	0.0391	0.003	0.00590	0.00011	0.4854	0.0481	0.00380	0.00193	0.00034	38.9	3.2	37.91	0.73	39	6.9	240	23	1.85E+06
QMP-z47-3	26.1	0.0377	0.002	0.00606	0.00008	0.0301	0.0450	0.00250	0.00180	0.00029	37.9	2.1	38.92	0.53	36.3	5.8	590	42	4.29E+06
QMP-z50-1	26.1	0.0407	0.004	0.00596	0.00016	0.2405	0.0500	0.00470	0.00186	0.00035	40.5	3.9	38.3	1.1	37.6	7.1	91	18	9.66E+05
QMP-z50-2	26.0	0.0363	0.003	0.00581	0.00010	0.0792	0.0456	0.00370	0.00186	0.00031	36.1	2.9	37.32	0.64	37.6	6.2	180	28	2.09E+06
QMP-z49-1	22.7	0.0369	0.001	0.00586	0.00008	-0.0036	0.0459	0.00150	0.00196	0.00031	36.74	1.1	37.65	0.53	39.6	6.3	1.80E+03	97	1.31E+07
QMP-z49-2	26.1	0.0393	0.002	0.00609	0.00009	-0.0500	0.0471	0.00230	0.00193	0.00032	39.1	1.9	39.1	0.6	39	6.5	580	46	4.36E+06
QMP-z60-1	20.5	0.0368	0.004	0.00597	0.00016	0.2025	0.0455	0.00480	0.00181	0.00037	36.6	3.8	38.4	1	36.5	7.4	270	26	1.28E+06
QMP-z60-2	26.1	0.0384	0.003	0.00595	0.00012	-0.0941	0.0469	0.00420	0.00173	0.00031	38.3	3.3	38.26	0.75	35	6.3	280	27	1.66E+06
QMP-z74-1	8.9	0.0399	0.004	0.00582	0.00013	-0.0282	0.0500	0.00500	0.00195	0.00032	39.7	3.7	37.39	0.8	39.4	6.5	1.70E+03	190	8.21E+06
QMP-z74-2	12.8	0.0390	0.004	0.00589	0.00010	-0.1632	0.0474	0.00470	0.00187	0.00032	38.8	3.8	37.83	0.66	37.8	6.5	570	78	4.18E+06
QMP-z72-1	26.1	0.0412	0.003	0.00587	0.00014	0.0358	0.0502	0.00460	0.00176	0.00032	41	3.3	37.75	0.88	35.6	6.5	110	14	9.33E+05
QMP-z72-2	26.1	0.0399	0.003	0.00604	0.00014	-0.0397	0.0479	0.00400	0.00190	0.00039	39.7	3.4	38.84	0.9	38.4	7.9	100	15	9.37E+05
QMP-z58-1	24.8	0.0394	0.004	0.00575	0.00012	-0.0946	0.0496	0.00520	0.00196	0.00036	39.2	4.0	36.98	0.8	40.3	7.5	1.10E+03	74	1.69E+06
QMP-z58-2	26.1	0.0423	0.003	0.00610	0.00011	0.0458	0.0501	0.00350	0.00190	0.00033	42.1	2.7	39.18	0.73	38.5	6.7	450	37	2.07E+06
QMP-z76-1	17.9	0.0369	0.002	0.00573	0.00008	-0.0350	0.0468	0.00240	0.00181	0.00031	36.7	1.9	36.85	0.53	36.6	6.2	2.90E+03	160	7.45E+06
QMP-z88-1	5.3	0.0394	0.003	0.00562	0.00014	-0.4775	0.0508	0.00400	0.00187	0.00030	39.2	2.5	36.14	0.89	37.8	6.1	1.40E+03	95	7.13E+06
QMP-z83-1	26.1	0.0406	0.004	0.00591	0.00015	0.0050	0.0503	0.00540	0.00201	0.00040	40.3	4.2	37.98	0.99	40.7	8	210	18	9.05E+05
QMP-z83-2	26.1	0.0389	0.003	0.00608	0.00013	-0.0809	0.0447	0.00430	0.00206	0.00040	38.7	3.2	39.07	0.84	41.6	8.1	350	24	1.13E+06
QMP-z84-1	7.0	0.0407	0.005	0.00621	0.00011	-0.2665	0.0473	0.00570	0.00191	0.00036	40.5	4.6	39.89	0.68	38.5	7.2	640	67	2.68E+06
QMP-z84-2	9.2	0.0420	0.003	0.00601	0.00012	-0.0856	0.0503	0.00390	0.00191	0.00032	41.8	3.1	38.63	0.75	38.5	6.5	320	58	4.09E+06
QMP-z69-2	26.0	0.0384	0.003	0.00616	0.00013	0.1213	0.0453	0.00320	0.00184	0.00031	38.2	2.6	39.59	0.83	37.2	6.2	800	43	2.35E+06
QMP-z56-1	20.0	0.0429	0.005	0.00613	0.00014	0.2065	0.0497	0.00510	0.00189	0.00034	42.6	4.6	39.37	0.9	38.1	6.9	210	27	1.21E+06
QMP-z56-2	26.0	0.0368	0.001	0.00587	0.00009	-0.0555	0.0457	0.00190	0.00205	0.00032	36.7	1.3	37.7	0.6	41.4	6.4	1.50E+03	94	7.68E+06
QMP-z78-1	26.1	0.0370	0.002	0.00571	0.00009	-0.1761	0.0470	0.00280	0.00179	0.00029	36.8	2.1	36.68	0.6	36.2	5.8	720	54	3.29E+06
QMP-z78-2	9.6	0.0388	0.004	0.00606	0.00020	0.2830	0.0457	0.00480	0.00212	0.00044	38.7	4.3	38.9	1.3	42.8	8.9	230	38	2.05E+06
QMP-z62-1	15.5	0.0433	0.003	0.00622	0.00014	0.2690	0.0508	0.00310	0.00193	0.00033	43	2.7	39.97	0.92	39.1	6.6	910	53	2.74E+06
QMP-z63-1	12.6	0.0355	0.002	0.00584	0.00011	0.2457	0.0437	0.00270	0.00185	0.00030	35.4	2.2	37.52	0.72	37.4	6.1	1.20E+03	83	6.26E+06
QMP-z63-2	12.1	0.0410	0.003	0.00584	0.00012	-0.1985	0.0510	0.00380	0.00199	0.00032	40.8	2.8	37.56	0.8	40.2	6.4	330	64	4.62E+06
QMP-z03-1	26.1	0.0389	0.003	0.00584	0.00014	0.0071	0.0477	0.00400	0.00176	0.00031	38.7	3.2	37.51	0.92	35.6	6.3	190	20	1.26E+06
QMP-z51-2	16.4	0.0382	0.002	0.00579	0.00011	0.2980	0.0481	0.00270	0.00182	0.00030	38	2.2	37.22	0.73	36.7	6.1	270	50	5.13E+06
Latite Porphyry																			
LP-z01-1	12.8	0.0462	0.002	0.00585	0.00009	0.0201	0.0573	0.00290	0.00212	0.00036	45.9	2.2	37.62	0.56	42.9	7.3	5.60E+03	340	9.20E+06

Identifier	Integ. length (s)	Final 207/ 235	Final 207/235 prop2σ	Final 206/238	Final 206/238 prop2σ	Error Corr. 6/38 vs. 7/35	Final 207/ 206	Final 207/206 prop2σ	Final 208/232	Final 208/232 prop2σ	207/235 Age	207/235 Age prop2σ	206/238 Age	206/238 Age prop2σ	208/232 Age	208/232 Age prop2σ	Pb206 CPS	Pb207 CPS	U238 CPS
GJ-1 - 7	26.583	0.812	0.022	0.0977	0.0011	0.071566	0.0607	0.0018	0.0301	0.0059	605	13	600.7	6.6	597	120	2.10E+03	140	3.70E+04
GJ-1 - 8	26.574	0.823	0.025	0.098	0.0011	0.26427	0.061	0.0019	0.0298	0.0062	609	14	602.8	6.4	591	120	2.40E+03	150	4.10E+04
GJ-1 - 9	26.555	0.811	0.028	0.0966	0.0014	0.42943	0.0614	0.002	0.0277	0.0061	605	15	594.5	8.1	550	120	2.20E+03	140	3.70E+04
GJ-1 - 10	26.569	0.826	0.026	0.0981	0.0013	0.40544	0.0611	0.0019	0.0342	0.0079	610	14	603.4	7.6	680	150	2.10E+03	160	3.40E+04
GJ-1 - 11	23.923	0.807	0.024	0.0981	0.0015	0.28397	0.0585	0.0015	0.0303	0.007	600	13	603.3	8.9	600	140	1.90E+03	120	3.50E+04
GJ-1 - 12	26.556	0.802	0.019	0.0976	0.0012	0.15342	0.0595	0.0016	0.0344	0.0066	600	11	601.8	7.4	682	130	2.20E+03	140	3.70E+04
GJ-1 - 13	26.555	0.823	0.024	0.0986	0.0013	0.3927	0.0612	0.0018	0.0247	0.0058	609	13	606.3	7.6	492	120	1.90E+03	140	3.10E+04
GJ-1 - 14	26.554	0.796	0.024	0.0971	0.0013	0.019735	0.0592	0.002	0.03	0.0064	596	13	597.4	7.5	596	130	2.20E+03	160	3.60E+04
GJ-1 - 15	26.59	0.826	0.021	0.098	0.0012	0.28308	0.0611	0.0017	0.0304	0.0073	611	12	602.8	7.2	600	140	2.00E+03	130	3.10E+04
GJ-1 - 16	26.562	0.821	0.023	0.0982	0.0011	0.32314	0.0607	0.0018	0.0331	0.007	608	13	603.6	6.5	660	140	2.00E+03	140	3.30E+04
GJ-1 - 17	26.56	0.821	0.026	0.0984	0.0014	0.40501	0.0604	0.002	0.0336	0.0074	607	15	605.1	8.4	660	150	2.10E+03	160	3.30E+04
GJ-1 - 18	26.564	0.817	0.025	0.0976	0.0015	0.31385	0.0606	0.0019	0.0321	0.0068	606	14	600.2	9	637	130	2.10E+03	110	3.10E+04
GJ-1 - 19	26.555	0.797	0.024	0.0979	0.0012	0.25843	0.0595	0.002	0.027	0.0063	597	14	601.8	7.2	537	120	2.00E+03	120	3.20E+04
GJ-1 - 20	26.598	0.797	0.03	0.098	0.0012	0.42842	0.0597	0.0023	0.0285	0.0061	597	17	602.9	6.9	565	120	2.00E+03	130	3.40E+04
GJ-1 - 21	26.553	0.811	0.023	0.0974	0.0013	0.087078	0.0597	0.0021	0.0309	0.0067	602	13	598.8	7.6	610	130	2.00E+03	120	3.20E+04
Temora - 1	23.004	0.512	0.051	0.0663	0.0015	0.54196	0.0543	0.0045	0.0251	0.0055	415	34	413.5	9.2	499	110	230	29	6.20E+03
Temora - 2	19.162	0.517	0.039	0.0663	0.0013	0.11082	0.0568	0.0044	0.0216	0.0036	421	26	414	7.6	433	71	890	78	2.00E+04
Temora - 3	26.607	0.501	0.028	0.0662	0.0013	-0.10862	0.0548	0.0031	0.0208	0.0036	411	19	413	7.7	416	71	620	38	1.30E+04
Temora - 4	26.711	0.5	0.023	0.0664	0.0012	0.14658	0.0553	0.0025	0.0198	0.0032	410	15	414.5	7.2	397	63	580	37	1.30E+04
Temora - 5	19.528	0.502	0.032	0.0658	0.0012	0.16981	0.0551	0.0035	0.0195	0.0035	412	22	410.7	7.4	390	69	850	64	1.70E+04
Temora - 6	14.08	0.51	0.04	0.0675	0.0014	0.23652	0.055	0.0043	0.0218	0.0045	416	27	420.9	8.3	434	89	420	47	1.20E+04
Temora - 7	26.559	0.505	0.031	0.0671	0.0011	0.10258	0.0547	0.0035	0.0199	0.0038	413	21	418.7	6.5	397	75	730	58	1.50E+04
91500 - 1	25.3	1.91	0.087	0.1794	0.0025	0.19551	0.0775	0.0036	0.0498	0.0079	1086	29	1063	13	981	150	970	100	9.20E+03
91500 - 2	19.998	1.863	0.088	0.1792	0.0033	0.36578	0.0748	0.0032	0.0481	0.0085	1076	31	1063	18	947	160	890	71	7.40E+03
91500 - 3	26.109	1.872	0.071	0.18	0.0027	0.12061	0.0753	0.0032	0.0546	0.0095	1068	25	1067	15	1090	190	880	70	7.90E+03
91500 - 4	11.324	1.852	0.085	0.1803	0.005	0.15465	0.0744	0.0036	0.053	0.011	1062	30	1069	27	1040	210	660	69	7.10E+03
91500 - 5	26.611	1.851	0.081	0.1797	0.0024	0.21954	0.074	0.0032	0.053	0.0091	1065	28	1065	13	1041	170	850	72	7.40E+03
91500 - 6	22.369	1.824	0.095	0.1797	0.0034	-0.090563	0.0739	0.0043	0.0579	0.011	1049	34	1065	19	1130	210	650	77	5.60E+03
91500 - 7	19.482	1.868	0.081	0.1818	0.0037	0.3037	0.0751	0.0033	0.0571	0.0095	1073	30	1077	20	1141	190	640	42	5.90E+03

Table S5:
LA-ICP-MS titanite trace element analyses

Sample	Si	P	Sc	Ti	V	Mn	Sr	Y	Zr	T°C[1]	Nb	Ba	La	Ce	Pr	Nd	Sm	Eu	Gd	Tb	Dy	Ho	Er	Tm	Yb	Lu	Hf	Ta	Th	U
	ppm	ppm	ppm	ppm	ppm	ppm	ppm	ppm	ppm	ppm	ppm	ppm	ppm	ppm	ppm	ppm	ppm	ppm	ppm	ppm	ppm	ppm	ppm	ppm	ppm	ppm	ppm	ppm	ppm	ppm
QLP2-1	143,299	201	9.2	209,624	629	896	54	1,928	383	686	1,886	23	1,398	5,788	1,025	4,648	937	184	644	80	419	72	192	24	144	18	30	143	463	131
QLP2-2	142,247	207	10.1	206,502	623	913	53	1,909	361	683	1,812	22	1,333	5,498	964	4,397	904	177	627	77	409	70	187	24	144	17	31	139	440	131
QLP2-5	144,012	320	7.0	209,140	756	787	73	1,799	448	694	1,429	28	1,631	6,531	1,140	5,157	1,000	205	660	78	406	68	178	23	133	16	33	120	473	125
QLP2-6	141,256	225	9.7	205,233	667	850	56	1,932	376	685	1,515	23	1,344	5,630	1,011	4,596	974	191	666	82	428	72	187	24	140	16	31	117	461	125
QLP2-8	150,874	233	10.6	209,854	656	966	57	1,957	428	692	1,668	24	1,451	5,960	1,063	4,803	993	191	688	85	428	73	193	23	147	17	32	126	446	134
QLP2-9	141,434	221	10.8	204,574	616	924	52	2,057	396	688	1,939	24	1,388	5,956	1,053	4,739	975	186	668	82	442	75	200	25	153	18	35	157	510	139
QLP2-10	146,620	236	8.5	209,809	701	835	63	1,778	392	687	1,463	25	1,492	6,078	1,060	4,731	928	188	618	74	391	66	175	23	133	16	29	111	448	116
QLP2-11	143,822	211	9.7	209,319	648	909	57	2,087	421	691	1,569	24	1,479	6,068	1,100	5,040	1,065	203	733	91	462	82	203	26	153	18	33	121	456	127
QLP2-12	142,951	242	9.9	205,931	669	836	67	1,687	431	692	1,679	27	1,714	6,657	1,127	4,955	949	179	614	74	373	63	160	20	122	15	33	130	434	115
QLP2-14	140,947	204	11.8	211,678	643	957	49	1,983	366	684	1,723	22	1,268	5,460	971	4,345	944	184	652	81	422	73	192	25	154	18	32	125	456	141
QLP2-15	138,213	251	7.2	203,785	708	784	63	1,573	362	683	1,485	21	1,274	5,115	886	3,905	753	170	509	65	326	57	155	20	122	16	30	113	489	127
QLP2-16	141,416	237	8.3	209,876	692	809	67	1,747	425	691	1,341	26	1,635	6,535	1,102	4,821	932	188	630	74	385	65	169	21	127	15	31	103	447	111
QLP2-17	142,050	223	10.2	213,456	637	920	55	2,028	407	689	1,703	23	1,479	5,942	1,069	4,896	1,007	192	697	87	457	78	201	26	150	18	34	128	456	131
QLP2-18	141,893	291	7.2	209,024	772	705	72	1,917	462	696	1,560	26	1,620	6,548	1,142	5,162	1,048	214	687	84	435	73	189	24	141	16	36	166	530	135
QLP2-21	141,849	80	3.4	211,739	865	394	28	400	541	704	142	19	1,953	4,391	500	1,712	248	66	156	18	88	15	38	5	32	4	33	4	107	51
QLP2-22	146,185	284	9.1	210,471	698	792	71	1,751	463	696	1,610	30	1,801	7,183	1,190	5,130	983	197	639	76	388	65	167	21	129	15	37	139	498	121
QLP2-23	142,570	226	8.9	209,180	664	848	61	1,890	383	686	1,737	23	1,369	5,779	1,038	4,615	970	195	680	82	431	73	187	24	135	16	30	132	432	120
QLP2-24	148,393	227	9.7	215,708	671	926	60	2,001	399	688	1,726	25	1,464	6,059	1,054	4,729	998	194	693	85	450	76	191	25	148	18	31	134	444	129
QLP1-1	140,140	93	4.4	214,077	800	290	54	321	152	641	149	19	1,681	4,474	540	1,819	242	80	144	15	74	12	29	4	21	3	19	6	41	22
QLP1-3	140,483	217	3.4	211,672	925	413	32	408	495	699	300	29	3,383	6,682	657	2,015	244	73	158	17	86	15	39	6	38	5	11	3	394	173
QLP1-5	142,520	297	7.8	207,963	728	748	78	1,787	471	697	1,421	30	1,911	7,394	1,268	5,455	1,050	209	684	80	410	70	175	22	133	15	36	125	476	110
QLP1-6	146,700	338	8.0	213,650	770	751	88	1,754	440	693	1,652	35	2,222	8,214	1,359	5,837	1,093	212	701	81	415	68	170	21	125	14	31	145	490	112
QLP1-8	137,907	149	2.4	210,061	840	371	31	325	314	676	238	25	2,913	5,644	572	1,809	221	53	137	15	73	12	30	4	27	4	9	2	268	107
QLP1-9	140,701	178	3.4	213,906	841	391	37	315	561	706	297	25	3,133	5,677	548	1,719	210	52	130	14	68	11	30	4	26	4	16	5	305	181
QLP1-11	143,898	276	8.8	209,121	684	828	69	1,877	442	693	1,848	30	1,781	7,205	1,208	5,261	1,046	199	677	81	418	70	177	22	136	16	34	160	520	125
QLP1-12	141,459	211	12.0	216,249	713	735	55	1,565	404	689	1,892	19	1,024	4,405	765	3,450	725	143	492	62	331	57	149	20	120	14	32	134	353	117
QLP1-13	141,158	232	9.3	205,362	717	792	63	1,775	456	695	1,369	26	1,629	6,451	1,078	4,895	975	177	620	75	396	65	169	21	123	14	32	122	376	123
QLP1-14	138,088	242	7.3	202,702	723	745	83	1,557	457	695	1,307	29	1,859	7,147	1,161	4,963	898	184	580	66	348	58	146	19	113	14	30	100	406	105
QLP1-16	138,782	201	9.7	198,465	643	882	53	1,833	388	687	1,663	22	1,327	5,397	948	4,247	899	168	610	76	396	67	177	22	141	16	31	121	393	125
QLP1-17	140,997	200	10.7	202,163	653	941	51	1,853	374	685	1,785	20	1,208	4,981	885	4,112	843	164	587	75	398	67	177	23	142	17	30	129	402	129
QLP1-18	140,166	248	8.6	201,842	682	778	66	1,603	387	687	1,444	26	1,583	6,277	1,037	4,604	854	175	556	68	341	60	151	19	118	14	28	106	401	104
QLP1-19	137,504	438	7.5	201,234	714	734	72	1,723	447	694	1,774	30	1,864	7,168	1,189	5,164	963	195	618	73	380	63	166	21	128	15	33	156	580	120
MKEDI	139,583	133	2.6	207,184	331	155	8	961	234	662	927	9	538	2,302	384	1,678	353	64	280	41	228	40	99	12	65	6	14	59	352	118
MKEDI - 2	140,521	133	2.8	210,596	332	154	7	945	238	662	951	9	513	2,232	382	1,590	357	64	283	41	234	40	101	12	64	6	15	61	346	121
MKEDI	141,372	159	3.0	209,015	331	171	9	1,012	262	667	1,026	13	563	2,372	402	1,704	372	67	294	42	234	42	103	13	67	6	16	69	393	131
MKEDI - 1	141,644	153	2.6	209,346	319	156	8	1,072	313	676	1,220	11	604	2,597	434	1,913	406	74	322	46	264	46	118	14	74	7	19	89	464	150
BLS - 1	142,664	110	5.4	203,603	263	708	319	667	1,575	763	7,507	8	455	1,819	318	1,466	313	71	224	32	182	31	83	10	60	6	38	278	317	145
BLS - 2	145,917	111	5.9	206,503	268	723	326	680	1,614	765	7,492	8	462	1,863	324	1,409	326	71	220	32	185	31	81	10	58	6	39	280	310	143
BLS	141,091	113	5.2	199,462	257	700	312	663	1,547	762	7,394	7	450	1,780	311	1,390	308	70	219	32	177	31	78	10	57	5	35	267	312	138
BLS	142,296	97	5.4	199,857	261	702	321	666	1,560	763	7,474	8	456	1,808	316	1,418	306	70	221	32	175	31	79	10	57	5	37	272	317	139

[1] Calculated crystallisation temperature applying the Zr-in-titanite thermometer by Hayden et al. (2008)

Table S6:
Input parameters for fractional crystallisation modelling

Parental Composition
assumed from most primative zircon

Gd	76.1
Yb	356

Partition coefficients

Element	amphibole (Nandedkar et al., 2014)	plagioclase (Rollinson, 1993)	biotite (Matsui et al., 1977)	quartz	titanite (Bachmann et al., 2005)	Zircon (Sano et al., 2002)
Gd	14.9	0.09	0.442	0.00001	855	8
Yb	9.6	0.077	0.67	0.00001	393	277

Modal abundances (based on Redmond et al., 2010)

QMP

phase	amphibole	plagioclase	biotite	quartz	titanite	zircon
Modal abu	15	42	3	1	0	0.1
mode %	25	68	5	2	0	0.2

LP

phase	amphibole	plagioclase	biotite	quartz	titanite	zircon
Modal abu	15	40	3	1	0.1	0.1
mode %	25	65	5	2	0.2	0.2

QLP

phase	amphibole	plagioclase	biotite	quartz	titanite	zircon
Modal abu	3	23	4	7	0.3	0.1
mode %	8	60	10	20	1	0.2